UNIVERSITÀ
DEGLI STUDI
DI PADOVA

DIPARTIMENTO
DI INGEGNERIA
DELL'INFORMAZIONE

DIPARTIMENTO DI INGEGNERIA DELL'INFORMAZIONE

CORSO DI LAUREA IN BIOINGEGNERIA PER LE NEUROSCIENZE

"TOWARD THE CONTROL OF A CURSOR ON THE SCREEN USING A FOUR CLASS MI BASED BCI"

Relatore: Prof. / Dott Tonin Luca

Laureando/a: Zanchi Luca

ANNO ACCADEMICO 2022 – 2023

Data di laurea 14/12/2023

INDEX

ABSTRACT

Brain-computer interfaces (BCIs) offer an alternative method of communication between the subject and the external environment, without relying on conventional communication channels. The ability to modulate its own electroencephalogram EEG signal during the imagination of specific movements can enable the actuation of specific movements to external devices, thus repairing or reinforcing some abilities that may have been lost. Herein, we propose two possible setups for a four-class MI BCI, which aim to test the feasibility of these endogenous BCIs to accurately control a cursor on the screen. To this end, an initial calibration phase has been conducted for each of the 12 healthy subjects to create two initial decoders, for the X and Y axes respectively; after this phase, three online test runs for each axis have been conducted to test the efficacy of these decoders, Subjects have been allowed to pass to the control of the cursor in 2D only if they reached at least 70% accuracy on each axis singularly. Those who passed to this final stage proved that a good control may be possible with adequate time to train, stating that a four-class MI BCI is a feasible, although at its beginnings, system able to provide an alternative communication channel.

CHAPTER 1: INTRODUCTION TO BCI

1.1 DEFINITION OF A BCI

Various definitions could be made about what is a BCI; probably, the best definition of a BCI system has been given by Wolpaw et al. as follows: “BCI can be defined as a system that measures Central Nervous System (CNS) activity and converts it into an artificial output that replaces, restores, enhances, supplements or improves natural CNS output and thereby changes the ongoing interactions between the CNS and its external or internal environment” [1]. From this definition, it is important to highlight some concepts that from a first reading may have been overlooked.

The physical components that compose a BCI systems are three: a user, from whom a neurophysiological signal, for example EEG, is extracted; a decoder, which gets as an input the processed signal, extracts useful information and returns as an output a command; and an output

device, which may vary from application to application. Examples of possible output devices may be the screen of a computer or robotic limb, which are given a determined input command in order to execute a specific task.

The essential requirement for a BCI system is fact that it must be a “close loop”: the user performs a specific mental task, the neural signal is acquired and processed, and specific features are extracted and classified by a decoder. Finally, the BCI translated the user’s intention in a command for the external device. The result of the classification serves as feedback to the user, so he/she can have a confirmation about the execution of the intended task [2]. The ultimate goal of a BCI system is to accurately interpret the user’s intentions and translate them into an appropriate command; with the aid of a training period, the user can achieve the ability to modify his/her brain patterns to evoke a desired outcome from the BCI system [3][4]. Seen from this point of view, learning to use a BCI is not different from learning a new skill [5][6], with one great difference: the user does not have a physical contact with the external device, but only a feedback; this inability to completely feel the outcome of the brain activity may influence the BCI performance.

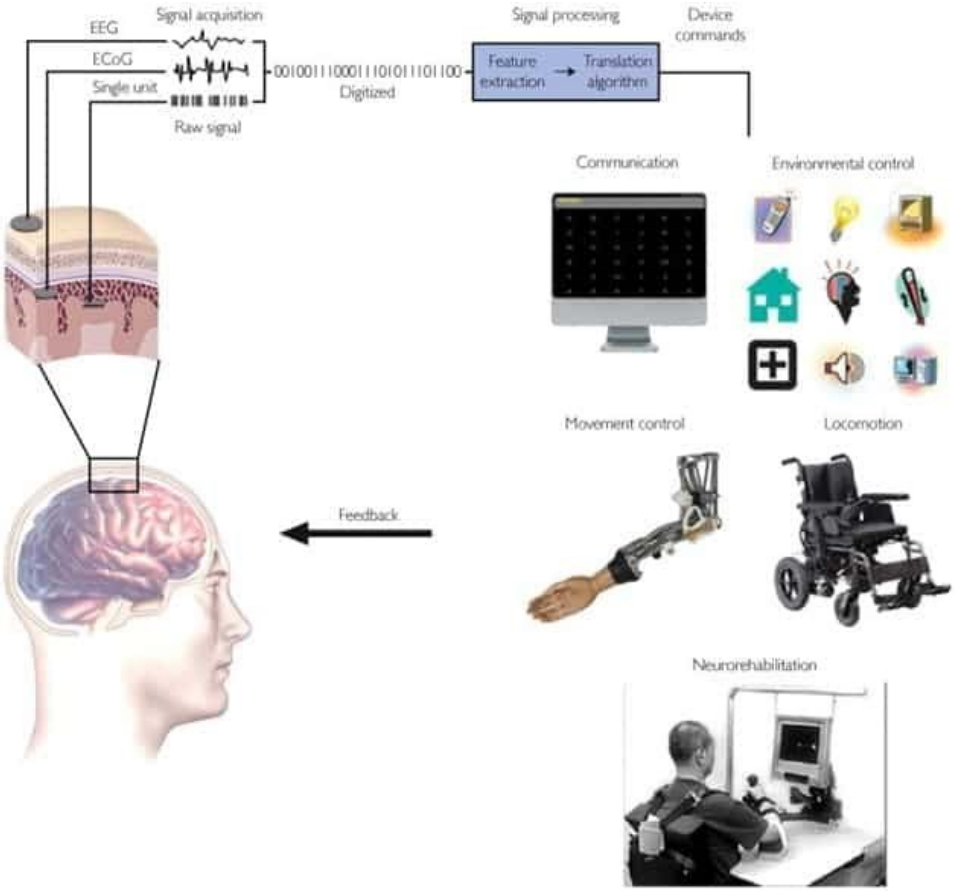

Figure 1 Main components of a BCI system. The feedback component is essential to close the loop between the user, which generates an electrical signal, and the computer parts, which processes the signal and translates it into a specific action [7]

1.1.1 AIM AND USEFULNESS OF A BCI

A BCI system enables a novel communication between the CNS and the environment, without relying on the standard CNS outputs (i.e., nervous stimuli or endocrine outputs); instead, a BCI converts the neural signal into an artificial output, which may or may not be linked to the original meaning of the CNS process taken in exam. For example, as shown later in this thesis, a particular type of BCI, known as Motor Imagery (MI) BCI, translates the kinesthetic imagination of a peculiar movement into a 2D direction of a cursor on the screen, without any movement on the user's side. The necessity of this further communication channel can be understood once the medical environment is taken into account: patients affected by various diseases may be partially or totally unable to efficiently communicate with the external environment, so BCI may result in an improvement of their quality of life. Since several diseases ultimately impede the normal communication channels, the researchers' interest in the BCI systems grew exponentially in these past decades.

Some of the aforementioned diseases are more known and common than other, like stroke, Amyotrophic Lateral Sclerosis (ASL), spinal cord injury or muscular dystrophies, whilst others like brainstem stroke and neuromuscular disorders are not, unfortunately, brought to the attention of the public as they should. All of these diseases ultimately lead to inefficient ways of communication with the external environment, and even though the incidence of them is not particularly high (exception made for strokes), the possibility of incurring in only one of these diseases and being constricted to rely on different ways of communication, even for little periods of time, exists. Just this one reason is enough to understand why researchers decided to invest time and money in improving the various BCI systems, but there are others.

From the first experiments using the EEG signal for a BCI in 1969 [8], technology made tremendous step forwards; but it is only around the late 80's that more accurate signal processing techniques and more powerful hardware reached the market, opening to researchers the possibility of investigating many unanswered questions and theories regarding the generation of the EEG and how the relation between the CNS and PNS (Peripheral Nervous System) works, both in animals and in humans. At present, we lack a whole and complete understanding of these processes, but BCI systems have been used in previous years as an ulterior way of investigating brain connections and functionalities. Suddenly, real-time BCIs became possible and feasible, and the research in this field also brought new important data on which grasp and test theories about the brain functioning. Moreover, progress in other research fields such as physics, computer science and computing made possible the approach to the BCI as interdisciplinary, integrating information from the aforementioned fields and granting them to progress further too.

The utility of a BCI systems does not only resides in providing ulterior communication channels, but also in the ability to exploit the characteristic of the CNS, once some of its paths are no more usable, to create new connections in the damaged areas surroundings, partially or, in some cases, totally restoring the previously lost ability [9]**.** This ability of the CNS is called neuroplasticity, and researchers found out that, after a brain damage caused by trauma or strokes, a good and prompt rehabilitation made in the subsequent period of convalescence is more likely to produce restoration of the lost functions. In this junction comes the BCI: by creating specific, repetitive and easy tasks, which can be made funny in order to stimulate the patient and diminish the possibility of him/her abandoning the rehabilitation, various studies [10][11][12] suggested that there may be a positive correlation between the usage of a BCI system as a parallel tool in the rehabilitation and the consequent good outcome of the rehabilitation.

Lastly, another interesting usage of a BCI system is to control robotic devices in order to carry out simple to difficult tasks, from grabbing and moving an object [13] to moving an exoskeleton [14]**.**

1.1.2 BCI SYSTEMS CLASSIFICATION

There exists no unique classification for a BCI system: each one can vary from the acquisition techniques and for the specific purpose (rehabilitation, control of robotic devices, social interactions, …). However, when referring to BCI, an initial difference can be made among exogenous and endogenous BCIs.

The exogenous BCIs use external stimuli, e.g. the P300 component of the ERP (Event-Related Potential) or the steady state visually evoked potential (SSVEP), to induce the activation of specific brain areas; these kind of BCIs are generally robust and easy to train, given the fact that the training phase required to obtain a model is short [15][16], however they rely on exogenous stimuli that induce non-spontaneous changes in brain areas, which should also follow an oddball paradigm to produce significative and detectable signal characteristics. Since the aim of this thesis is to control a cursor on the screen to reach a random target, the premises of the oddball paradigm are not respected, and thus the use of an exogenous BCI is not recommended.

Endogenous BCIs rely, instead, on self-initiated, voluntary modulation of brain rhythms, providing a more flexible and natural control for a wide range of applications [5]. Both these typologies use electrodes to gather brain signal, and if these electrodes are placed over the scalp we are facing a non-invasive BCI, while if they are placed inside the scalp, generally over the cortex or even internally, we can talk about an invasive BCI [17].

Another important aspect of a BCI system is its ability to work in real-time, an essential requirement to provide good support for a potential user. Working in real-time is not a trivial task: the signal

processing steps that are needed to extrapolate relevant feature must be kept relatively easy to require little processing time, the system should not be hardware demanding and the signal should be the cleanest possible [18].

For these reason, the most popular BCI systems that are used in laboratories, especially for the training of a decoder, are the synchronous BCIs, generally referred to as cue-based, in which the brain signal is analyzed only during predetermined time windows, in which the user is required to stay focused on one specific task; out of these windows, the user is free to move, relax and blink the eyes, since the disturbances and artifacts that will appear in the signal will not be analyzed. Asynchronous BCIs, or self-paced BCIs, on the other hand make no use of time windows; instead, they analyze the signal continuously. This emulates a more natural human-machine interaction, but comes with consequences, such as artifacts in the brain signal and disturbances, that must be dealt with [19][20].

1.2 FROM RAW SIGNAL TO CONTROL OUTPUT

There are several acquisition techniques that allow to acquire neural signals and to process them in order to obtain useful results from the BCI system. Among these techniques, the two that are most used, thanks to their high temporal resolution, are the electroencephalography (EEG) and the electrocorticography (EcoG) [1], that allow the distinction between non-invasive and invasive BCIs, respectively; both of them provide pros and cons that must not be ignored during the decision of which acquisition technique to use. Both techniques use electrodes, which can be placed invasively or not invasively, and the resulting signal greatly differs in quality. Working with implanted electrodes placed just above the cortex, or internally, the resulting ECoG overcomes one of the main EEG problems, the low spatial resolution that imposes the necessity of using spatial filters [21]. This benevolent condition comes with no little implications, from moral to possible harmful consequences: to place electrodes inside the skull, medical surgeon is necessary, requiring very strict studies of biocompatibility to produce proper electrodes that can remain inside the subject's body for long periods of time, and ethical issues must not be underestimated. On the pros side, however, a much cleaner signal, without the noise that volume conduction inside the cortex and through the skull and scalp arise, can be gathered and analyzed, allowing the study of more interesting setup and cognitive task. EEG, instead, is considered much more feasible, not having ethical and harmful consequences at its disposal, but the result is a much noisier and more complex signal that requires more pre-processing steps in order to reduce its complexity and avoid the appearance of artifacts [22].

Other modalities for signal acquisition include fNIRS, fMRI and MEG, each one having their own pros and cons, but generally they have one of these three problems: they are not affordable and are very expensive; they have poor temporal resolution; the quality price ratio is not worth [2][23].
ECoG is indeed the cleanest signal that researchers could work with, having both high temporal and spatial accuracy, but its invasiveness raises many problems; in the end, the most used signal to work with remains the EEG [24], recorded on the scalp by a variable number of electrodes, which can be active or passive. Since they are placed over the scalp, the majority of the signal that they acquire comes from the cerebral cortex, that is responsible for the control of high cognitive, sensory and motor functions such as planning, language and thinking. In this section we will undergo the main passages that needs to be performed to extract useful information from an EEG signal and how to turn it into an actual output for the BCI.

1.2.1. SIGNAL PROCESSING

The EEG signal needs to be processed before its analysis, given its poor SNR and the various possible disturbances that may alter the information that should be extracted. These interferences, generally referred to as artifacts, can be classified among endogenous and exogenous [25]. Among the endogenous artifacts there can be found electromyography signal deriving from muscle contraction; rhythmic cardiac activity; eye and movement and low frequency pattern arising from other brain activities. Many of them are characterized by low frequencies, so a high pass filter with a cutting frequency of 1 or 2 Hz is sufficient to clean the signal; the only exception is muscle activity, which presents higher frequencies.
On the other hand, exogenous artifacts arise from electromagnetic interference, lightening conditions and the equipment used to extract the EEG signal (i.e., the amplifier), and have a frequency that oscillates from 50 to 60 Hz [26]. A good low pass filter cutting frequencies above 40 Hz should be more than enough to highlight the range of frequencies we are interested in, that are the μ and β bands, which range from 8 to 12 Hz and 18 to 30 Hz respectively.
Other methods used to extract a cleaner signal include the independent component analysis (ICA) or the principal component analysis (PCA); the first one aims to find the sources that generate the EEG signal, sources that do not translate to the single neurons, but to population of neurons responsible for a portion of the signal, while the second one's goal is dimensionality reduction, given the fact that the EEG signal, collected from, generally, many electrodes and carrying noise from a poor SNR, can be simplified extracting only the signal components that carry the most information [23].
Volume conduction another problem when working with the EEG: the signal generated by each electrode is influenced only by half from the neuron population below the said electrode, in a 3 cm

radius; the remaining half is influenced by adjacent populations [27]. Moreover, other sources, like the visual cortex or muscle artifacts, may hide relevant features in the frequency range of μ and β bands [28]. To reduce the influence of nearby signal sources, many spatial filters can be used, most known being the Laplacian, Common Average Reference (CAR) or Common Spatial Patterns (CSP) filters. In this thesis, the spatial filters kept into account is the Laplacian one, a reference-free that emphasize the activity below each electrode by calculating the second derivative of the instantaneous spatial voltage distribution [29] and can be seen as a high pass filter that reduces interference signals produced from distant sources.

1.2.2. FEATURE EXTRACTION AND SELECTION

With the pre-processing phase, the main goal is to obtain a clean and reliable signal from each electrode. Even with this expedient, the EEG signal remains a highly complex, non-stationary and multi-sources signal, so a key aspect of research is to find constant characteristics, called features, able to represent and describe it. The importance of finding good features is critical, since the decoder that will analyze the signal in real-time will search for these features and classify a portion of the signal into one of the possible classes the decoder works with. There are many domains from which features can be extracted, all of them potentially carrying useful and well-distinguishable information to comprehend the signal at best [30].

The most common domains used for the feature extraction are Time, Frequency and Time and Frequency, all of them requiring many parameters to be tuned and techniques to know to establish if they are suitable or not for the situation. Techniques such as auto-regressive (AR) models, Wavelet Transform and Power Spectral Density require to determine, respectively, subject-specific order of the model, mother wavelet and channel-frequency pairs to exhibit right features to extract [31]. Neurophysiological notions like brain connectivity models can be added to the equation to distinguish where and what to look for [32]. Moreover, given the fact that the EEG signal is multi-source, the number of signals to analyze are at least equal to the number of electrodes at disposal, generally making dimensionality reduction methods like PCA or ICA really useful [33].

1.2.3. CLASSIFICATION

Once the features have been selected, a classifier can be made with different algorithms. It can be created using various Machine Learning (ML) and Deep Learning (DL) techniques, and determining which one reaches the best accuracy is greatly debated in literature [34][35][36].

In the last years, the opportunity to link the feature extraction phase with simple to complex DL models got the attention of many teams around the world [37][38][34], reaching high accuracy even on datasets that present more than two possible tasks, the so called multiclass MI BCI datasets; however, training these models require time, and the application of DL concepts with such little datasets to train on can lead to bias. For this reason, simpler ML models, such as Linear Discriminant Analysis, Random Forest and Quadratic Discriminant Analysis, still remain the most used, since their properties of reaching good accuracy and getting update if necessary, while being fast to train [1].

1.3 BCI DRIVEN APPLICATIONS

In the past decades, technology has increased to a point where the main obstacle to work online has been overcome, namely powerful, yet affordable, hardware. Their main objective is to compute even complex models within milliseconds [8]. One of the main application of a BCI system is its use in the neurorehabilitation field [10][39], in which many papers report better results at the end of the rehabilitation using a BCI system instead of conventional rehabilitation protocols [40][41]. The typology that seems to produce more reliable and satisfactory results is the MI BCI, probably given the intrinsic property of linking an imagined movement to the actuation of the same movement onto a prosthesis of a robotic device, which gives a more familiar feedback compared to brain activation that people generally do not correlate, in everyday life, to specific commands, as happens, instead, in other types of BCIs [42]. However, even if the results tend to be positive and encouraging, the lack of a sufficient amount of data is not enough to determine the supremacy of the rehabilitation using a BCI system over the conventional methods; they just hint that, at least for now, implementing the aforementioned system may prove to be helpful in parallel with the conventional physiotherapy [43][44].

One of the first implementations of BCIs is communication for patients which suffer from severe neurological diseases that greatly impair the ability to communicate verbally with the external environment [12]. From a virtual keyboard, the patient can select the letters that compose the phrase he/she wants to say, and at the end a digital voice reproduces the phrase [45]. The use of a BCI, however, in this case in not very recommended, since there are easier to implement and interpret systems that can do the same, for example a camera or myoelectric signal derived from ocular muscles. Nonetheless, some BCI systems proved to produce relevant results in the communication field, especially in the case of patients affected by neurological disorders such as ALS, most of them relying not on MI tasks, but on SSVEP [46], P300 [47] or a non EEG-based BCI, called fNIRS BCI, based

upon the functional Near Infrared Spectroscopy that explores the blood-oxygenation level of the cortex [48].

Furthermore, BCIs can be used to control external devices to partially restore the lost functions, for example to move an electric wheelchair or a neuro-prosthesis [49][50][51]. Such changes in the life of the users may not just improve their ability to interact with the environment, but even their emotional and psychological state, which may affect the therapy's efficacy [51][52]. However, these setups assumes that the user is free to move, which rises the problem of how to handle artifacts in the EEG that will be present in the signal.

BCI applications are not applied only to medical research: another emerging trend is the entertainment field, in which various types of BCIs are being currently tested. At the time, complex games and scenarios are out of reach, but simple games as a surrogate of Space Invaders or even complex games that does not require time limits like chess seems to obtain quite good results [53]. One of the main problems regarding the use of the BCI is that is a technology mainly studied in laboratories or research centers on a limited number of users, so the quantity of data acquired is not enough to produce more generalizable models that can be applied to larger populations. In the near future, however, if these technologies would be opened to wider categories of users, more data could be gathered to produce more accurate and generalized models; one of the most promising of these categories is represented by the gamers, given their tendency to invest considerable amount of time to master determined skills, in which the BCI can be fit in [54].

1.3.1 MI BCI OVERVIEW

MI BCI relies heavily on the concept of brainwaves and the identification of particular brainwaves patterns, relegated in two specific ranges of frequencies. These ranges are commonly known as μ waves and β waves and can be seen from the scalp during the planning of an imagined or real movement, more specifically over the somatosensory (SM) cortex.

During the execution of a MI task, a phenomenon known as Event-Related Desynchronization (ERD) takes place, and it consists mainly of a decrease in power of the Sensory Motor Rhythms (SMR) over specific electrodes, due to the fact that in the area below the neuronal population fires at different frequencies from point to point, resulting in a less powerful signal in the μ and β bands. On the other Hand, when the MI task finishes, the opposite phenomenon takes over: the neuronal population starts to fire in a more synchronized way (ERS), and the power of SMR increases.

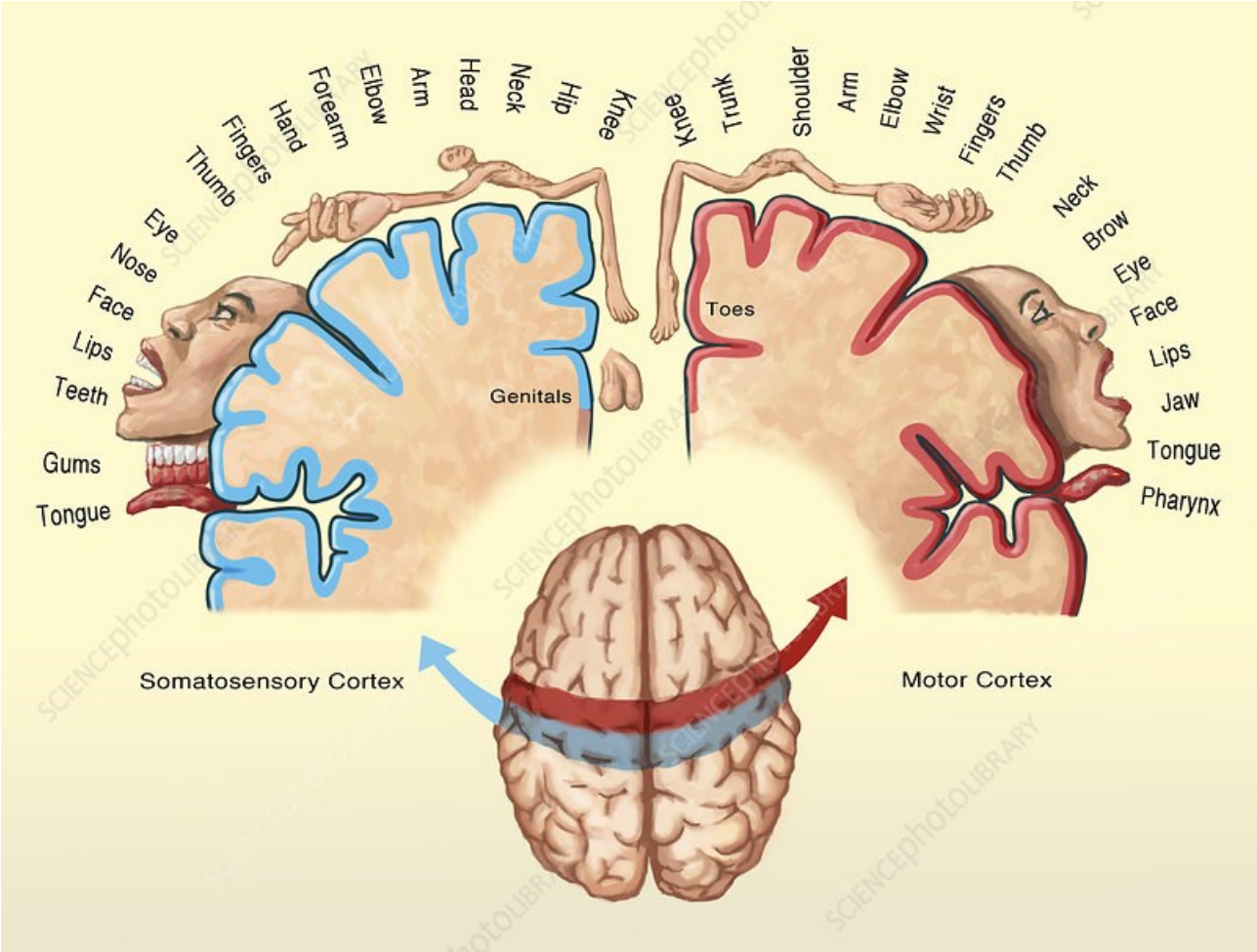

Figure 2: Somatosensory cortex. From this figure can be created the cortical homunculus, a human figure with limb and body parts extension proportional to the surface that those parts occupy in the somatosensory cortex. It can be seen that the MI tasks chosen occupy broad areas. Credit to Spencer Sutton/Science Source/SCIENCE PHOTO LIBRARY

For example, during the kinesthetic imagination of the Left Hand, an ERD will be visible over the contralateral somatosensory cortex responsible for controlling that specific body part, according to the cortical homunculus. In this case, the ERD should be visible mainly over the C4 electrode, using the 10-20 system.

The main advantages about using this kind of BCI consist in maintaining a certain degree of correlation between the imagined movement and the actualization of that specific thought process, and in the ability, by the user, to get used and gradually control more efficiently the entire system [55]**.** This preserves a more natural approach to the BCI, as the user is engaged even in the calibration phase, avoiding tasks such as looking at a blinking object on the screen, which are much less entertaining. However, this advantage is accompanied by some disadvantages, such as longer and more challenging calibration phases in order to train a good model, and a general lesser efficiency compared to other types of BCIs [56].

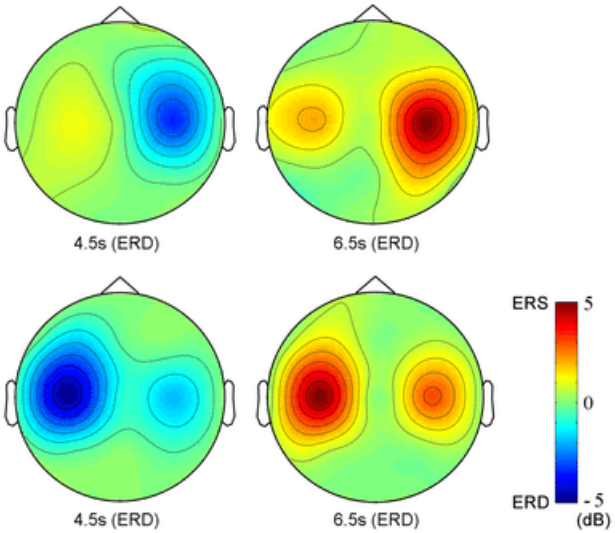

Figure 3: An ideal case of ERD/ERS over electrode C3 and C4. A greater ERD can be seen over one electrode than the other, highlighting which Hand movement is being imagined at that time. In the top row we can affirm that the user is trying to imagine the movement of the left Hand, while in the bottom row we can affirm the opposite. It is important to notice that there is still and ERD/ERS effect even on the ipsilateral side [58].

1.4 PRINCIPAL CHALLENGES TO OVERCOME

It is commonly accepted that the threshold of 70% accuracy in 2-class BCI is the minimum requirement to say that the user is skilled enough to use the system [57]. Increasing the number of possible tasks reduce the threshold, mainly due to a reduction of the confidence level. Unfortunately, BCI systems present some obstacles that may be really hard to overcome, if not impossible for few people, for example the ability to make the use of the system a passive skill, that needs little to no mental effort [5]. A very much more likeable situation is indeed the opposite: the user needs to concentrate a lot even to achieve little results, and, with long online sessions (or repeated short ones), fatigue and emotional states as frustration or even overjoy are capable of produce an EEG signal that can mask the user important features that drive the BCI.

1.4.1 BCI ILLITERACY

BCI illiteracy has been described as the “lack of knowledge and proficiency in using BCI systems within a standard training period” [59] and is a relatively new concept highly debated and criticized. Generally, the main arguments that are carried to justify the use of the terminology of “BCI illiteracy”

can vary from the inability to impede little muscle spasms, to some artifacts and, ultimately, to anatomical differences in brain volumes and neuron populations that alter the EEG signal [60]. These obviously represent some possible problems that may limit the ability of the user to perform well, but all of them can be resolved trying different techniques or different paradigms; indeed, Lee et al. stated that, between three different BCI paradigms exposed to the same users, no universally BCI illiterate could be found, while there was a good percentage of users that were, instead, BCI literate, able to use all types of BCIs [61]. This supports the vision of controlling a BCI system as a skill that first of all needs to be learned [6][62], and sometimes this learning process may be longer in some individual respect to others.

Another critical aspect of the definition of BCI illiteracy is the time limit in which a user, generally a healthy one, must remain to be considered a successful user [63]. There are two main problems to discuss. Firstly, the insertion of a time limit is not a sufficient statement to imply that a person is unable to use the BCI, if anything it can distinguish between successful or unsuccessful user, and it is valid only for the experiment at hand. Secondly, BCI systems are tested mainly on healthy subjects, even if the system is thought to be used by disabled people to improve their quality of life. This is due to the difficulty of having the true end-users that may benefit from this technology, which, if the BCI proves to be efficient, will have plenty of time to learn how to use the system efficiently.

Beside the physical factors described above, psychological, behavioral or motivational factors can highly influence the ability to correctly control a BCI. Conditions like fatigue, engagement and concentration are indeed responsible for the variation in outcome of a user's performance [64], and have been gathered inside the BCI illiteracy, recognized as impactful factors; however, once time limitations are removed, these factors can be modulated or integrated in subject-specific setups to obtain good performance.

1.5 MOTIVATION AND OBJECTIVES OF THE THESIS

In this thesis, the aim is to create an asynchronous, noninvasive multi-class MI BCI.

The goal consists in assessing the feasibility of a 4-class MI BCI in order to control a cursor in a 2D plane. Among all possible BCI typologies, MI is "able to provide a more intuitive mapping of direction between BCI interfaces and control commands" [65], and this is due to the fact that the possible MI tasks available (namely Both Hands, Both Feet, Right Hand, Left Hand and Tongue) can be highly correlated to commands sent to control external devices. The more natural this correlation is, the easier it would be to be in control of the BCI system [66]; however, depending on the structure of the BCI, some tasks are easier to discern from others, and will be discussed later. It is for this reason that two possible BCI systems have been investigated during this thesis, one focused on easier to discern

MI tasks, the other based on naturalness of the correlation between the MI tasks and the output commands.

Aiming to control a cursor in a 2D screen, the main focus was to have two pair of different MI tasks both in the horizontal and vertical direction. For the first setup, the control of the X axis is based upon the discernment between the classes Both Hands and Both Feet to move right and left the cursor, respectively; instead, the classes that control the Y axis are the contemporaneous activation of Both Hands and Both Feet vs the Rest class to move upward and downward. In the second setup, the classes assigned to control the X axis are Right Hand and Left Hand to move right and left, which maintains the naturalness between the task and the direction the cursor should move to, while on the Y axis the classes used to go upward and downward are Both Feet and Rest.

Diagonal movements are allowed, but this implies a very important assumption, that is to say that two different MI classes can be active at the same time and can be detected by the system. This can be hard to see from a first look at the first setup, since the classes of the X axis are present, united, on the Y axis, but in the MI BCI users are able to modulate their brain activity in order to overcome this issue [67].

A feasible MI BCI could be applied in every possible field of application for the BCI: in communication it may improve the velocity in composing words, avoiding one of the main problems of ERP BCIs that imposes randomness in the letters appearance [16], substituted by selecting directly the wanted letters; in movement control of external devices and locomotion it offers a more variety of possible commands, directly correlated to the increase of the classes the system works with; lastly, in neurorehabilitation, MI can greatly help in functional recovery by reinforcing and increase the effective use of damaged or impaired brain areas [68].

CHAPTER 2: METHODS

2.1 PARTECIPANTS

The EEG signal of 13 users (30% female) is acquired through 16 electrodes placed on the somatosensory cortex according to the 10-20 EEG system and processed with ROS-Neuro [69][70][71]. The average subject's age is 24 ± 3.54 years old. Five users already had experience with the BCI; the remaining ones did not have any previous experience, and an initial exposition about what they would do and imagine in order to use a MI BCI was given.

Focusing on the X axis, for the Both Hands task, users were asked to imagine a familiar movement linked to the use of both the hands, recommending simple tasks like closing and opening the fists; for the Both Feet tasks similar instructions were given, recommending focusing on sensations like stomping the feet or rising on the toes. Proceeding to the Y axis, for the Both Hands and Both Feet task the union of the aforementioned instructions were advanced, while for the Rest task a recommendation about focusing only on inspiring and exhaling from the abdomen region was given.

2.1.1 CALIBRATION PHASE

The experiment was composed of two sessions, and between the first and the second at least a day passed. On the first day, after the explanation of the protocol, each user had the possibility to get comfortable with the feeling of the kinesthetic imagination of the various tasks before two calibration phases, on for each axis.

The first calibration consists in three runs containing 10 trials of Both Hands and 10 trials of Both Feet each, for a total of 30 trials for the two classes. Once a run started, a visual paradigm of 900x800 pixels, created using Python, as presented in Figure 4, containing two bars with atop an image of the corresponding task, is showed.

The trials began when a white cross below the bars disappeared, replaced by the image of the task to perform. After 1 second, the task-corresponding bar started filling for a random time between 4.5 to 5.5 second; once full, the bar illuminated itself for 1 second, stating the end of one trial, and the cycle can repeat until all trials have ended.

Once a run finished, data were inspected visually to confirm if the user manifested features that matched previous literature [72]; features in the μ and β bands over electrodes C4, C4 and Cz, and relative neighbors, were expected. At the end of the first three calibration runs, a decoder for the classes Both Hands and Both Feet is created.

The second calibration phase is pretty much equal to the first one, exception made for the introduction of the last two MI tasks: contemporaneous activation of Both Hands and Both Feet vs Resting state. Data were visually inspected once again to extract the relevant features in the aforementioned positions; this time, however, identical features that appeared in both calibration were excluded, if not too impactful, that is to say if they did not reach dark red or orange color in Figure 6**.** At the end of this second calibration phase, a second decoder, able to discern between the Both Hands and Both Feet class vs Rest class is created.

2.1.2 ONLINE CONTROL ON ONE AXIS AT A TIME

These two calibration phases could take up to an hour in the worst-case scenario, and the quantity of mental work without any feedback can be disarming and frustrating, resulting in just fatigue and a sense of bitterness. In order to get the users familiar with the sensation of controlling the cursor, after the calibration phase a first experience of the online control is proposed, limiting the movements of the cursor to only one axis at a time.

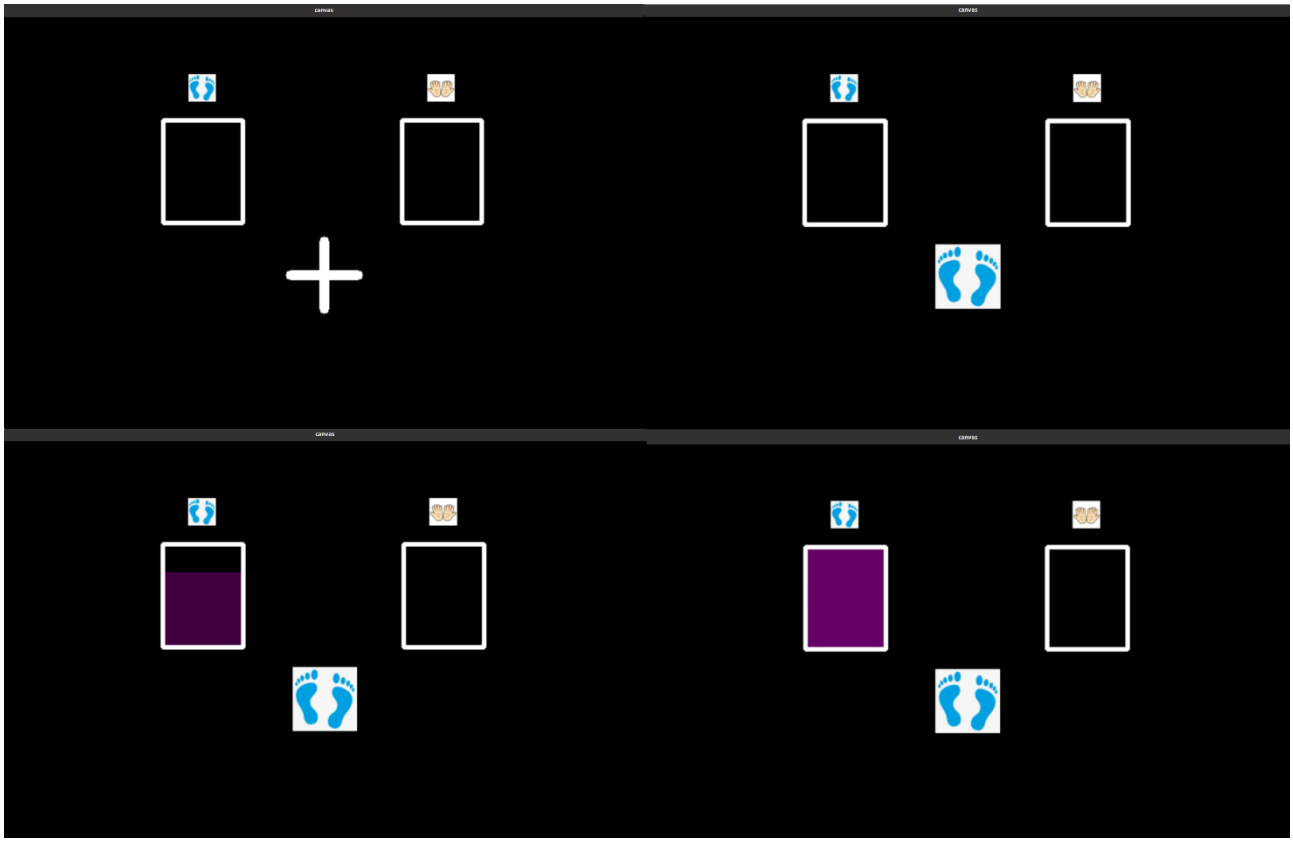

Figure 4: Image of the 4 phases that composes each task in the calibration phase. This represents a Both Hands vs Both Feet run: at the top left there is the fixation period; at top right the cue, in which appears the task the user is about to perform; at bottom left the continuous feedback, in which the user performs the corresponding task; at the bottom right the boom, stating that the task is finished and the user is allowed to rest a little.

A different virtual environment is shown, with eight possible targets to reach, as shown Figure 5, created with Python again**.** The maximum cursor speed allowed is 192 pixels on the horizontal and 160 pixels in the vertical axis per second (12 and 10 pixels per refresh rate). Limiting the circle movements to only the x or y axis means that the user can reach only a subset of targets, which are numbered 5,6,7 and 8. This first experience presents no constraints about the time needed to reach one target; its utility resides in giving the user a visual feedback useful to complete the loop that composes a BCI system and allow to experience the feeling of controlling the circle with a specific MI task. The aim is to strengthen the neural connections used to perform the various tasks, therefore mastering the skill to control the system. Moreover, adding a little bit of fun directly in the calibration phase allow the users to be more involved in the experiment, an important factor that seems to have a good impact on the final outcome [54]. From this last experience we are able to understand early on if the user has the ability to perform correctly the MI tasks necessary to complete the experiment, since reaching each target in little time is a good indicator that the decoder is performing correctly, and that the user is able to control his/her mental state to recreate accurately the same sensations felt during the calibrations.

On the second day of the experiment, the user is asked to perform once again the control of the same cursor in one dimension, but this time a time limit of 20 seconds is introduced. This exercise is carried out three times, and for each run the user is asked to reach 20 targets, 10 in one semiaxis of the direction in control, and 10 on the opposite side. There are two possible outcomes for this phase: the user is able to perform correctly and reach an accuracy of at least 70%; the user activates features different from the ones the decoder is based on, preventing him/her to reach the accuracy threshold of 70%, probably because of the intra-variability phenomenon. We will focus a little more on this second possibility before proceeding onto the final stage, which is the 2D control of the simulated cursor.

There may be many different factors that influence the inability to control properly a BCI [73], like the right amount of sleep, the attention level, fatigue, frustration and even confidence. Once a trial started, a bad control scenario consisted of a drift of the cursor in just one direction, independently from which task the user was supposed to perform, which translated to the decoder assigning only one class. This happened if he/she presented different features from those the decoder is searching for, and users were given the instruction not to deconcentrate or get frustrated if this happened, since these new data could be used to create an updated decoder. If this was the case, the first two runs were used as an ulterior calibration phase, whilst the last one was used to confirm or not the ability of the user to reach the threshold of 70% accuracy with the updated decoder. This process is repeated on both axes. It is important to note, however, that if the necessity of a decoder update rose, the burden

for the user rose too, given the fact that these new calibration runs, with trials of 20 seconds in the unassigned class, were much longer.

This last scenario appeared quite often unfortunately, but generally only one decoder of the two created before did not work, allowing us not to extend the experiment's duration too much. Once at this point, the user must have shown that he/she is able to reach the accuracy threshold in both the 1D online setups; if this were not the case, the user was considered a dropout and could not proceed onto the final stage, that is the control of the cursor in 2D.

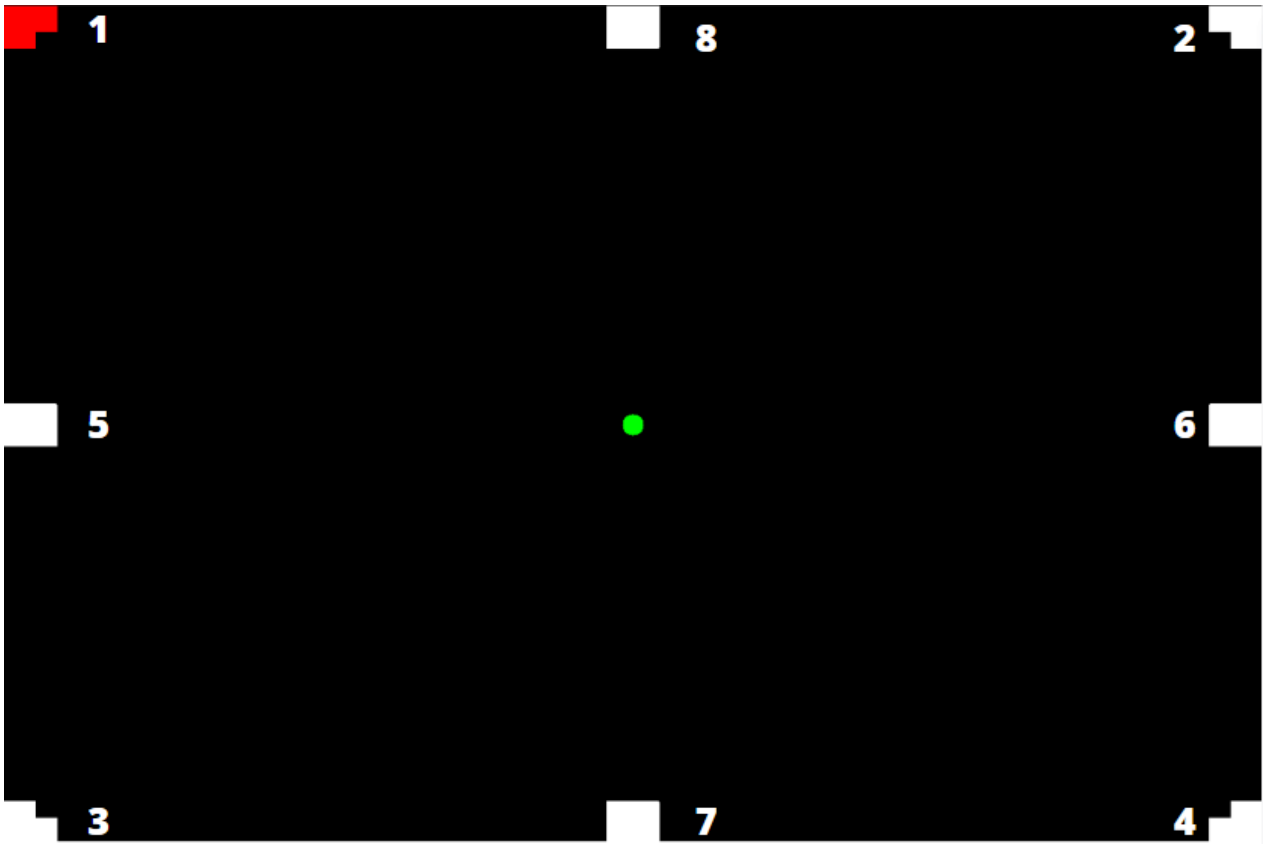

Figure 5: Graphical interface of the 1D and 2D environments. The little green circle in the middle is the simulated cursor that the user controls to arrive at the marked target in red. In a 1D control, one of the two possible dimension is disable: during the control of the x axis the cursor can move only towards targets 5 and 6, while during the control of the y axis only target 7 and 8 are available.

2.1.3 2D CONTROL

The final stage of the protocol consists of reaching each possible target that is highlighted in the 2D environment shown above. Since this is the hardest task that the user performs, a little bit of extra time is given, reaching a time limit of 30 seconds. In total, two 2D online runs took place, both consisting of reaching each target two times, resulting in a 16 tasks per run. One of the main obstacles we expected in this stage is a diagonal drift of the cursor that favorites the targets at the top right and

bottom left corners. In the passage from calibration to online, the user needed to adapt to the abrupt change of the goals: in the offline, he/she needed to focus on just a MI task without feedback, while in the online 1D, the cursor's movement, the actual visual feedback, indicated where the cursor was moving, and the goal changed from just concentrating on a task to reaching one of two targets. Here, the user passes from two possible targets to eight, requiring the simultaneous activation of one or two of the four possible MI tasks. The diagonal drift in just one of the two possible diagonals of the rectangular interface is not casual, but due to the experiment setup: the Both Hands tasks appears both in commanding the cursor up and right, and the absence of the Both Hands task may activate the other two, making the cursor go left and bottom; to correct this phenomenon, an Evidence Accumulated Framework, discussed more clearly in section 2.4.1**,** is introduced, making it a little bit easier to separate the X and Y movement, resulting in a little more independent decoders. This framework, abbreviated EAF, made easier even the particularly difficult task of reaching a target controlling one dimension while maintaining constant the coordinate of the other one, a setup already seen in 1D control, but here far more difficult.

2.2 EEG PROCESSING

A key aspect of the good outcome in controlling a BCI system is the selection of relevant features from the EEG signal; once correctly identified and voluntary activated, the right commands can be sent to the external devices. There are various methods to extract such information, some of which do not even require an expert to look at the data to decide which features are considered relevant and which should be discarded. Such methods, however, tend to limit the interaction between the user in his/her first experiences and the expert that follows the experiment, which may result in an incomplete understanding of the correct performance from the user's side. Having the possibility to rely on visual feedback, after the first calibration runs, that highlight the good or bad outcome of the first trials is indeed a powerful instrument that slows down a little the time needed to carry out the experiment but helps greatly both the user and the expert to understand if there are critical issues or everything is going on as planned. For these reasons, the method chosen in order to extract, visualize and select relevant feature is a Power Spectral Density (PSD) based analysis, with the ultimate goal of providing what can be seen in Figure 6, the so-called Fisher Score Matrix.

2.2.1 PSD ANALYSIS

Having talked about the μ and β rhythms, a frequency domain analysis method must be used to extract the power contained in those two rhythms, and here the PSD analysis comes into play. Given the non-

stationarity of the EEG signal, however, we cannot calculate its total energy, since we should acquire the EEG for an infinite time; however, its average power is limited and meaningful, even if estimated from a limited period of time [74].

Mathematically, we can view the spectrum of the signal, $S_{XX}(w)$, as:

$$S_{XX}(w) = F_{r_{XX}}(w) = \frac{1}{\sqrt{2\pi}} \int_{-\infty}^{\infty} r_{XX}(t) e^{-iwt} dt$$

$S_{XX}(w)$ is calculated using the FFT of the signal r_{XX}; since we do not have an infinite signal r_{XX}, what we compute is an estimate of the true spectrum, from which, based on Welch's method [75], the aim to arrive to a spectrogram, so that in the end we arrive at a PSD composed of [windows x frequencies x channels]. A little improvement of the Welch's method is used, which helps to reduce the computational time needed to calculate the various FFT coefficients and obtain the spectrogram for each instant of time. Before diving in the details of the technique, however, an overview of how data are stored and analyzed must be done.

Once every run starts, data are collected into a Buffer of 512 samples x 16 channels; since the sampling rate is 512 Hz, the Buffer contains the last 1 seconds of data for each channel. With a frequency of 16 Hz, 32 new samples for each channel are stored in the Ring Buffer, implying that the first 32 samples x 16 channels are deleted, and the rest of the Ring Buffer translated in order to accommodate new data. At a frequency of 16 Hz, the PSD is computed; the result of each computation is a window of frequency x channels, each pair containing its relative power. This process returns the aforementioned PSD of [windows x frequencies x channels].

Normally, we should compute the Welch's method for each of these windows, but, since they are overlapping between each other, meaning that quite a bunch of the FFT coefficients calculated at the window at time n are equal to the coefficients calculated at the window at time n+1; if we store these values, the only coefficients left to calculate are the ones relative to the Welch's sub-windows that contains the new data. Having less operations to do translates to reducing the computational time, which opens the way to work in real-time.

2.2.2 FISHER SCORE MATRIX

Once the PSD has been computed, we still maintain some information about the time, encoded in the windows dimension. From this point, we are able to mark and consider only the portion of the signal relative to the various MI tasks and to compute the so-called Fisher Score Matrix in order to highlight if there are significant differences in power in the μ and β bands while performing the tasks. To compute the Fisher Score Matrix, we use the following formula:

$$FS(k) = \frac{abs(\mu_{C1}(k) - \mu_{C2}(k))}{\sqrt{\sigma_{C1}^2(k) + \sigma_{C2}^2(k)}}$$

Where μ_{C1} and μ_{C2} are the mean for classes C1 and C2 (Both Hands vs Both Feet or Both Hands and Both Feet vs Rest, in this case), while σ_{C1} and σ_{C2} are their relative standard deviations (STD). These values are calculated from the cue period until the end of the continuous feedback, so to say the interval of time in which we know the user is performing, possibly, the task presented on the screen. This process returns a 2D matrix of [frequencies x channels], also called discrimancy maps as shown in Figure 6, and if one of these pairs shows a value close to 0, that means that during the performance of the two classes, the selected frequency over the selected electrode show no difference in power; otherwise, if the value is different from 0, there is a difference in the selected pair during on task or the other. Selecting the most discriminant features now means that we search the [channel x frequency] pairs that remains constantly different from 0 through the various calibration runs; not only, we will select just a few of these pairs, those related to the μ and β bands with the highest values.

2.3 DECODER CREATION

From the visualization of the Fisher Score matrixes, we are able to understand if the user will reach good performance during the online trials or if more time will be needed to understand at best the MI tasks and how to control the BCI. It is important to note that if a user show no particularly good features, maybe due to task-unrelated thoughts during the trials or inability to remain concentrated for a long period of time, during the online trials this situation may greatly change. In this last scenario, the user will tend to exhibit relevant features at high frequencies; since we are interested in very specific sub bands, however, only the most prominent features in those ranges that still manage to come out will be selected, even if the subsequent trained decoder does not show great results. The good outcome of the experiment will depend on the user to adapt and learn to prioritize the selected features during the online trials, generally resulting in the disappearance of features located at higher frequencies and the strengthening and appearance of sub-bands related features.

Figure 6: Examples of possible Fisher Score matrices. In the top section of both the windows we can see the channel-frequency pairs that indicate, through the colors, which pair present the most difference in power between the tasks during the three calibration runs, while in the bottom there is an interface that highlight the common features present, which can be selected automatically or manually.

At the end of the calibration phase and, eventually, two online trials, the related Fisher Score matrixes are visualized, and the relevant features selected. Once we have the [channel x frequency] pairs that seems to discern at best the various MI tasks, a QDA decoder can be created and tested on unlimited time online trials in order to tune other external parameters that will be discussed in Chapter 2.4.

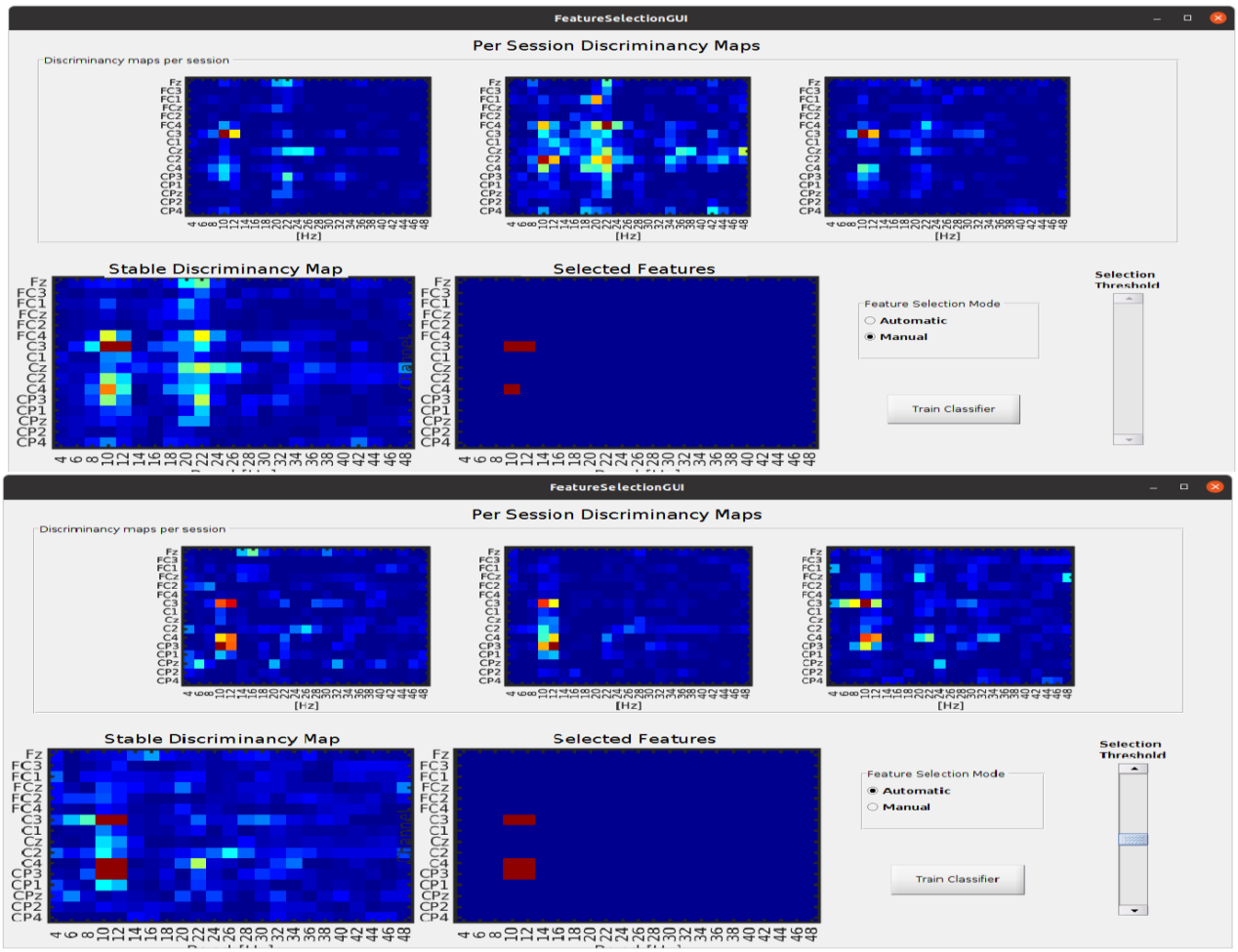

2.3.1 QDA ANALYSIS

The main goal of a Discriminant Analysis (DA) classifier, both Linear and Quadratic, is to create decisions boundaries out of a $\Re^m$ space, where m is the number of the features that are able to describe the sample they have been extracted from. The boundaries separate the $\Re^m$ space in k subspaces, where k is the number of classes we are considering [76]; in the case of this thesis, k is set equal to 2, since we will be working with two binary classifiers working in parallel to distinguish 4 MI tasks. Once a new sample arrives, it will be represented by a new point in the $\Re^m$ space and will inevitably fall into one of the two possible regions that the space is separated into, thus determining the label of the new sample.

DA classifiers are based on the Bayes rules, which aims to calculate the probability of a sample to belong to a specific class:

$$P(x = \omega_i|x) = \frac{P(x|\omega = \omega_i)P(\omega_i)}{P(x)}$$

where:

- x is the sample currently at hand

- ω_i is the class considered
- $P(x = \omega_i \mid x)$ is the probability for the sample x to belong to class ω_i
- $P(x| \omega = \omega_i)$ is the likelihood of class ω_i
- $P(\omega_i)$ is the a priori probability of having class ω_i
- P(x) is the evidence and is calculated as follows:

$$P(x) = \sum_{i=1}^{k} P(x|\omega = \omega_i)P(\omega_i)$$

An important aspect of the DA classifiers is that they assume the likelihood to follow a gaussian distribution, having, for each class, specific mean μ_i and covariance Σ_i. We are not able to precisely assess these two parameters, but we can estimate them from the data we gathered during the calibration phase. The main aspect that differentiates between a Linear Discriminant Analysis and a Quadratic Discriminant Analysis is that in the LDA there is an ulterior assumption, so that the covariance of each class is the same, while in the QDA they may differ. This determines different boundaries in the $\Re^m$ space: linear boundaries in the LDA, quadratic boundaries in the QDA.
Having estimated the likelihood for each class, once a new sample arrives, all that remains to do is to compare its likelihood to belong to one or the other class and calculate the relative probabilities; the class that has higher likelihood will be chosen as the label for this new sample.

2.4 EVIDENCE ACCUMULATION FRAMEWORK

The objective of the decoder is to understand the user's intentions correctly and classify them; of course, this is the ideal case, where the classes that we are dividing our MI tasks are perfectly separable with no possible errors. This scenario is obviously not possible, but from a look at the probability, for a chunk of EEG data, to belong to one of two classes, we can manipulate the decoder's output to send the right command to the cursor on the screen.
From the decoder we can extract two characteristics, which are the class that the data contained in the Buffer belongs to, and its related probability. Working with just the classes' labels is feasible in the case we are interested in maximizing the classification accuracy, but in this thesis what we are most interested in is the stream of probabilities that comes from the decoder, which will be converted into a similar, but more reliable, output that helps to classify the user's intentions in a better way. This data manipulation technique is called Evidence Accumulation Framework, abbreviated EAF.

2.4.1 EXPONENTIAL SMOOTHING

By definition, the probability for a sample of data to belong to a class or another, in a binary classification problem, goes from 0 to 1, with numbers tending to 0 stating that the sample does not belong to a specific class with high reliability, and vice versa. If the decoder works well, theoretically it will provide only high probability to belong to one class and low probability for the other, but since the EEG signal presents low SNR, is non-stationary, there is the intra-subject variability and the features extracted are not always the best possible, the values we expect at most are probabilities above 0.5, but much below 1 or even 0.9. In the fortunate case in which the decoder returns a high probability for one class, this does not imply that for the subsequent instants of time the decoder will return those same high values, so a system that just follows this very unstable stream does not match with the BCI characteristic to deliver a specific command continuously. We would prefer something derived from the stream of probabilities that once above or below certain thresholds delivers a command, but is more stable, even if it means introducing a delay in the feedback. The EAF fits perfectly in these necessities.

The proposed EAF can be considered as a way to integrate the posterior probability given by the decoder, following this formula:

$$D(t) = D(t-1) * \alpha + pp(t) * (1-\alpha)$$

D(t) can be seen as the state in which the system is at time t, and is equal to the state that the system was in the previous instant of time multiplied by a smoothing factor α plus the probability of the state being in a specified class multiplied by 1-α. Normal values of the smoothing parameter α range from 0.9 to 0.99; the higher the smoothing parameter is, the slower the response of the system will be. At the beginning of the online trials, the state vector D(t=0) is set to 0.5, stating that the system is waiting for subsequent data to adjust itself and explore its possible range, that remains in the interval [0,1], the same range as the probabilities.

Given the fact that we are using a binary classification, it follows that if at a time instant t the decoder returns a probability equal to ω for the first class, the second one has a probability equal to 1-ω; we can condense all this information into the state vector D(t), saying that if its value is close to 0 we are observing one class, while values around 1 states that we have observed for a long period of time the other class. The last case left to be discussed is when D(t) is around 0.5: if the state keeps remaining in this situation, we can consider it as the decoder being unable to assign neither one class or the other, hinting that maybe a different MI task or a not considered mental state is currently being executed.

The main advantage of using an EAF resides, so, in its ability to enclose the state of the BCI system in a limited number that needs time to reach meaningful values, and so considers, in a way, the past decisions of the user. The problem of the decoder not reaching high values may remain, if an incorrect setup is made or the user is not particularly able to perform the MI tasks, but we have greatly reduced the impact of erratic behaviors and misclassified samples, which, if followed strictly, may result in abrupt changes in command delivered to the cursor and in a misleading feedback.

2.4.2 FROM CLASSIFICATION TO CURSOR VELOCITY

All the considerations said earlier support an ideal classification that oscillates around the 0.5 value if the decoder is unable to distinguish between the two classes. This may not be the case, but fortunately the EAF proved to be robust and easy to set up in order to face this problem.

One of the easiest setup to input a command to the cursor could be to look at the state vector D(t) and compare its value to two different thresholds, τ_{top} and τ_{bottom}: if D(t) is higher than τ_{top}, we can give the command related to the MI task corresponding to state values closer to 1; if D(t) is lower that τ_{bottom}, we can affirm that the user is performing the opposite MI task; if D(t) is not above τ_{top} nor is below τ_{bottom}, the decoder is having a hard time assigning the same class with good probability for a long period of time, and so the user is performing no one of the two possible MI tasks. The command given to the cursor will go accordingly, with no movement given as input in the case the state does not reach τ_{top} nor τ_{bottom}.

With this setup, the control of one axis and, consequently, two axis seems quite simple: one command is given if the state reaches one of the two thresholds, and a null command is given otherwise. If the gap between τ_{top} and τ_{bottom} is too large, however, the user may experience long periods of time in which the cursor stands still, with no hints about how well the task he/she wants to perform is being carried out. Still, having an interval of values in which the cursor does not move can be important while learning to modulate brain rhythms, since if the user is executing a task in a correct, albeit weak, way, the cursor does not move in the opposite direction if the probability of the correct class returned by the decoder is slightly below 50%.

To avoid this situation, while preserving the possibility for the cursor to not move, two ulterior thresholds have been implemented, τ_{vel_top} and τ_{vel_bottom}. In this setup, when the state of the system firstly reaches one of these two values, it starts moving the cursor with a velocity proportional to the distance of the state from these thresholds and the distance between these thresholds and the top/bottom once:

$$v(t) = abs(int\left(\frac{D(t) - \tau_{vel_{top}\ or\ vel_{bottom}}}{\tau_{vel_{top}\ or\ vel_{bottom}} - \tau_{top\ or\ bottom}}\right))vel_{max}$$

Using this formula, when the state reaches τ_{vel_top} or τ_{vel_bottom}, it still has a velocity equal to 0, but the more the state increases/decreases, the higher the velocity of the cursor will be, until reaching the maximum speed of vel_{max}. Now the user has a reduced interval of state values in which the cursor does not move, and once it starts moving, the speed of the cursor can be seen as a feedback: if the direction is correct and the task is being performed intensely, the cursor rapidly gets to vel_{max} and to the target; on the other Hand, if the task is performed poorly or the decoder does not reach high probability, the cursor won't move with great speed, letting the user to adapt the mental state and try to focus correctly on the task before the cursor travelled too much distance.

These parameters, τ_{vel_top}, τ_{vel_bottom}, τ_{top} and τ_{bottom}, must be set up before the beginning of the run by the researcher, and the unlimited time trials proved to be an excellent test ground. It is important to state that one controlling just one axis, the values of , τ_{vel_top} and τ_{vel_bottom} won't be too distant from the state value of 0.5; those same values cannot be used in the control of both axis, because the complexity of actually performing correctly two MI tasks at the same time favors one of the two classes per axis, thus inducing to pose the idle state sometimes far from 0.5, up to 0.75.

CHAPTER 3: RESULTS

3.1 NATURAL OR USER-FRIENDLY HORIZONTAL CONTROL

The main objective of this thesis is to prove that a simultaneous identification of two possible MI tasks is feasible and easy to implement to control a cursor in 2D. One of the main arguments was which MI tasks should be performed on the x and y axis, so a preliminary test was conducted to verify which setup, between Both Hands vs Both Feet and Right Hand vs Left Hand, achieve the most accuracy. The results led to use Both Hands vs Both Feet setup, which achieved an overall accuracy between 6 subjects of 69 % ± 8.3, compared to the overall accuracy of Right Hand vs Left Hand of 63.2 % ± 6.6. The accuracies of every subject can be found in Table 1:

Classes	s1	s2	s3	s4	s5	s6	Mean_accuracy
Bh vs Bf	67.1494	75.6024	71.3110	67.8916	77.7896	54.3598	69.0173
Lh vs Rh	60.6555	69.2771	65.4421	58.4789	71.2348	54.0549	63.1905

Table 1 Accuracies between MI Both Hands vs MI Both Feet tasks and MI Right Hand vs MI Left Hand tasks for each of the preliminary users.

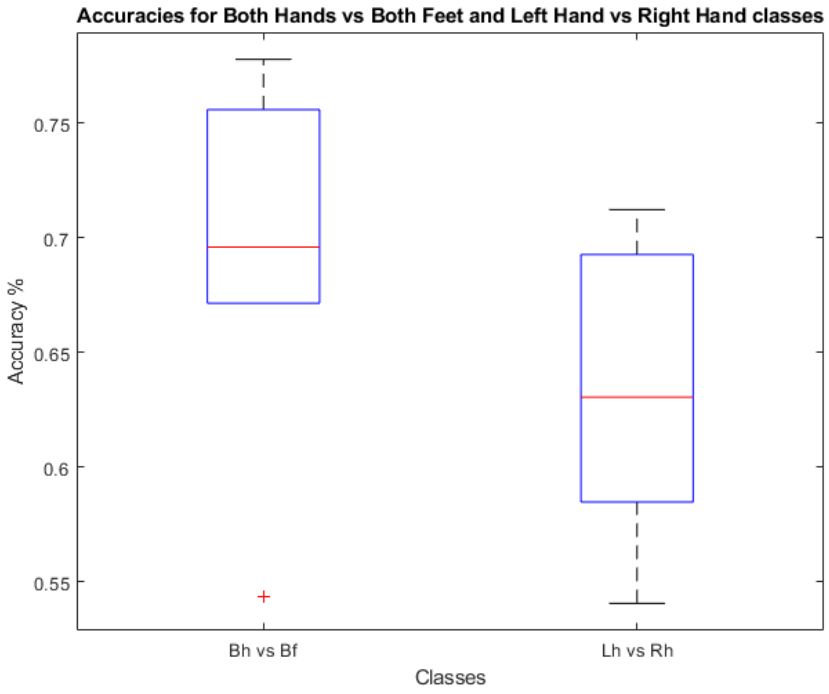

Figure 7: Boxplot of overall accuracy for the Both Hands vs Both Feet MI tasks and Left Hand vs Right Hand MI tasks. From the picture, we can clearly see that the mean accuracy of Both Hands vs Both Feet corresponds to the 75th percentile of Right Hand vs Left Hand, thus declaring the superiority of the first presented setup respect to the second.

The two distributions are statistically different, with a p-value of 0.0061 (t-test).

Supported by these results, an initial setup composed of MI tasks Both Hands and Both Feet to move the cursor right/left and the MI tasks of contemporaneous activation of Both Hands and Both Feet and Rest to move it upwards/downwards was chosen, assuming that the features of Both Hands and Both Feet altogether could be well distinguished from those of Both Hands and Both Feet taken singularly.

Data of class Both Hands and those of class Both Feet are acquired in the first calibration; since class Both Hands and Both Feet is the sum of the other two classes conceptually, it is important to verify if data of this class can be reproduced fusing data from the other two classes or not. If Both Hands and Both Feet data could be derived, just one calibration phase could be sufficient to gather all the data necessary to create the decoders, simply introducing a third bar representing the Rest class. The main advantage would be a much shorter calibration phase, generally renown as the most tedious part of the experiment.

To verify this part, data from the first six users, the same that confirmed that classes Both Hands and Both Feet could be better classified than classes Left Hand and Right Hand, were used to emulate data of the class Both Hands and Both Feet; these data have been compared lately with true class Both Hands and Both Feet data derived from the second calibration, and, as Figure 8 shows, a second calibration is indeed required and data of this class cannot be replicated.

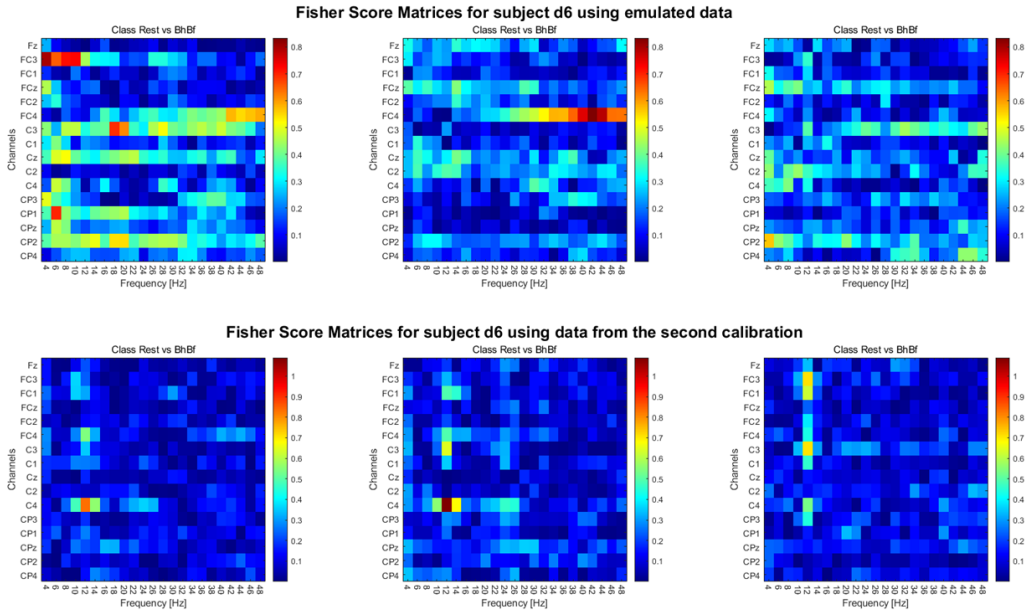

Figure 8: Example of discordant features derived from simulated data (top) and real data (bottom) between the classes Both Hands and Both Feet vs active Rest.

3.2 CONTROL IN 1D

3.2.1 ACCURACY OVER THE AXIS

Out of the 11 users that volunteered to participate to this experiment, 8 of them reached the final phase of controlling the cursor in 2D, establishing the percentage of users able to perform at the very first times at 73%, confirming what Brendan et al. assessed [60]. Data comings from these subjects are not reported, since they did not reach the end of the protocol. The only exception is subject s1, which already had previous experience with the BCI, even if he/she did not reach the threshold of 70% on the Y axis, probably for the unfamiliarity of the MI tasks required; still, in 2D control proved to be one of the best pilots.

As Table 2 and Table 3 show, neither the X axis nor the Y proved to be much more easier to maneuver than the other, but almost every user reported that controlling the Y axis was less tiring. Someone reported signals of sleepiness induced by the Rest task; overall the performances on only one axis confirmed that the system was feasible and easy to control, albeit mentally challenging and exhausting for a protracted period of time.

s1	s3	s5	s6	s7	s8	s9	s11
90,00	95,00	55,00	50,00	50,00	90,00	50,00	50,00
80,00	80,00	50,00	85,00	65,00	70,00	85,00	75,00
80,00	80,00	90,00	95,00	65,00	100,00	65,00	75,00
83,33	85,00	65,00	76,67	60,00	86,67	66,67	66,67

Table 2: accuracy for every user during the control of the x axis. The last row is their overall mean accuracy.

s1	s3	s5	s6	s7	s8	s9	s11
50,00	50,00	50,00	50,00	95,00	95,00	50,00	50,00
40,00	50,00	70,00	55,00	90,00	80,00	65,00	95,00
55,00	85,00	90,00	95,00	75,00	95,00	95,00	85,00
48,33	61,67	70,00	66,67	86,67	90,00	70,00	76,67

Table 3: accuracy for every user during the control of the y axis. The last row is their overall mean accuracy.

Many users experienced some level of frustration or dejection during the first or up to the second run both in the X and Y axis because of the intra-subject variability from day to day. This generated a drift of the cursor in just one direction, even if the users were instructed not to focus on the cursor's direction but only on the task. This phenomenon has been observed in every run that reached 50% accuracy. The case of subject s5 with 55% accuracy can be due to the user's momentaneous ability to activate features showed on the previous day, immediately losing control afterwards.

Even if a user managed to activate the same features the first decoder works with, after the second run the visualization of the Fisher Score matrices and the creation of a new decoder was generally always necessary. Adapting the decoder to the new features the user was manifesting on the second day largely increased the performance of the users if the drift phenomenon was observed; maintaining the first decoder generally translated, however, in a slight drop of accuracy.
Keeping into account the best runs for each subject, thus ignoring those ones in which there was the drift phenomenon, the overall accuracy for X and Y axis reached, respectively, 88.75% and 88.13%, once again stating that no great distinction can be made about which MI pair tasks performs better.

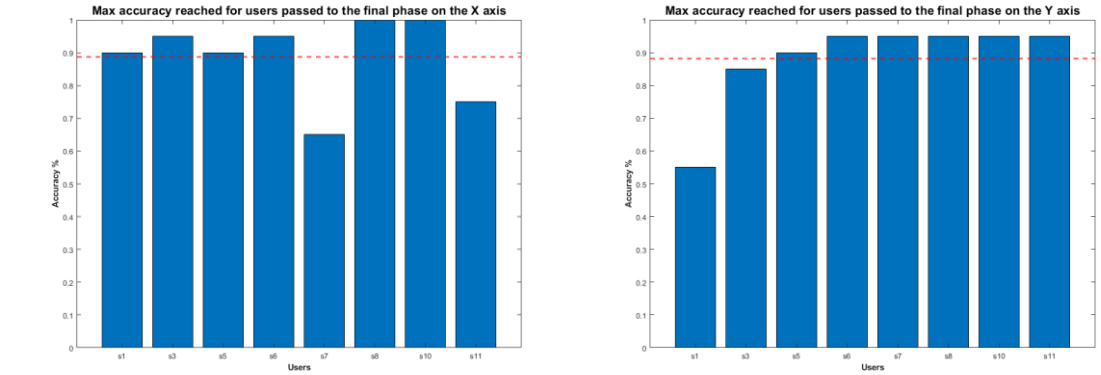

Figure 9: Max accuracy reached for each axis for every user that passed to the final phase.

3.2.2 TIME PER TRIAL

Focusing now on the time needed to complete a trial, the Y axis seems to be the direction that needs less time to achieve the hoped result. Given the rectangular shape of the environment, this axis contains less pixels that the user needs to travel among in order to reach the target, but this aspect has been corrected normalizing the distance among the Y direction. Yet, data leads to indicate that it is easier to identify the MI tasks on the vertical axis instead of the tasks of the horizontal one, even if, from the users' report, the first ones are more difficult to master.

Time	s1	s3	s5	s6	s7
Mean_time_trials	7.7340	9.6911	6.7760	7.6114	6.1438
Mean_time_bh_trials	8.4725	9.9578	5.8930	8.7609	12.0924
Mean_time_bf_trials	6.8110	8.9798	7.6591	6.3342	4.3592
Time	s8	s10	s11	Mean	Std
Mean_time_trials	10.2258	8.3101	5.6201	7.6954	1.5262
Mean_time_bh_trials	12.8336	11.7863	6.2085	9.5385	2.4703
Mean_time_bf_trials	7.6180	5.8768	4.9475	6.3674	1.5514

Table 4: Mean time of Both Hands and Both Feet trial for all the users. Mean and Std refers to all users.

Time	s1	s3	s5	s6	s7
Mean_time_trials	7.4973	9.0734	7.0673	6.4256	7.2495
Mean_time_bhbf_trials	8.3086	10.8562	5.8368	5.8913	9.1367
Mean_time_rest_trials	3.8463	7.0678	8.0517	7.0193	5.1526
Time	s8	s10	s11	Mean	Std
Mean_time_trials	9.1907	4.6505	8.1428	7.4121	1.4741
Mean_time_bhbf_trials	10.2004	6.4304	6.1272	7.8484	2.0459
Mean_time_rest_trials	8.0688	3.0485	9.9569	6.5265	2.3353

Table 5: Mean time of Both Hands and Both Feet and Rest trials for all the users. Mean and Std refers to all users.

3.2.3 STATE VECTOR ANALYSIS

Figure 9 also seems to confirm what the Table 4 and Table 5 hinted: the trials relative to the Y axis seems to be easier to distinguish respectively to the trials on the X axis, and this is highlighted by the fact that both the Both Hand and Both Feet and Rest classes present a clear peak for the completion of tasks within 4 seconds, while this is true for the BF class, but not for the BH class on the X axis.
Figure 10 offers an interesting graphical way to undestand the ability of a user to control his/her mental state to adequately control the BCI system. Each ellipses enclose data relaitve to a specific task, with the direction of the major axis indicating what axis of the cursor the task controls. The ideal user should have the centers of the ellipses as distant as possible, stating that the he/she learned to use the decoder very well.
Figure 11 shows the state vector values throughout the best X and Y runs for user s6. The red segmented green line indicates the value of 0.5, the hypothetical threshold that distinguishes between one axis' pair of classes: the most wanted scenario would be that in the BH tasks, the state vector values should be greater than 0.5, tending to 1, while for the BF class these should go towards 0; the same concept applies for the Y axis. This user perfectly fits in this scenario; being able to reach very high or very low values is a good indicator of the ability of the user to control properly the BCI on the 2D control, although not the only one, as has happened with user s1.
From Figure 11 and Figure 13 two different scenarios are clear. On the X axis we have a good situation, where the point of distinction between the tasks is probably around 0.5, with the majority of the outputs of the decoder being higher that this point for Both Hands and lower for Both Feet; on the Y axis, however, the range of possible values always revolves around 0.5, indicating that the decoder is not reliable when it comes to distinguish the two MI tasks controlling this axis.

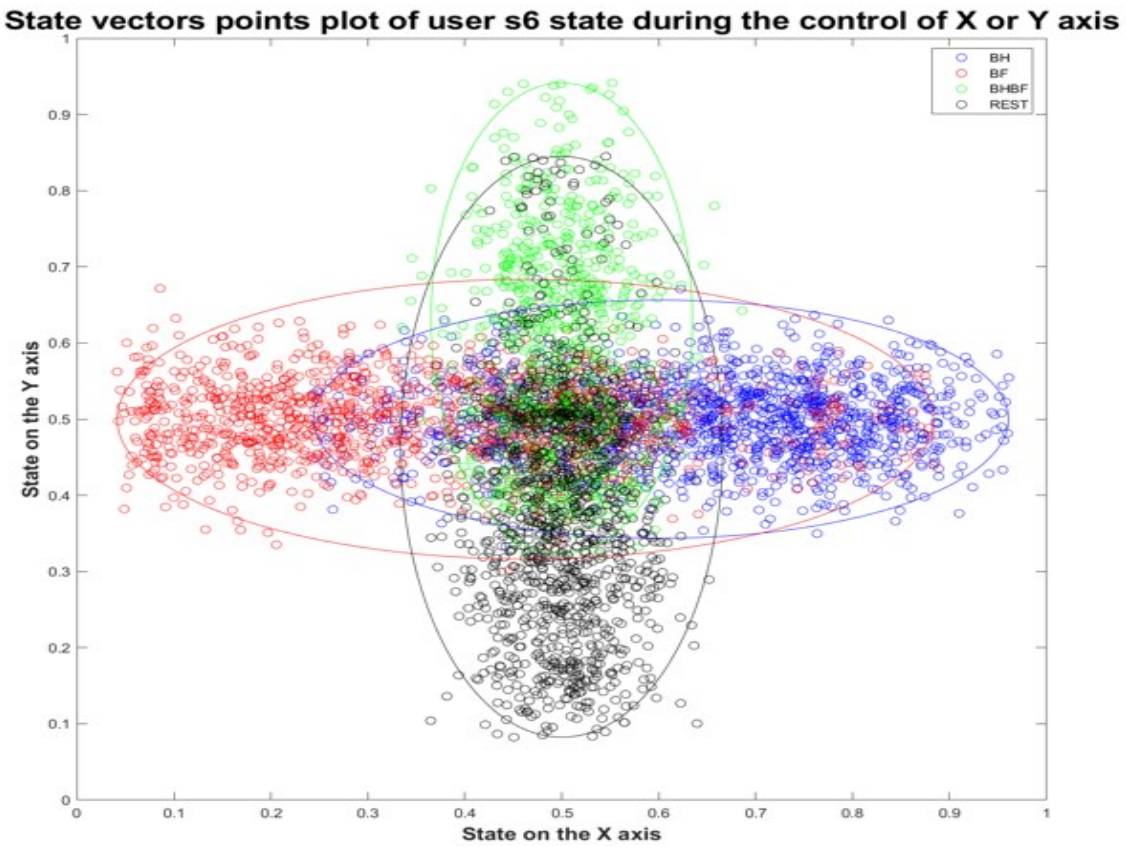

Figure 10: Plot of all the state vector values achieved during the run with best performance for subject s6, one of the best pilots in the 2D control.

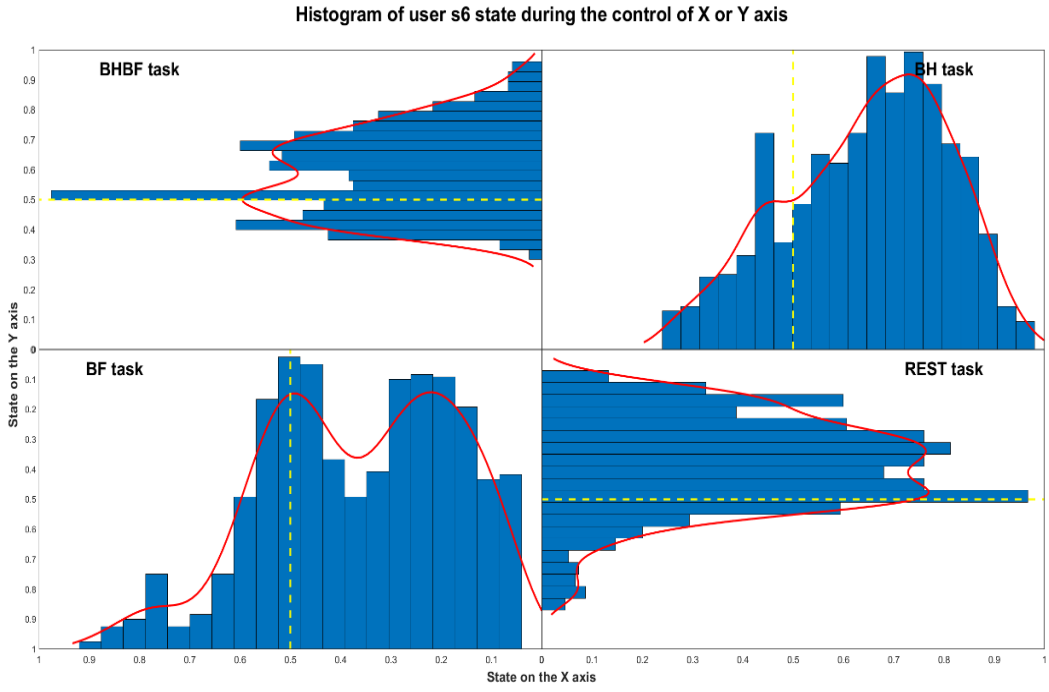

Figure 11: Histograms of all the state vector values achieved during the run with best performance for subject s6, one of the best users in the 2D control.

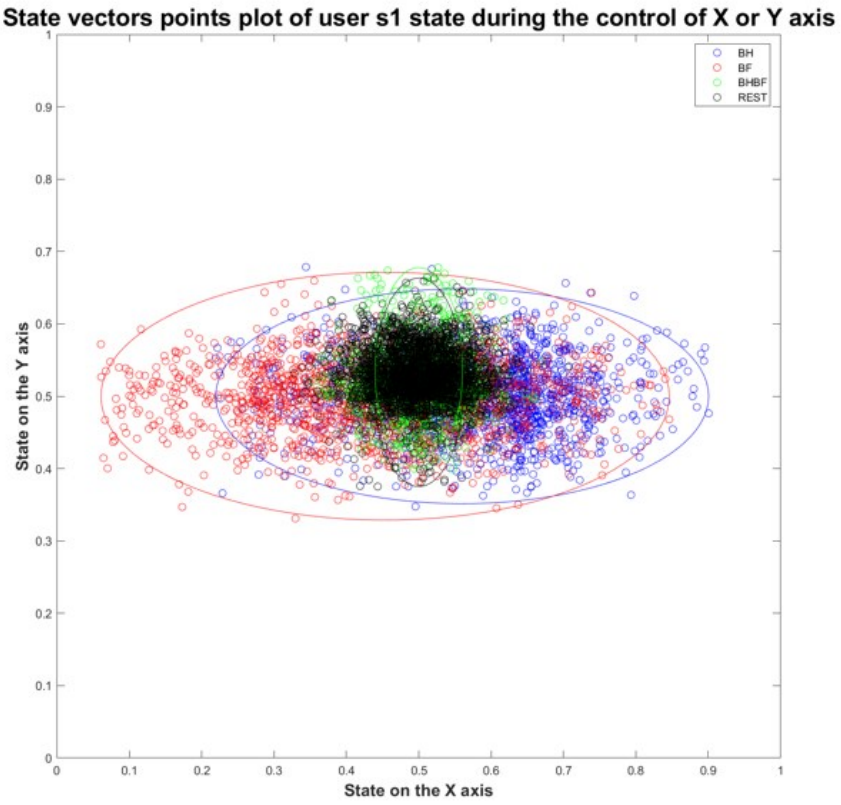

Figure 12: Plot of all the state vector values achieved during the runs with best performances for subject s1. It can be noted a good differentiation between the horizontal ellipses, but almost an overlap of the vertical ones.

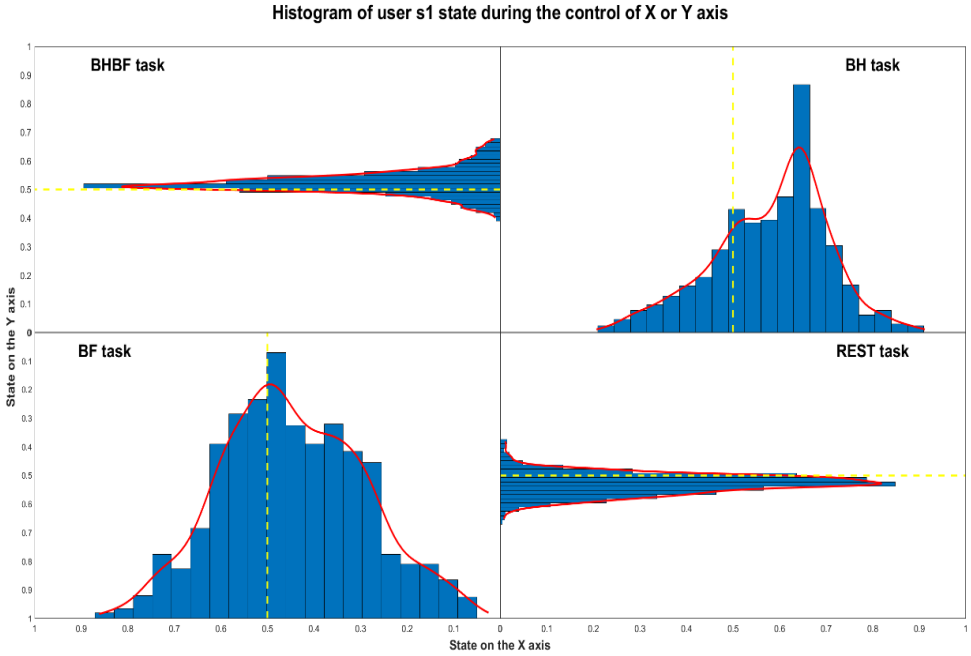

Figure 13: Histograms of all the state vector values achieved during the run with best performance for subject s1. In this case, high/low state vector values are not reached and are, instead, restricted to the median value of 0.5 in the Y axis, but still user c7 performed well during the 2D control.

3.3 CONTROL IN 2D

3.3.1 ACCURACY

Exception made for users s1 and s3, every other user that arrived in this final phase showed constancy between the two time-limited, online, 2D runs at their disposal. Considering only the best run for each subject, the mean accuracy overall is 51.56%, while if every run is kept into account, the overall accuracy lowers to 44.14%. As shown in Table 6, the two main reachable targets are target 2 and target 3, the top-right corner and the bottom-left corner ones, which have been reached in 65.25% and 59.375% of their appearances, followed by targets 6 and 7. The most difficult target to reach is target number 1, the top-left one, which has been reached in 31.25% of the times. These considerations finds confirmation in Table 7, in which the mean time necessary to reach each target, excluding those greater than the 30 seconds time limit, is presented: the targets that required the least mean time to be reached are again targets number 2 and 3, but this time the target that seems to be very hard to achieve is target number 8, the middle-top one, with 18.379 seconds.
Lastly, the best performances for each target are summarized in Table 8.
The ideal shortest time possible can be obtained going only through the Y axis, reaching a middle-bottom or middle-top target, in 2.43 seconds (390 pixels / 160 pixels per second). Some of the times displayed in Table 8 are very close to this asymptotic value, highlighting the feasibility of the system with a good training. These results are close to what Wolpaw et al. developed in a very similar experiment [77].

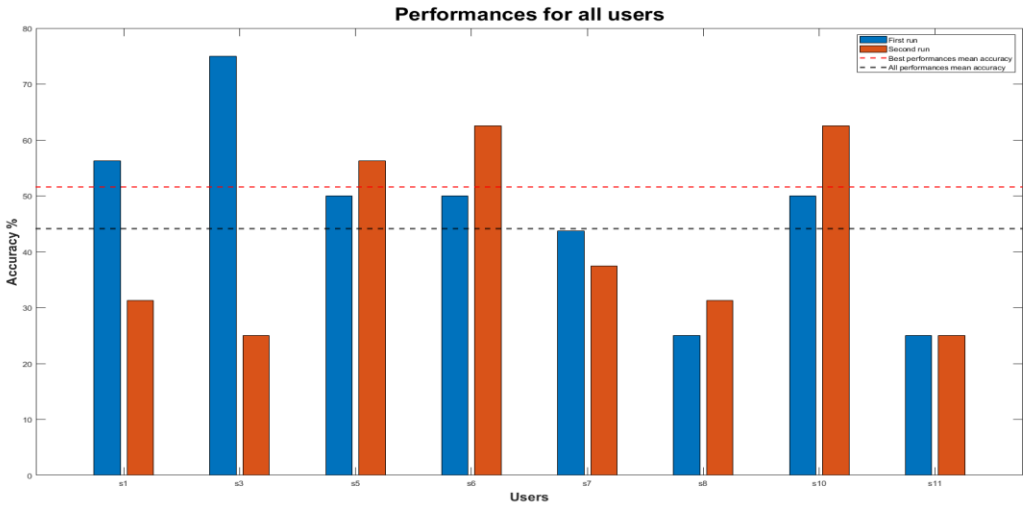

Figure 14: Accuracy of all the users during the 2D control of the cursor. The dotted lines refer to the mean accuracy among the best trials (red line) and among all trials (black line)

Accuracy per target	S1		S3		S5		S6		Mean
	First run	Second Run	First run	Second Run	First run	Second Run	First run	Second Run	
Target 1	50	0	100	0	0	0	100	50	31,25
Target 2	100	100	100	50	50	100	100	50	59,375
Target 3	50	50	50	100	50	100	100	0	65,625
Target 4	50	0	50	0	100	100	0	50	34,375
Target 5	50	0	100	0	50	0	50	100	37,5
Target 6	50	50	50	0	100	50	0	100	46,875
Target 7	0	0	50	50	50	100	0	50	40,625
Target 8	100	50	100	0	0	0	50	100	37,5
Accuracy per target	S7		S8		S10		S11		Mean
	First run	Second Run	First run	Second Run	First run	Second Run	First run	Second Run	
Target 1	0	0	0	0	100	100	0	0	31,25
Target 2	0	100	100	0	0	50	0	50	59,375
Target 3	100	0	50	50	100	50	100	100	65,625
Target 4	100	0	0	100	0	0	0	0	34,375
Target 5	0	0	0	0	50	100	50	50	37,5
Target 6	50	100	50	50	0	50	50	0	46,875
Target 7	100	50	0	50	100	50	0	0	40,625
Target 8	0	50	0	0	50	100	0	0	37,5

Table 6: Accuracy of each target for every user during the two time-limited, 2D control runs.

Mean Time per Target	Target 1	Target 2	Target 3	Target 4	Target 5	Target 6	Target 7	Target 8
Time	15,954	12,321	12,062	14,770	15,098	13,387	13,022	18,379

Table 7: Mean time for each target in seconds

Targets	Taget 1	Taget 2	Taget 3	Taget 4	Taget 5	Taget 6	Taget 7	Taget 8
Best Time	4,55	5,02	4,55	5,02	3,07	5,47	5,53	3,22
User	s3	s8	s3	s8	s11	s7	s11	s1

Table 8: List of minimum time required to reach each target among every user.

3.3.2 PREFERENTIAL PATTERNS

The only method to evaluate each users' performance is the ability to reach the highlighted target within a time window of 20 seconds in one dimension, 30 in two dimensions. Once a target is marked as the active one, coloring it in red, the others stay present in white, and if the cursor passes on these, no penalties are given. This implies that the paths the cursor can take can greatly vary from ideal trajectories, generally hitting other targets before landing on the highlighted one. Figure 15 shows user s6 trajectories used in his/her best run: the central heat map represents all paths taken during all the trials, while the heat maps at the corners represent the trajectories travelled during each target's trials. Targets are indicated by the yellow rectangles; the color code ranges from blue (background, cursor never moved to these coordinates: low coverage) to orange (most common cursor coordinates: high coverage). Another example of heat maps is presented in Figure 17, making possible to visually see the differences in what was expected and what was discovered, as will be discussed in Chapter 4.2.

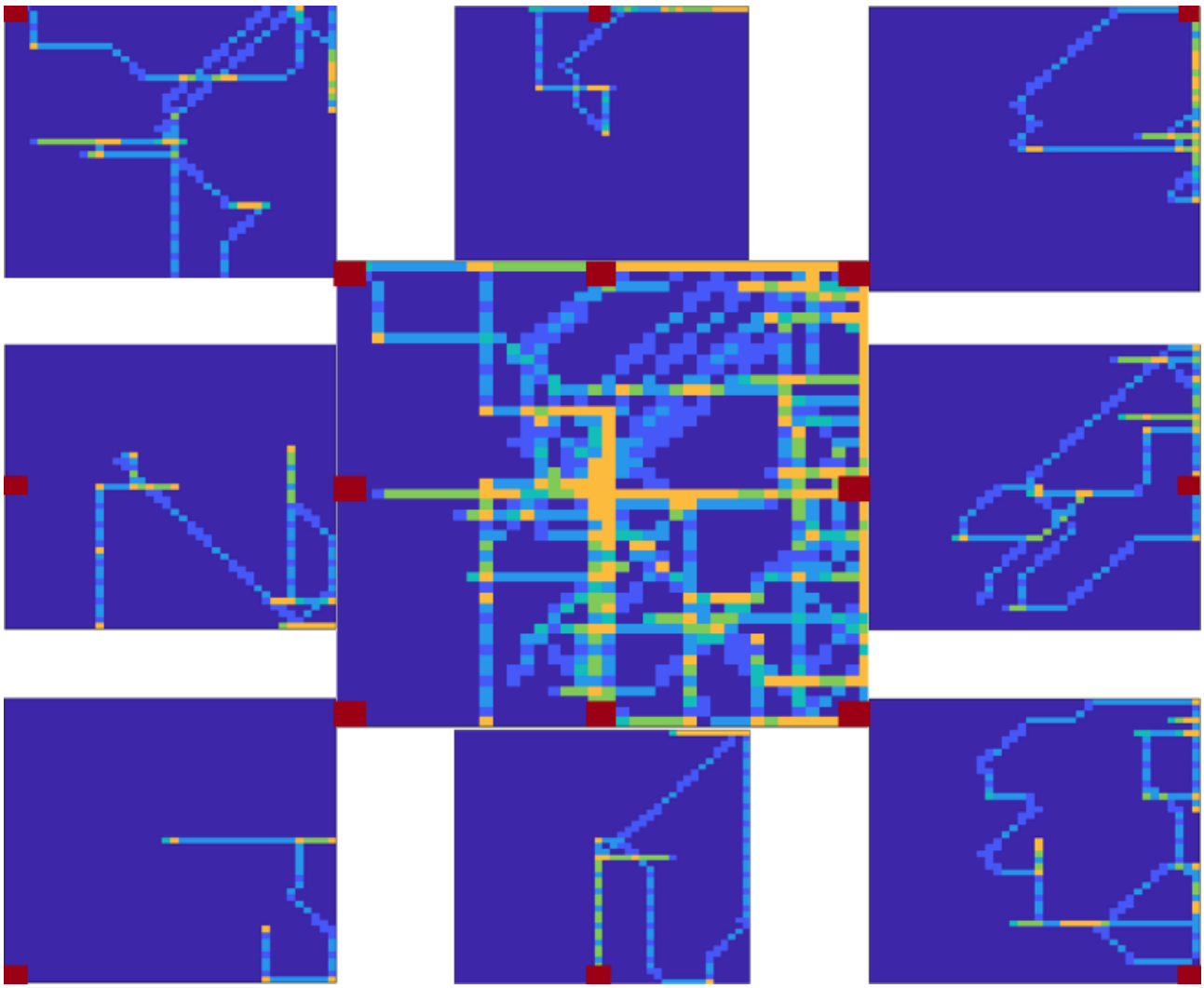

3.4 2D CONTROL WITH DIFFERENT MI TASKS

The only difference between the first and second setups are the MI tasks used to control the axis; in this last case, to control the horizontal movement the tasks Left Hand and Right Hand are used to move the cursor to the left and right, respectively; for the vertical movement, the tasks Both Feet and Rest handle the upward and downward movement respectively.

Due to time constraints, only five subjects (40% female) underwent the test of this setup, all of them having at least tries to control a BCI system once before.

Figure 15: Heat maps representing the coordinates of the cursor through the trials of subject s6. The central heat map highlights the trajectories taken during all the runs; the border heat maps represent each one the corresponding targets and the trajectories taken in the two trials related to it.

3.4.1 ACCURACY

Exception made for s3, which did not complete the second run, every other user showed a good constancy from run to run. Given the limited number of users, data should be taken accordingly, but from an initial analysis it can be seen that there is an increase in the mean accuracy of this BCI system setup, both considering only the best runs for each user, which increased to 60%, and the overall accuracy, which increased to 54.37% (Figure 16).

Focusing on the time necessary to reach each target, we have a significative increment in the users' performances, lowering the mean time to reach of almost every target below 10 seconds, that could not be achieved in the previous setup. A t-test has been conducted on the mean times of the two setups, resulting in a p-value of 7.9280e-04, stating that the two population are indeed different and that the second setup presents a better solution, time performances side. Even the best times for each target seem to be lowered, but not to a level to refuse the null hypothesis of the t-test; still, this last p-value is very close to the threshold, being equal to 0.0506.

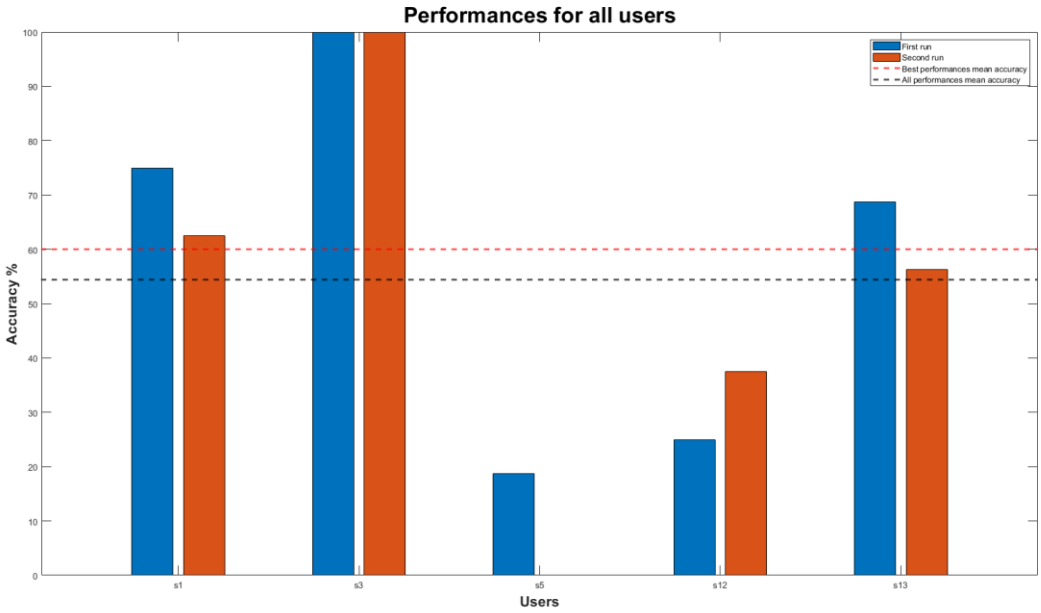

Figure 16: Bar plot of the accuracies reached in every run by the users. The red dashed line indicates the mean accuracy of the best runs for each user; black-dashed line states the mean accuracy overall.

Targets	Target 1	Target 2	Target 3	Target 4	Target 5	Target 6	Target 7	Target 8
Best Time	6.34	3.29	3.10	4.04	3.40	5.35	3.22	2.91
User	s3	s3	s3	s3	s3	s3	s3	s13

Table 9: Best performance achieved for each target. Notice that, unlike before, now S2 claimed almost every record, probably given the fact that the experience factor now acquires more relevance.

Mean time per Target	Target 1	Target 2	Target 3	Target 4	Target 5	Target 6	Target 7	Target 8
Time [s]	6,34	5,55	9,28	9,75	6,53	11,77	12,89	11,06

Table 10: Mean time among all users to reach each target. Unlike before, many targets can be reached in less than 10 seconds, condition that is not true with the previous setup.

Acuracy per target	S1		S3		S5		S12		S13		Mean (%)
	First run	Second run	First run	Second run	First run	Second run	First run	Second run	First run	Second run	
Target 1	100	100	100	100	0	~	0	0	50	50	55,55556
Target 2	100	0	100	100	0	~	50	0	100	0	50
Target 3	50	50	100	100	100	~	100	100	100	100	88,88889
Target 4	50	100	100	100	50	~	0	100	100	100	77,77778
Target 5	100	100	100	100	0	~	0	0	0	50	50
Target 6	0	50	100	100	0	~	0	0	50	50	38,88889
Target 7	100	100	100	100	0	~	0	100	100	50	72,22222
Target 8	100	0	100	100	0	~	50	0	50	50	50

Table 11: Accuracy for every target and user during the both the 2D online runs. Subject S3's second run is kept null since he/she did not execute it. With this setup, only one target seems to be difficult to achieve, Target 6 (middle-right), with a mean accuracy below 50%, while every other target has accuracy ≥ 50%.

Table 11 presents the accuracy of each target from run to run; having less data to work with, gained from users with previous experience with the BCI, results can lead to a bias, but still a clear improvement can be seen at the level of the mean accuracy for each target. Only target 6, the middle-right one, has a mean accuracy below 50%, being the only one that lowered its accuracy from the previous setup (46.875). A t-test has been conducted to verify if these two populations, the mean accuracy of each target in the previous and new setup, are different, resulting in a p-value of 0.0463, once again confirming that the second setup seems to be superior.

3.4.2 PREFERENTIAL PATTERNS

Similar to Figure 15**,** Figure 17 offers a clear vision of the position the cursor took during the best run of user S2, which scored 100% accuracy in both the 2D online runs. Aside from top-left quadrant, in the overall preferential patterns located at the center of the figure, there are more distinct and less chaotic patterns if compared to the heat maps of the previous setup. Even the single targets preferential patterns seem to point in a cleaner and less dispersive way to the respective goals, with less deviation from an ideal straight pattern.

The difference in path potential is made clearer if data from every user is taken to generate the heat maps, as shown in Figure 18. Here, in the first setup two paths prevaricate among all the possible ones, which are the down-left diagonal and the left path. All the right side of figure is darker, in the top-right quadrant there is a prevalence of diagonal movements, and the top-left quadrant still results quite dark. Note that among the most used paths there are the borders of the figure.

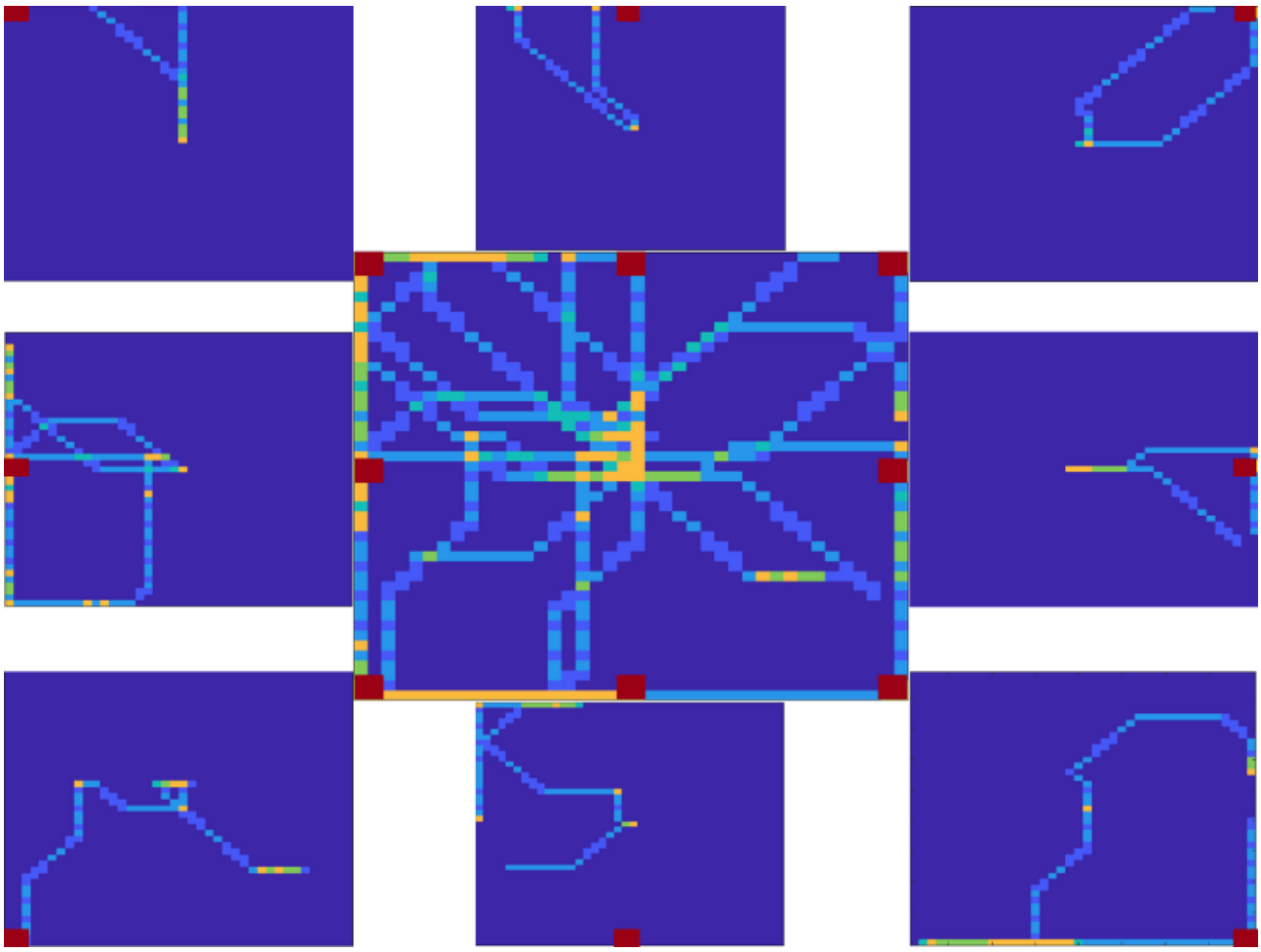

Figure 17: Heat maps representing the coordinates of the cursor through the trials of subject s3. The central heat map highlights the trajectories taken during all the runs; the border heat maps represent each one the corresponding targets and the trajectories taken in the two trials related to it.

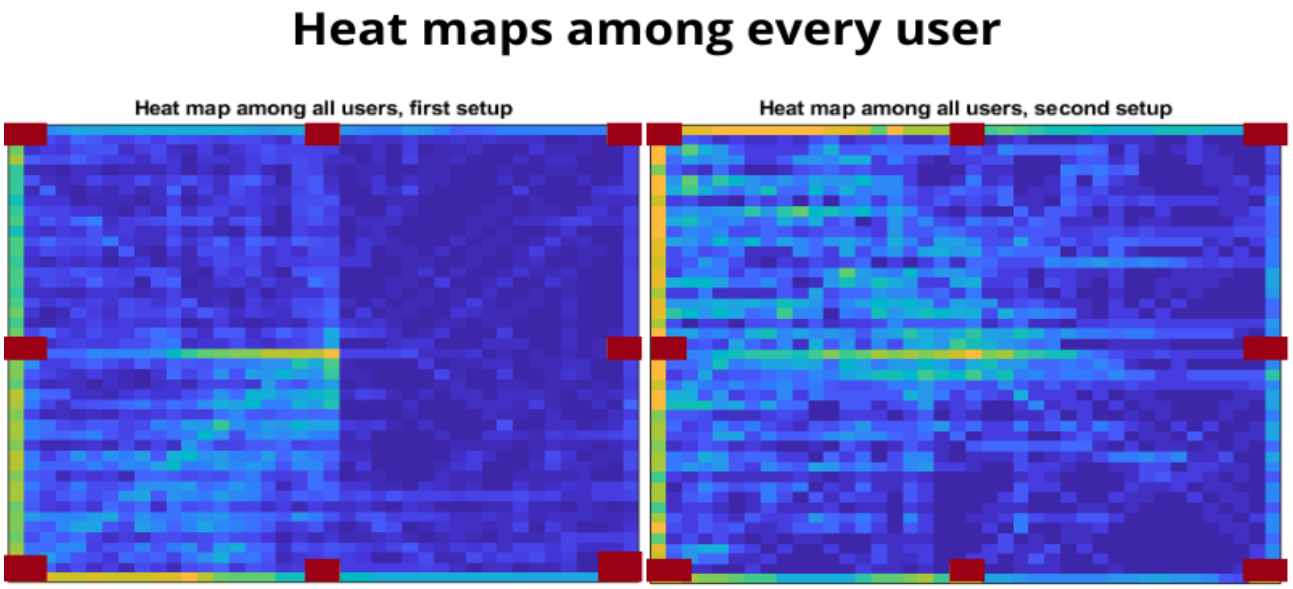

Figure 18: Heat maps among each user in both setups. Borders are very highlighted in both the figures, but it can be easily noted that in the second setup there seems to be more control of the cursor.

A different situation happens in the second setup, in which in every quadrant there are brighter colors, the right side is clearly more accessible and one of the hypothetically most difficult targets, the top-left one, seems to be, actually, the most visited.

CHAPTER 4: DISCUSSION

This thesis presented two possible setups for a multi class MI BCI for a hypothetical use of the systems in daily life operations. Most of the research is now more focused on finding the best possible methods for feature extraction and classification based on online available datasets [78][38][79][35], given the possibility, hardware wise, to support more complex Machine Learning or Deep Learning models. Although there exist some examples of BMI continuous control [80][66][81], they mainly focus on the pre-processing and classification steps or the feature extraction one. The control framework is kept relatively easy, which required participants to take a good amount of training to be able to control effectively the BCI system. This thesis proved that focusing more on the control approach to translate the BMI decoder output into a control signal, while maintaining simple and already tested pre-processing and feature extraction and classification phase, may produce good results with little time involvement, even on subjects that did not have any previous BCI experience; moreover, there are good hints that with a little longer training, many users would be able to complete the presented trials with little efforts.

4.1 EVALUATION OF 1D PERFORMANCE

One of the most important, critical aspects to determine before starting the experiment was the choice of which MI tasks to use to control the two axes singularly, especially on the vertical one. In literature there are papers which focus on using only two tasks to perform a great variety of commands, simply using a diagram control protocol [82], which represents a very simple and practical approach for easy tasks with not restricted time-constraints; in this scenario, the MI Both Hands and Both Feet are two easy to perform and distinguishable tasks which require little training time to be performed very well. Left Hand and Right Hand, however, are more difficult to master, probably due to the fact that, as can be seen in the topomaps of Figure 3, there is a clearer ERD/ERS over the dominant hand's region instead of the non-dominant one, but the diversity between these two regions may not differ much. This situation remains in the ERD/ERS of Both Hands, even if hidden by other factors, but since the focus is to distinguish between hands and feet and not between hands, it poses no problem. See Appendix for graphical reference.

A similar situation appears while controlling the Y axis, in which the features related to the imagination of Both Hands tend to be the most discriminative, relegating the Both Feet class as a more supportive than a determinant one. Still, this does not prove to be a problem when controlling only the Y axis, as Table 5 shows.

As a skill that needs to be trained [6], the more a user experience the BCI, the better he/she is able to control it. If the correct parameters are set, theoretically the user will be able to maneuver the system, resulting in the BCI correctly assigning the user's intentions to the right command for the external device. More skilled users imply the reinforcement of the neuronal connections that create the mental state the decoder is able to identify, resulting in higher probability for the decoder to assign the right class. Higher probability translates to a state vector, for each axis, that tends to the values of 0 or 1, depending on the user's intention, and the time necessary to reach the
thresholds will be much shorter; finally, achieving the maximum velocity in a lesser period of time shortens the time required to reach a target.

From the aforementioned hypothesis, we should expect that at first there will be successful trials that take long time to be completed, because the user needs to interiorize the sensation of controlling the cursor, but, the more the time passes, the more the user gets able to recall the MI task sensations, the lesser the time to reach significative velocity and the lesser the time to reach a target will be. It does not surprise, in the end, that the majority of the trials passed have been cleared within 6 seconds, after which the number of trials cleared in more seconds drops drastically, as seen in Figure 18.

Another powerful instrument investigated a posteriori as a good marker to discern if a user would result in good accuracy or not, or at least if there were some problems that needed more attention like a new decoder, is the plot of all the values of the state vector during the trials, as shown in Figure 10 : as can be seen in Appendix, users that showed good results tend to have more independent, non-overlapping ellipses, with centers far away from each other, while users that still managed to pass to the 2D trials but had more overlapping ellipses ended in worse accuracies.

Even though the lack of time to properly gather online 1D data on the second setup, given the fact that the chosen users already had experience with the BCI and although the classification of Left Hand and Right Hand proved to be harder, we could expect a similar histogram as shown in Figure 19 as a result, with many targets reached below a certain time-limit, maybe a little more than 6 seconds for the task is more difficult to perform.

From the fatigue point of view, almost every user reported that fatigue and exhaustion when only two MI tasks were involved derived mainly from the misclassification of the decoder rather than performing the task, because this situation resulted in longer trials in which users needed to significantly focus more on the tasks, generally implying little face muscles activation or the induction of tension in different region of the body. Other than that, if a user resulted in good ability to operate the BCI, the control of the cursor in one dimension was reported as interesting and relatively easy.

Each user was instructed to perform hands or feet movement imagination as closing and opening the fists for hands and elevating and lowering the toes for feet, and many first time BCI experience users followed this lead; other, however, reported that associated different tasks imagination, always

connected to the MI tasks that should be performed, like squeezing a ball or sinking the feet into sands, which they reported as more natural and easier to imagine movements and sensations. The imagination of different movements proved to be effective in the second setup, where users were instructed to imagine opening and closing one hand and rotating the other.

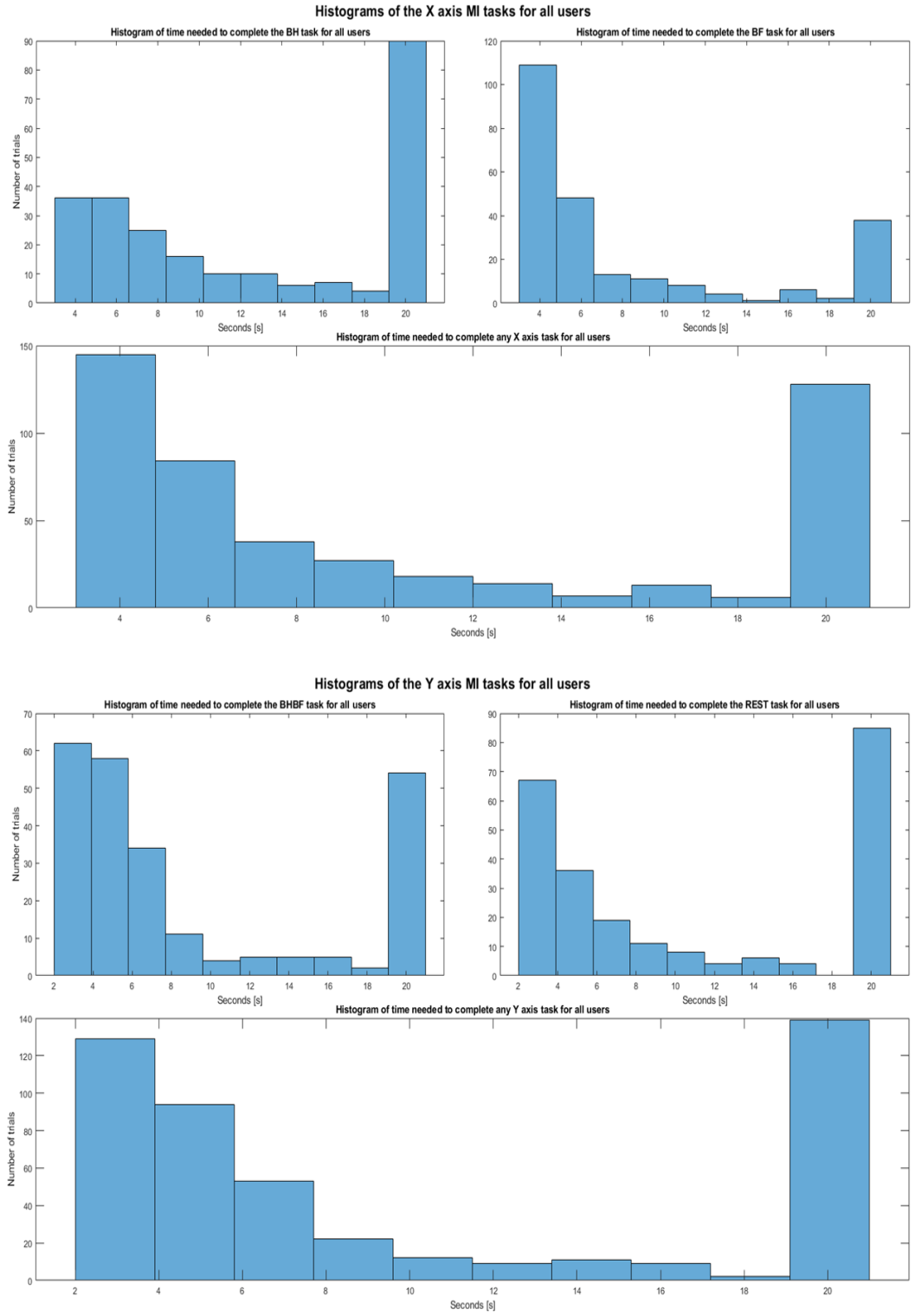

Figure 19: Histograms of time needed to complete every X or Y task for all users.

4.2 EVALUATION OF 2D PERFORMANCE

Focusing in finding a way to control an external device in real time, like a robotic prosthesis or a virtual avatar that have to mimic a variety of commands similar to the ones the user would perform in real life, the multi class approach appears more natural, especially if those tasks represent familiar movements. This naturalness is the key point of the second BCI setup, in which, depending on what objective has to be achieved, the control over the Y axis can easily be seen as a move forward with the feet and move backward or stay still while resting. Indeed, the move forward movement using the imagination of the feet can be normally linked to walking or accelerating while driving, two very common commands that even users with motor disabilities at least relate to in real life, just by observing. Moreover, the tasks chosen over the X axis, while more difficult to master as shown in Figure 8, are more independent from the tasks over Y, highly reducing the possibility to accidentally activate an unwanted command on the wrong axis. This factor can be easily seen in Figure 17 and Figure 15, the first one showing straighter, less chaotic and cleaner paths that focuses mainly on vertical or horizontal movements instead of diagonal ones, hinting a finer control and the possibility to avoid overlapping features that derived in diagonal, unwanted movements.

On the other hand, the first setup has been created keeping into account that more common and easier to perform tasks should be performed, helping a potential user with no experience with the BCI in seeing good results from the beginning and with little training. Unfortunately, this setup proved to be easy to implement, but hard to master in little time, the main obstacle being having non-independent tasks over the two axis and requiring a non-trivial mental effort to maintain the concentration during the online trials. This proved to be a crucial point, and here training is probably the main factor in order to achieve feasibility: almost every user showed little to high overlap between features for the X and the Y axis, resulting in having to be able to rapidly learn to modulate their brain activation patterns to obtain less unwanted diagonal movements in the 2D trials. This movements are generally caused by the presence or absence Both Hands class, which proved to be the most discriminative aspect of vertical navigation, since trying to move upwards only using the feet resulted in failure and having, instead, a bottom-left drift as a result. With the use of just Both Hands, the cursor did indeed tend to move right, but even upwards, resulting in a most unwanted diagonal drift that made very difficult to achieve targets not placed at the extremes of the monitor.

Figure 20 offers a more common situation in the first setup: many diagonal paths often leading to different directions instead of the target position, opening to the necessity to adjust the concentration of the task, leading to longer and more tiring trials. As Table 6 highlight, the a priori knowledge about this setup proved to be right, having target 1 and 4 as two of the most difficult to reach, with targets

5 and 8 making their appearance. Once again, these last two targets could be expected to be difficult: since a fine control could not be taken for granted, users generally resorted to different strategies to reach affordable targets like number 6 and 7, like reaching the right border of the screen and then trying to adjust only the vertical coordinate for target 7 or inducing a diagonal movement down-right for target 6. This was possible since for these two movements the use of Both Hands is not required, which rose the likelihood to go downwards and downleft; being on the left upper side, targets 6 and 7 needed the use of Both Hands to maintain or gain the Y coordinate, which instead rose the likelihood of a right oriented movement. Surprisingly enough, 5 out of 8 users managed to reach an accuracy of 50% or higher in the first setup. This outcome is good for many reason: first of all, 3 of these 5 users, all female, were at their first experience with the BCI; secondly, having to work with four classes and keeping into account that just following with the eyes the cursor movements is one of many factors of distraction, expectancy of reaching good accuracies was low; lastly, given the little time at their disposal, these users managed to modulate their brain patterns activation in order to reach a finer control of the cursor. Unfortunately, the lack of penalties if the cursor reaching a wrong target does not let us assess the feasibility of this BCI setup, and this factor can once again be seen in the various heat maps showing many trajectories on the borders of the screen that passed through unwanted targets before arriving at their true destination.

A more promising situation is offered by the second setup, in which not only there is an increment of the mean accuracy among the users, but also the reduction of the mean time needed to reach a target. The cursor velocity has been kept equal in both the setup, so it is of no surprise that the minimum time for each target tends to remain similar. On this regard, while in the first setup there is not a single user that achieved almost every minimum time for each target, in the second the situation is inverted, with user S3 scoring the best time almost everywhere. This may be due to two factors: first, he/she was the most experienced user with both the BCI setups; second, the classification of Left Hand and Right Hand is more difficult than the classification of Both Hand and Both Feet, so experience in this case seems to have a greater impact on the performance. This translates, obviously, into the conclusion that the first BCI setup can be seen as more new-user friendly, but more time consuming to master, whilst the second one requires at least a little bit of experience to potentially produce far better results. This hypothesis seems to be supported by users S1 and S13 furthermore, the first one increasing his/her performance from 56 to 75%, the latter being an experienced BCI user which tested this setup for the first time and being able to reach 68% accuracy on the first attempt. User S5, on the other hand, got significantly worse, from 50% to 18%, mainly because of the inability to create a good decoder for the Y axis.

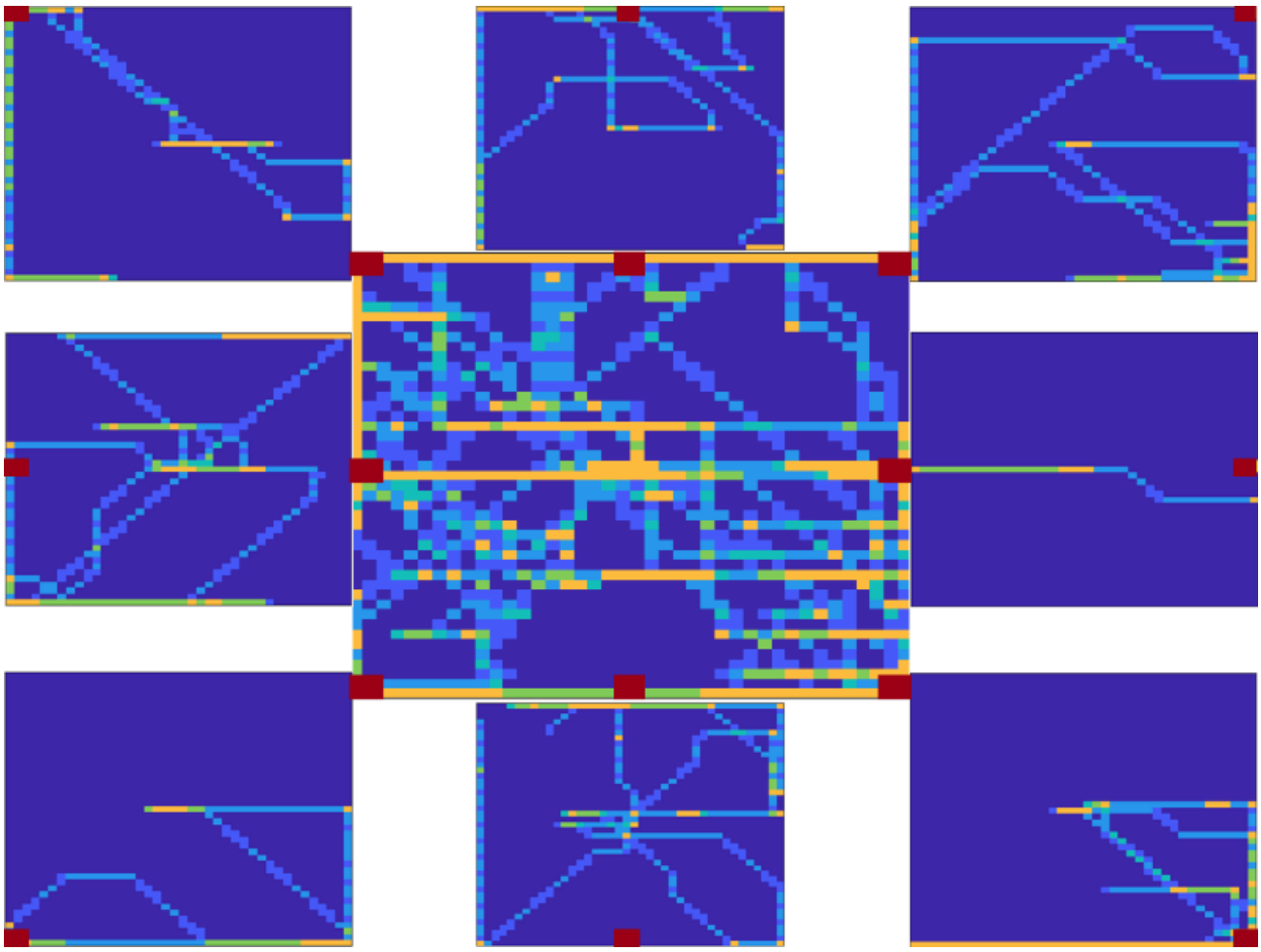

Figure 20: Heat maps of user s7. Overall paths taken can be seen in the central figure, while trajectories undertaken during each target's trials can be seen on the border figures. As the overall paths figure shows, there are too many positions that the cursor placed itself into, hinting that its control user side is not as fine as hoped.

Independently from which setup used, almost every user reported that in 2D the mental load required to complete the entire run can be labeled as exhausting, comparing this sensation to a full dive, all day long study session similar to what studying for an exam could represent. The only exception to this is represented by users S3, partly, and S6, both of them being able to score very good results and being able to add a joyful component through the various trials, hinting that enjoyment and engagement could lead to better results, as stated by Prahm et al [83]. This conclusion may seem obvious since the ability to accurately control the system results in lesser time needed for each run, greatly diminishing the mental challenge and avoiding frustration consequent to the decoder misclassification; however, entertainment and enjoyment can lighten the weight that frustration and vexation have on mental exhaustion. Still, almost every user showed good constancy with the 2D control, stating that the fatigue phenomenon does not influence heavily the outcome.

Lastly, while it may sound obvious that if a user shows good features, he/she should result in good control, this is not granted, since other factors heavily influence the outcome, like environment change and distraction deriving from the circle's movements. Many users reported that seeing the emulated

cursor moving to the opposite intended direction or even approaching the correct target may trigger different mental states that interfere and hide the right features read by the decoder, creating a hindrance and a sense of frustration in loop.

4.3 FUTURE WORK

Considering that the control framework can be viewed as very basic and needed the presence of an operator to set the various thresholds, future works may reside in improving both of these aspects. Human intervention should be kept at minimum in order to possibly reduce any source of variability in the performance; as possible solution to this, heat maps and histograms of state vectors offer two powerful instruments to adjust parameters and predict the output of the various tasks with the optimal thresholds. Moreover, manual setting of the parameters is a time-consuming activity, both when the operator has to adjust them and when the user needs to try them in a mock run; while offering to the user a little time to rest while the parameters are being set up, the possibility of having to do many mock trials may greatly influence user's concentration and fatigue.

From the control point of view, a simple scaling velocity of the cursor showed positive impact on the results of the experiment, being not a very good brake whenever the intended MI task was performed incorrectly, but a good feedback in the opposite case: indeed, if the user was not very good in performing one task, the possibility of slowly moving toward the intended direction was a good indicator of what to think and to stay concentrated to in order to move in the right direction.

Still, advanced option of controls could be introduced, like a slow speed in the initial phase with a constant acceleration if the task is maintained for a defined period of time, or using many simple, binary models in a one-vs-rest or one-vs-one Machine Learning approach to more accurately classify the various MI classes [36][35][66]. A more complex velocity control was investigated in the beginning, using two repulsors or two repulsors and one attractor with different influences depending on the probability vector given by the decoder, that showed potential on mock data. The implementation of this system is, however, at its beginning.

BIBLIOGRAPHY

[1] J. R. Wolpaw, “Brain-computer interfaces,” in *Handbook of Clinical Neurology*, Elsevier B.V., 2013, pp. 67–74. doi: 10.1016/B978-0-444-52901-5.00006-X.

[2] J. R. Wolpaw, N. Birbaumer, D. J. Mcfarland, G. Pfurtscheller, and T. M. Vaughan, “Brain-computer interfaces for communication and control,” 2002. [Online]. Available: www.elsevier.com/locate/clinphCLINPH2001764

[3] L. Tonin, T. Carlson, R. Leeb, and J. Del R. Millan, “Brain-controlled telepresence robot by motor-disabled people,” *Proc. Annu. Int. Conf. IEEE Eng. Med. Biol. Soc. EMBS*, pp. 4227–4230, 2011, doi: 10.1109/IEMBS.2011.6091049.

[4] P. G., G. C., M. G., K. G., and N. C., “Brain oscillations control hand orthosis in a tetraplegic.,” *Neurosci. Lett.*, vol. 292, no. 3, pp. 211–214, 2000.

[5] E. A. Curran and M. J. Stokes, “Learning to control brain activity: A review of the production and control of EEG components for driving brain-computer interface (BCI) systems,” *Brain and Cognition*, vol. 51, no. 3. Academic Press Inc., pp. 326–336, 2003. doi: 10.1016/S0278-2626(03)00036-8.

[6] D. J. McFarland and J. R. Wolpaw, “Brain–computer interface use is a skill that user and system acquire together,” *PLoS Biol.*, vol. 16, no. 7, pp. 10–13, 2018, doi: 10.1371/journal.pbio.2006719.

[7] “Brain Computer Interface (BCI) System Overview & Applications,” *May 27*, 2023. https://how2electronics.com/brain-computer-interface-system-overview-applications/

[8] A. Kawala-Sterniuk *et al.*, “Summary of over fifty years with brain-computer interfaces—a review,” *Brain Sci.*, vol. 11, no. 1, pp. 1–41, 2021, doi: 10.3390/brainsci11010043.

[9] E. E. Fetz, “Chapter 12 - Restoring motor function with bidirectional neural interfaces,” in *Sensorimotor Rehabilitation*, N. Dancause, S. Nadeau, and S. B. T.-P. in B. R. Rossignol, Eds., Elsevier, 2015, pp. 241–252. doi: https://doi.org/10.1016/bs.pbr.2015.01.001.

[10] N. Robinson, R. Mane, T. Chouhan, and C. Guan, “Emerging trends in BCI-robotics for motor control and rehabilitation,” *Current Opinion in Biomedical Engineering*, vol. 20. Elsevier B.V., Dec. 01, 2021. doi: 10.1016/j.cobme.2021.100354.

[11] R. Leeb *et al.*, “Transferring brain-computer interfaces beyond the laboratory: Successful application control for motor-disabled users,” *Artif. Intell. Med.*, vol. 59, no. 2, pp. 121–132, 2013, doi: 10.1016/j.artmed.2013.08.004.

[12] C. Neuper, G. R. Müller, A. Kübler, N. Birbaumer, and G. Pfurtscheller, “Clinical

application of an EEG-based brain-computer interface: A case study in a patient with severe motor impairment," *Clin. Neurophysiol.*, vol. 114, no. 3, pp. 399–409, 2003, doi: 10.1016/S1388-2457(02)00387-5.

[13] E. C. Lee, J. C. Woo, J. H. Kim, M. Whang, and K. R. Park, "A brain-computer interface method combined with eye tracking for 3D interaction," *J. Neurosci. Methods*, vol. 190, no. 2, pp. 289–298, 2010, doi: 10.1016/j.jneumeth.2010.05.008.

[14] A. Colucci *et al.*, "Brain–Computer Interface-Controlled Exoskeletons in Clinical Neurorehabilitation: Ready or Not?," *Neurorehabil. Neural Repair*, vol. 36, no. 12, pp. 747–756, 2022, doi: 10.1177/15459683221138751.

[15] U. Hoffmann, J. M. Vesin, T. Ebrahimi, and K. Diserens, "An efficient P300-based brain-computer interface for disabled subjects," *J. Neurosci. Methods*, vol. 167, no. 1, pp. 115–125, 2008, doi: 10.1016/j.jneumeth.2007.03.005.

[16] F. Nijboer *et al.*, "A P300-based brain-computer interface for people with amyotrophic lateral sclerosis," *Clin. Neurophysiol.*, vol. 119, no. 8, pp. 1909–1916, 2008, doi: 10.1016/j.clinph.2008.03.034.

[17] D. Steyrl, R. J. Kobler, and G. R. Müller-Putz, "On Similarities and Differences of Invasive and Non-Invasive Electrical Brain Signals in Brain-Computer Interfacing," *J. Biomed. Sci. Eng.*, vol. 09, no. 08, pp. 393–398, 2016, doi: 10.4236/jbise.2016.98034.

[18] B. Citation Venkata Phanikrishna, P. J. Pławiak, and A. Prakash, "A Brief Review on EEG Signal Pre-processing Techniques for Real-Time Brain-Computer Interface Applications," pp. 0–16, 2021, doi: 10.36227/techrxiv.16691605.v1.

[19] L. F. Nicolas-Alonso and J. Gomez-Gil, "Brain computer interfaces, a review," *Sensors*, vol. 12, no. 2, pp. 1211–1279, 2012, doi: 10.3390/s120201211.

[20] A. A. Nooh, J. Yunus, and S. Mohd Daud, *A Review of Asynchronous Electroencephalogram-based Brain Computer Interface Systems*. 2011.

[21] Y. Li *et al.*, "Gesture Decoding Using ECoG Signals from Human Sensorimotor Cortex: A Pilot Study," *Behav. Neurol.*, vol. 2017, 2017, doi: 10.1155/2017/3435686.

[22] B. Graimann, G. Townsend, J. E. Huggins, S. P. Levine, and G. Pfurtscheller, "A Comparison between using ECoG and EEG for direct brain communication," *IFMBE Proc. EMBEC05 3rd Eur. Med. Biol. Eng. Conf.*, no. September 2017, 2005, [Online]. Available: https://www.researchgate.net/publication/307135204

[23] H. Banville and T. H. Falk, "Recent advances and open challenges in hybrid brain-computer interfacing: a technological review of non-invasive human research," *Brain-Computer Interfaces*, vol. 3, no. 1, pp. 9–46, Jan. 2016, doi: 10.1080/2326263X.2015.1134958.

[24] M. Keerthi Kumar, B. D. Parameshachari, S. Prabu, and S. L. Ullo, "Comparative Analysis

to Identify Efficient Technique for Interfacing BCI System," *IOP Conf. Ser. Mater. Sci. Eng.*, vol. 925, no. 1, 2020, doi: 10.1088/1757-899X/925/1/012062.

[25] Z. Jamil, A. Jamil, and M. Majid, "Artifact removal from EEG signals recorded in non-restricted environment," *Biocybern. Biomed. Eng.*, vol. 41, no. 2, pp. 503–515, 2021, doi: https://doi.org/10.1016/j.bbe.2021.03.009.

[26] H. Yadav and S. Maini, "Electroencephalogram based brain-computer interface: Applications, challenges, and opportunities," *Multimed. Tools Appl.*, 2023, doi: 10.1007/s11042-023-15653-x.

[27] D. J. McFarland, "The advantages of the surface Laplacian in brain-computer interface research," *Int. J. Psychophysiol.*, vol. 97, no. 3, pp. 271–276, 2015, doi: 10.1016/j.ijpsycho.2014.07.009.

[28] B. Blankertz, R. Tomioka, S. Lemm, M. Kawanabe, and K. Muller, "Optimizing Spatial filters for Robust EEG Single-Trial Analysis," *IEEE Signal Process. Mag.*, vol. 25, no. 1, pp. 41–56, 2008, doi: 10.1109/MSP.2008.4408441.

[29] D. J. McFarland, L. M. McCane, S. V. David, and J. R. Wolpaw, "Spatial filter selection for EEG-based communication," *Electroencephalogr. Clin. Neurophysiol.*, vol. 103, no. 3, pp. 386–394, 1997, doi: 10.1016/S0013-4694(97)00022-2.

[30] undefined Pooja, S. K. Pahuja, and K. Veer, "Recent Approaches on Classification and Feature Extraction of EEG Signal: A Review," *Robotica*, vol. 40, no. 1, pp. 77–101, 2022, doi: DOI: 10.1017/S0263574721000382.

[31] P. Boonyakitanont, A. Lek-uthai, K. Chomtho, and J. Songsiri, "A review of feature extraction and performance evaluation in epileptic seizure detection using EEG," *Biomed. Signal Process. Control*, vol. 57, pp. 1–28, 2020, doi: 10.1016/j.bspc.2019.101702.

[32] A. E. Hramov, V. A. Maksimenko, and A. N. Pisarchik, "Physical principles of brain–computer interfaces and their applications for rehabilitation, robotics and control of human brain states," *Physics Reports*, vol. 918. Elsevier B.V., pp. 1–133, Jun. 25, 2021. doi: 10.1016/j.physrep.2021.03.002.

[33] A. Subasi and M. I. Gursoy, "EEG signal classification using PCA, ICA, LDA and support vector machines," *Expert Syst. Appl.*, vol. 37, no. 12, pp. 8659–8666, 2010, doi: 10.1016/j.eswa.2010.06.065.

[34] R. Zhang, Q. Zong, L. Dou, and X. Zhao, "A novel hybrid deep learning scheme for four-class motor imagery classification," *J. Neural Eng.*, vol. 16, no. 6, p. 66004, 2019, doi: 10.1088/1741-2552/ab3471.

[35] E. B. Sadeghian and M. H. Moradi, "Continuous detection of motor imagery in a four-class asynchronous BCI," *Annu. Int. Conf. IEEE Eng. Med. Biol. - Proc.*, pp. 3241–3244, 2007,

doi: 10.1109/IEMBS.2007.4353020.

[36] G. Liu, L. Tian, and W. Zhou, “Multiscale time-frequency method for multiclass Motor Imagery Brain Computer Interface,” *Comput. Biol. Med.*, vol. 143, no. February, p. 105299, 2022, doi: 10.1016/j.compbiomed.2022.105299.

[37] H. Altaheri *et al.*, *Deep learning techniques for classification of electroencephalogram (EEG) motor imagery (MI) signals: a review*, vol. 35, no. 20. Springer London, 2023. doi: 10.1007/s00521-021-06352-5.

[38] J. Xu, H. Zheng, J. Wang, D. Li, and X. Fang, “Recognition of eeg signal motor imagery intention based on deep multi-view feature learning,” *Sensors (Switzerland)*, vol. 20, no. 12, pp. 1–16, 2020, doi: 10.3390/s20123496.

[39] N. Robinson, R. Mane, T. Chouhan, and C. Guan, “Emerging trends in BCI-robotics for motor control and rehabilitation,” *Curr. Opin. Biomed. Eng.*, vol. 20, p. 100354, 2021, doi: 10.1016/j.cobme.2021.100354.

[40] C. P. Sensorimotor and R. Can, “Finger Extension after Stroke,” vol. 15, no. 5, pp. 1–30, 2019, doi: 10.1088/1741-2552/aad724.Controlling.

[41] Z. Bai, K. N. K. Fong, J. J. Zhang, J. Chan, and K. H. Ting, “Immediate and long-term effects of BCI-based rehabilitation of the upper extremity after stroke: A systematic review and meta-analysis,” *J. Neuroeng. Rehabil.*, vol. 17, no. 1, pp. 1–20, 2020, doi: 10.1186/s12984-020-00686-2.

[42] M. A. Cervera *et al.*, “Brain-computer interfaces for post-stroke motor rehabilitation: a meta-analysis,” *Ann. Clin. Transl. Neurol.*, vol. 5, no. 5, pp. 651–663, 2018, doi: 10.1002/acn3.544.

[43] L. Carelli *et al.*, “Brain-Computer Interface for Clinical Purposes: Cognitive Assessment and Rehabilitation,” *Biomed Res. Int.*, vol. 2017, 2017, doi: 10.1155/2017/1695290.

[44] D. Wen *et al.*, “Combining brain–computer interface and virtual reality for rehabilitation in neurological diseases: A narrative review,” *Ann. Phys. Rehabil. Med.*, vol. 64, no. 1, p. 101404, 2021, doi: 10.1016/j.rehab.2020.03.015.

[45] B. Chambayil, R. Singla, and R. Jha, “Virtual keyboard BCI using Eye blinks in EEG,” *2010 IEEE 6th Int. Conf. Wirel. Mob. Comput. Netw. Commun. WiMob’2010*, pp. 466–470, 2010, doi: 10.1109/WIMOB.2010.5645025.

[46] N. Shi *et al.*, “Steady-state visual evoked potential (SSVEP)-based brain–computer interface (BCI) of Chinese speller for a patient with amyotrophic lateral sclerosis: A case report,” *J. Neurorestoratology*, vol. 8, no. 1, pp. 40–52, 2020, doi: 10.26599/jnr.2020.9040003.

[47] P. Cipresso *et al.*, “The combined use of Brain Computer Interface and Eye-Tracking technology for cognitive assessment in Amyotrophic Lateral Sclerosis,” *2011 5th Int. Conf.*

Pervasive Comput. Technol. Healthc. Work. PervasiveHealth 2011, pp. 320–324, 2011, doi: 10.4108/icst.pervasivehealth.2011.246018.

[48] S. B. Borgheai *et al.*, "Enhancing Communication for People in Late-Stage ALS Using an fNIRS-Based BCI System," *IEEE Trans. Neural Syst. Rehabil. Eng.*, vol. 28, no. 5, pp. 1198–1207, 2020, doi: 10.1109/TNSRE.2020.2980772.

[49] R. Leeb, D. Friedman, G. R. Müller-Putz, R. Scherer, M. Slater, and G. Pfurtscheller, "Self-paced (asynchronous) BCI control of a wheelchair in virtual environments: A case study with a tetraplegic," *Comput. Intell. Neurosci.*, vol. 2007, 2007, doi: 10.1155/2007/79642.

[50] J. Tang, Y. Liu, D. Hu, and Z. T. Zhou, "Towards BCI-actuated smart wheelchair system," *Biomed. Eng. Online*, vol. 17, no. 1, pp. 1–22, 2018, doi: 10.1186/s12938-018-0545-x.

[51] C. Vidaurre, C. Klauer, T. Schauer, A. Ramos-Murguialday, and K. R. Müller, "EEG-based BCI for the linear control of an upper-limb neuroprosthesis," *Med. Eng. Phys.*, vol. 38, no. 11, pp. 1195–1204, 2016, doi: 10.1016/j.medengphy.2016.06.010.

[52] T. I. Voznenko, G. A. Urvanov, A. A. Dyumin, S. V. Andrianova, and E. V. Chepin, "The Research of Emotional State Influence on Quality of a Brain-Computer Interface Usage," *Procedia Comput. Sci.*, vol. 88, pp. 391–396, 2016, doi: 10.1016/j.procs.2016.07.454.

[53] A. Y. Kaplan, S. L. Shishkin, I. P. Ganin, I. A. Basyul, and A. Y. Zhigalov, "Adapting the P300-based brain-computer interface for gaming: A review," *IEEE Trans. Comput. Intell. AI Games*, vol. 5, no. 2, pp. 141–149, 2013, doi: 10.1109/TCIAIG.2012.2237517.

[54] A. Nijholt, *BCI for games: A "state of the art" survey*, vol. 5309. 2008. doi: 10.1007/978-3-540-89222-9_29.

[55] A. Singh, A. A. Hussain, S. Lal, and H. W. Guesgen, "A comprehensive review on critical issues and possible solutions of motor imagery based electroencephalography brain-computer interface," *Sensors*, vol. 21, no. 6, pp. 1–35, 2021, doi: 10.3390/s21062173.

[56] P. Wierzgała, D. Zapała, G. M. Wojcik, and J. Masiak, "Most popular signal processing methods in motor-imagery BCI: A review and meta-analysis," *Front. Neuroinform.*, vol. 12, no. November, pp. 1–10, 2018, doi: 10.3389/fninf.2018.00078.

[57] C. Guger *et al.*, "How many people could use an SSVEP BCI?," *Front. Neurosci.*, no. NOV, 2012, doi: 10.3389/fnins.2012.00169.

[58] Z. Tang, H. Yu, C. Lu, and P. Liu, "Single-trial classification of different movements on one hand based on ERD/ERS and corticomuscular coherence," *IEEE Access*, vol. PP, Aug. 2019, doi: 10.1109/ACCESS.2019.2940034.

[59] D. H. Kim, D. H. Shin, and T. E. Kam, "Bridging the BCI illiteracy gap: a subject-to-subject semantic style transfer for EEG-based motor imagery classification," *Front. Hum. Neurosci.*, vol. 17, no. Mi, 2023, doi: 10.3389/fnhum.2023.1194751.

[60] B. Z. Allison and C. Neuper, “Could Anyone Use a BCI?,” 2010, pp. 35–54. doi: 10.1007/978-1-84996-272-8_3.

[61] M. H. Lee *et al.*, “EEG dataset and OpenBMI toolbox for three BCI paradigms: An investigation into BCI illiteracy,” *Gigascience*, vol. 8, no. 5, pp. 1–16, 2019, doi: 10.1093/gigascience/giz002.

[62] S. Perdikis, L. Tonin, S. Saeedi, C. Schneider, and J. del R. Millán, “The Cybathlon BCI race: Successful longitudinal mutual learning with two tetraplegic users,” *PLoS Biol.*, vol. 16, no. 5, pp. 1–28, 2018, doi: 10.1371/journal.pbio.2003787.

[63] M. C. Thompson, “Critiquing the Concept of BCI Illiteracy,” *Sci. Eng. Ethics*, vol. 25, no. 4, pp. 1217–1233, 2019, doi: 10.1007/s11948-018-0061-1.

[64] S. C. Kleih and A. Kubler, “Psychological Factors Influencing Brain-Computer Interface (BCI) Performance,” *Proc. - 2015 IEEE Int. Conf. Syst. Man, Cybern. SMC 2015*, pp. 3192–3196, 2016, doi: 10.1109/SMC.2015.554.

[65] S. Park, J. Ha, D. H. Kim, and L. Kim, “Improving Motor Imagery-Based Brain-Computer Interface Performance Based on Sensory Stimulation Training: An Approach Focused on Poorly Performing Users,” *Front. Neurosci.*, vol. 15, no. November, pp. 1–12, 2021, doi: 10.3389/fnins.2021.732545.

[66] H. S. An, J. W. Kim, and S. W. Lee, “Design of an asynchronous brain-computer interface for control of a virtual Avatar,” *4th Int. Winter Conf. Brain-Computer Interface, BCI 2016*, pp. 1–2, 2016, doi: 10.1109/IWW-BCI.2016.7457463.

[67] D. Coyle, J. Stow, K. McCreadie, J. McElligott, and Á. Carroll, “Sensorimotor modulation assessment and brain-computer interface training in disorders of consciousness,” *Arch. Phys. Med. Rehabil.*, vol. 96, no. 3, pp. S62–S70, 2015, doi: 10.1016/j.apmr.2014.08.024.

[68] J. N. Mak and J. R. Wolpaw, “Clinical Applications of Brain—Computer Interfaces: Current State and Future Prospects,” *IEEE Rev. Biomed. Eng.*, vol. 2, pp. 187–199, 2009, doi: 10.1109/RBME.2009.2035356.

[69] L. Tonin, G. Beraldo, S. Tortora, and E. Menegatti, “ROS-Neuro: An Open-Source Platform for Neurorobotics,” *Front. Neurorobot.*, vol. 16, no. May, pp. 1–7, 2022, doi: 10.3389/fnbot.2022.886050.

[70] L. Tonin, G. Beraldo, S. Tortora, L. Tagliapietra, J. D. R. Millan, and E. Menegatti, “ROS-neuro: A common middleware for BMI and robotics. the acquisition and recorder packages,” *Conf. Proc. - IEEE Int. Conf. Syst. Man Cybern.*, vol. 2019-October, no. October, pp. 2767–2772, 2019, doi: 10.1109/SMC.2019.8914364.

[71] G. Beraldo, S. Tortora, E. Menegatti, and L. Tonin, “ROS-Neuro: Implementation of a closed-loop BMI based on motor imagery,” *Conf. Proc. - IEEE Int. Conf. Syst. Man Cybern.*,

vol. 2020-October, pp. 2031–2037, 2020, doi: 10.1109/SMC42975.2020.9282968.

[72] W. Yi *et al.*, "Evaluation of EEG Oscillatory Patterns and Cognitive Process during Simple and Compound Limb Motor Imagery," *PLoS One*, vol. 9, no. 12, p. e114853, Dec. 2014, [Online]. Available: https://doi.org/10.1371/journal.pone.0114853

[73] G. Huang *et al.*, "Discrepancy between inter- and intra-subject variability in EEG-based motor imagery brain-computer interface: Evidence from multiple perspectives," *Front. Neurosci.*, vol. 17, no. February, pp. 1–11, 2023, doi: 10.3389/fnins.2023.1122661.

[74] Y. Zhang and Y. Wang, "Research on Feature Extraction Algorithm Commonly Used in Brain-computer Interface Technology," *J. Phys. Conf. Ser.*, vol. 1861, no. 1, 2021, doi: 10.1088/1742-6596/1861/1/012027.

[75] O. Trigui, W. Zouch, and M. Ben Messaoud, "Hilbert-huang transform and welch's method for motor imagery based brain computer interface," *Int. J. Cogn. Informatics Nat. Intell.*, vol. 11, no. 3, pp. 47–68, 2017, doi: 10.4018/IJCINI.2017070104.

[76] A. Tharwat, "Linear vs. quadratic discriminant analysis classifier: a tutorial," *Int. J. Appl. Pattern Recognit.*, vol. 3, no. 2, p. 145, 2016, doi: 10.1504/ijapr.2016.079050.

[77] J. R. Wolpaw and D. J. McFarland, "Control of a two-dimensional movement signal by a noninvasive brain-computer interface in humans," *Proc. Natl. Acad. Sci. U. S. A.*, vol. 101, no. 51, pp. 17849–17854, 2004, doi: 10.1073/pnas.0403504101.

[78] A. Jafarifarmand and M. A. Badamchizadeh, "Real-time multiclass motor imagery brain-computer interface by modified common spatial patterns and adaptive neuro-fuzzy classifier," *Biomed. Signal Process. Control*, vol. 57, p. 101749, 2020, doi: 10.1016/j.bspc.2019.101749.

[79] R. Mahamune and S. H. Laskar, "Classification of the four-class motor imagery signals using continuous wavelet transform filter bank-based two-dimensional images," *Int. J. Imaging Syst. Technol.*, vol. 31, no. 4, pp. 2237–2248, 2021, doi: 10.1002/ima.22593.

[80] J. W. Choi, B. H. Kim, and S. Jo, "Asynchronous Motor Imagery Brain-Computer Interface for Simulated Drone Control," *9th IEEE Int. Winter Conf. Brain-Computer Interface, BCI 2021*, 2021, doi: 10.1109/BCI51272.2021.9385309.

[81] D. Coyle, J. Garcia, A. R. Satti, and T. M. McGinnity, "EEG-based continuous control of a game using a 3 channel motor imagery BCI: BCI game," *IEEE SSCI 2011 - Symp. Ser. Comput. Intell. - CCMB 2011 2011 IEEE Symp. Comput. Intell. Cogn. Algorithms, Mind, Brain*, pp. 88–94, 2011, doi: 10.1109/CCMB.2011.5952128.

[82] Y. Yu *et al.*, "Toward brain-actuated car applications: Self-paced control with a motor imagery-based brain-computer interface," *Comput. Biol. Med.*, vol. 77, pp. 148–155, 2016, doi: 10.1016/j.compbiomed.2016.08.010.

[83] C. Prahm, F. Kayali, A. Sturma, and O. Aszmann, “PlayBionic: Game-Based Interventions to Encourage Patient Engagement and Performance in Prosthetic Motor Rehabilitation,” *PM R*, vol. 10, no. 11, pp. 1252–1260, 2018, doi: 10.1016/j.pmrj.2018.09.027.

APPENDIX

User s1 – first setup

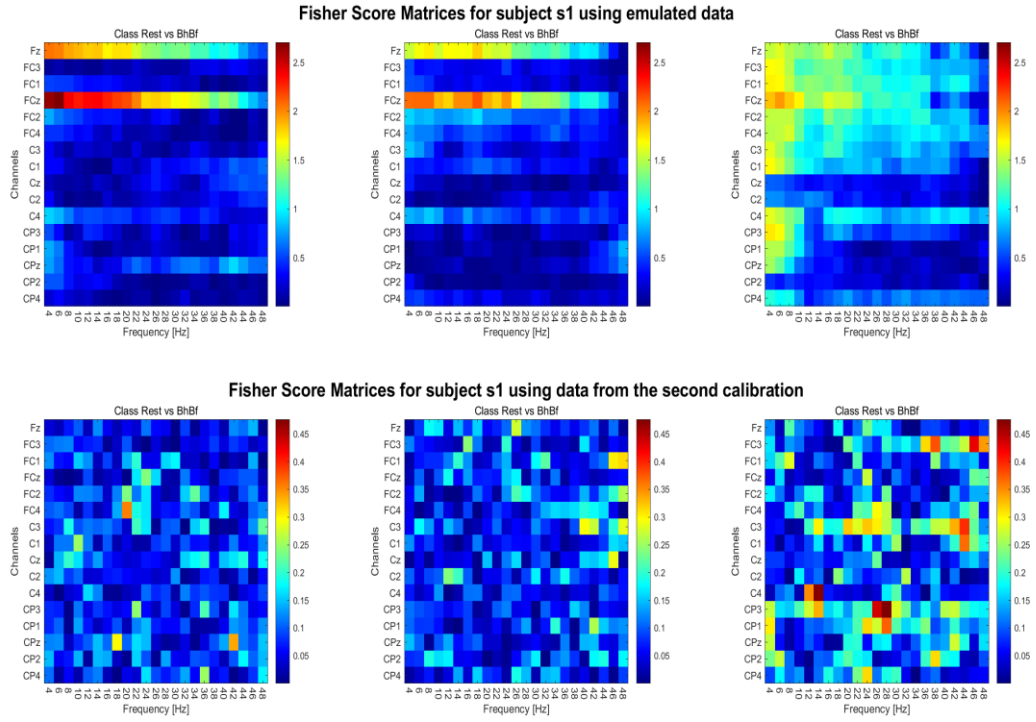

Figure 21: Fisher Score matrices of subject s1 to prove that class Both Hands and Both Feet cannot be derived from class Both Hands and class Both Feet data.

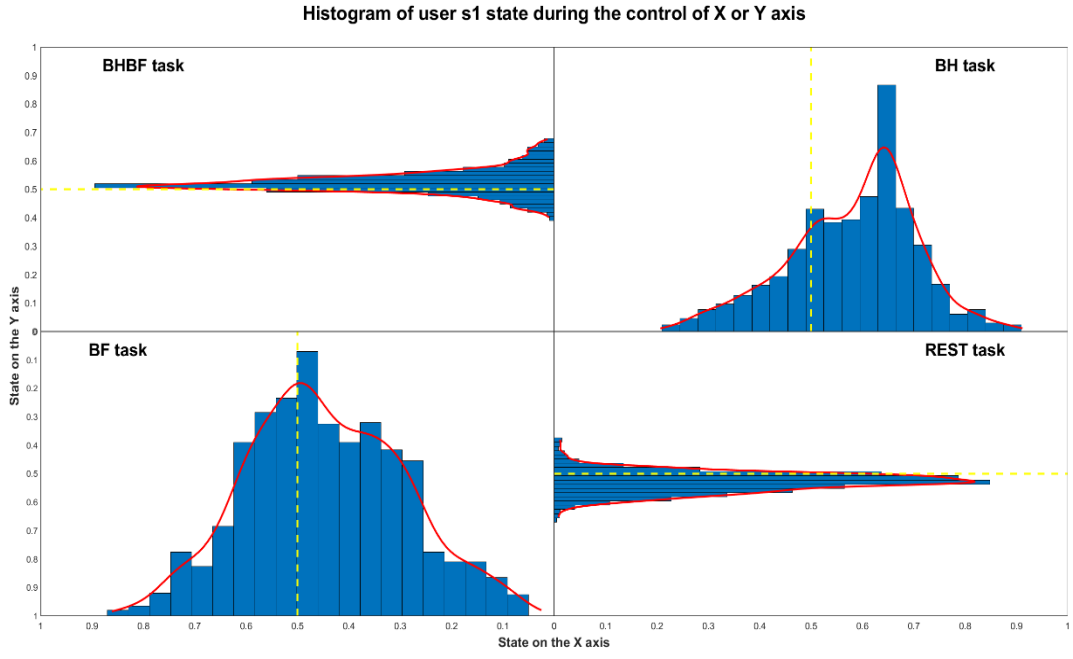

Figure 22: Histograms of all the state vector values achieved during the run with best performance for user s1.

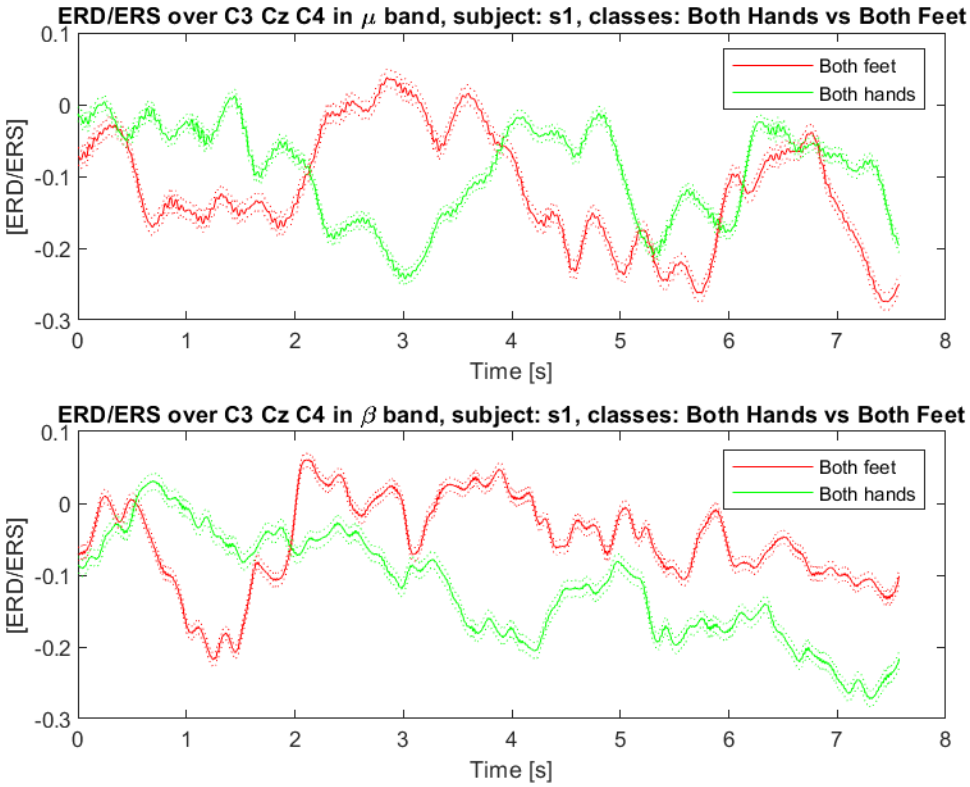

Figure 23: ERD/ERS over main target electrodes in μ and β bands for classes Both Hands and Both Feet, user s1.

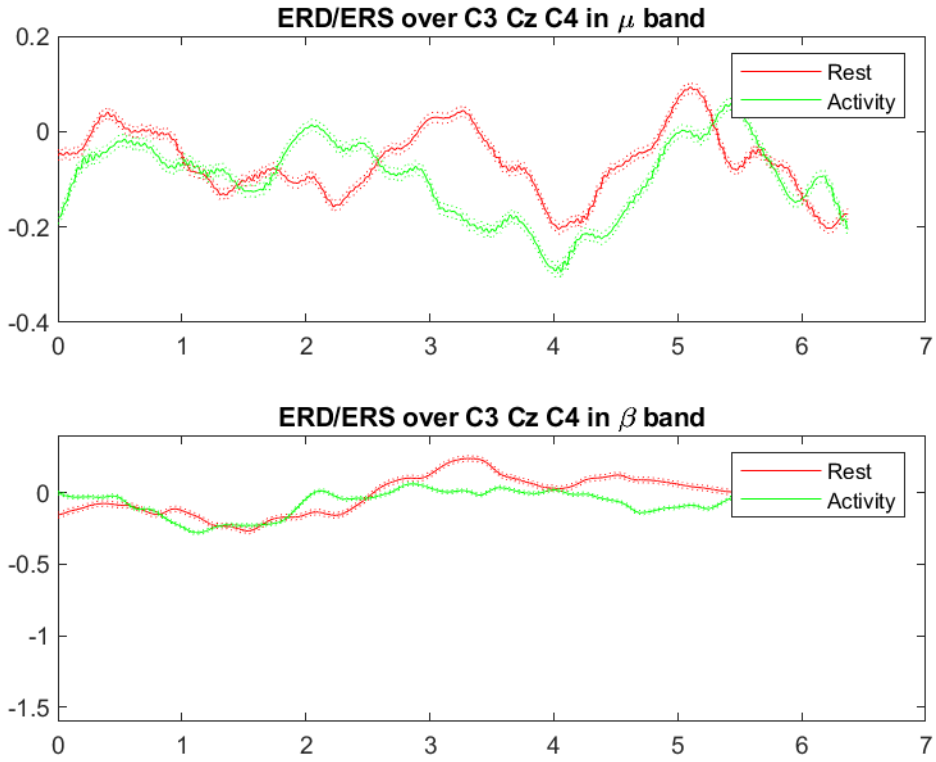

Figure 24: ERD/ERS over main target electrodes in μ and β bands for classes Activity (Both Hands and Both Feet together) and Rest, user s1.

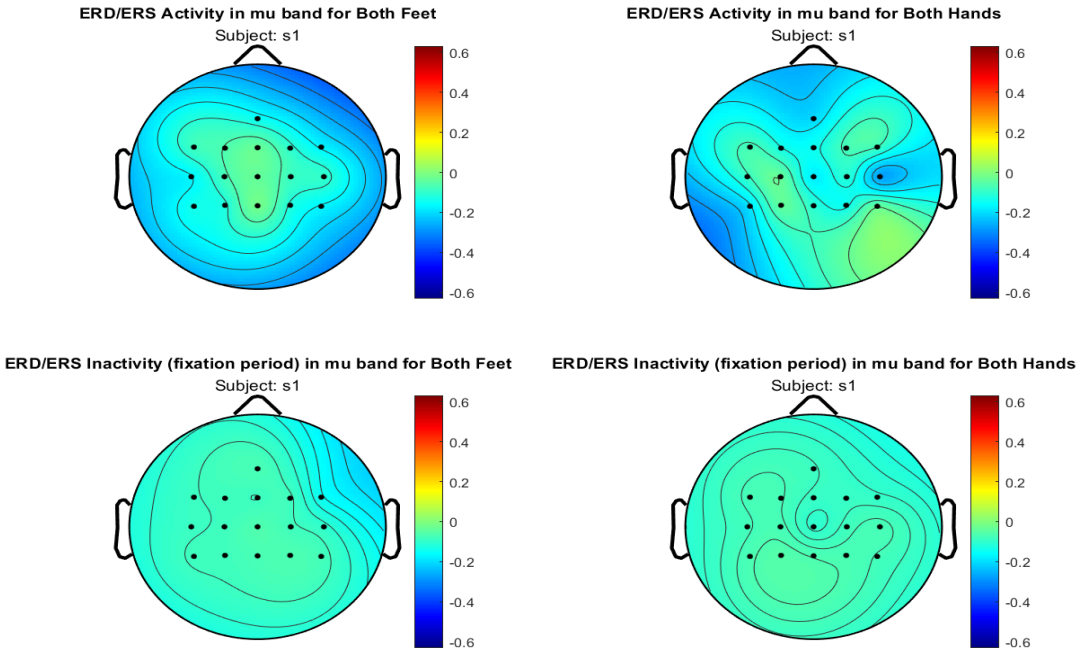

Figure 25: Topomaps related to the ERD/ERS of classes Both Hands and Both Feet, user s1.

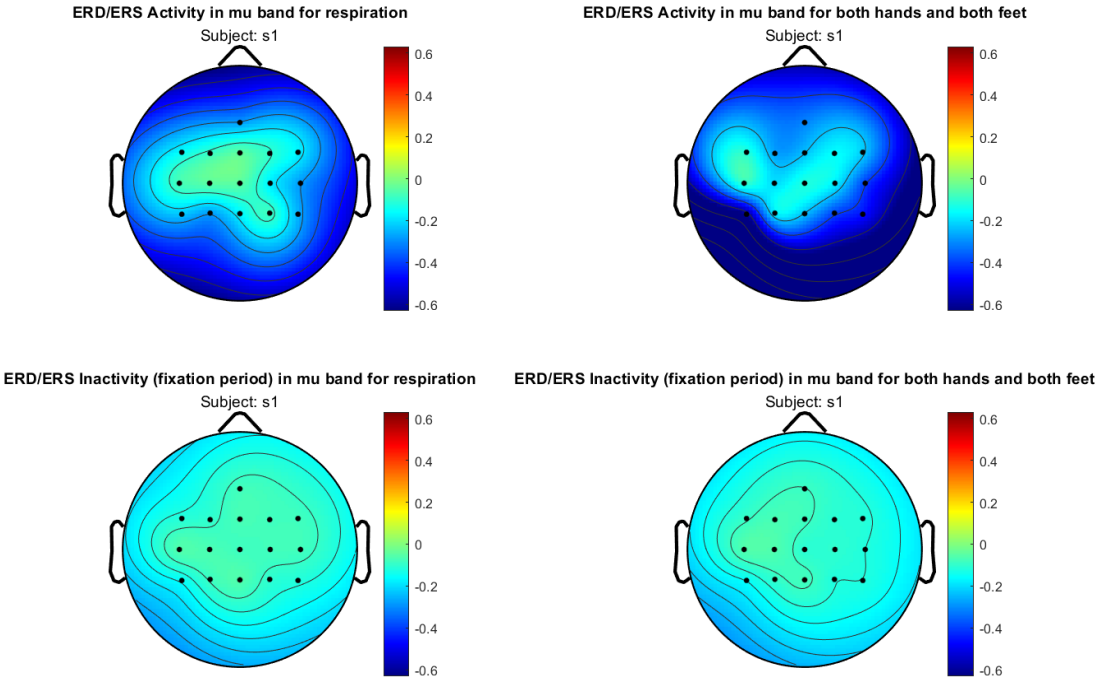

Figure 26: Topomaps related to the ERD/ERS of classes Activity (Both Hands and Both Feet) and Rest (respiration), user s1.

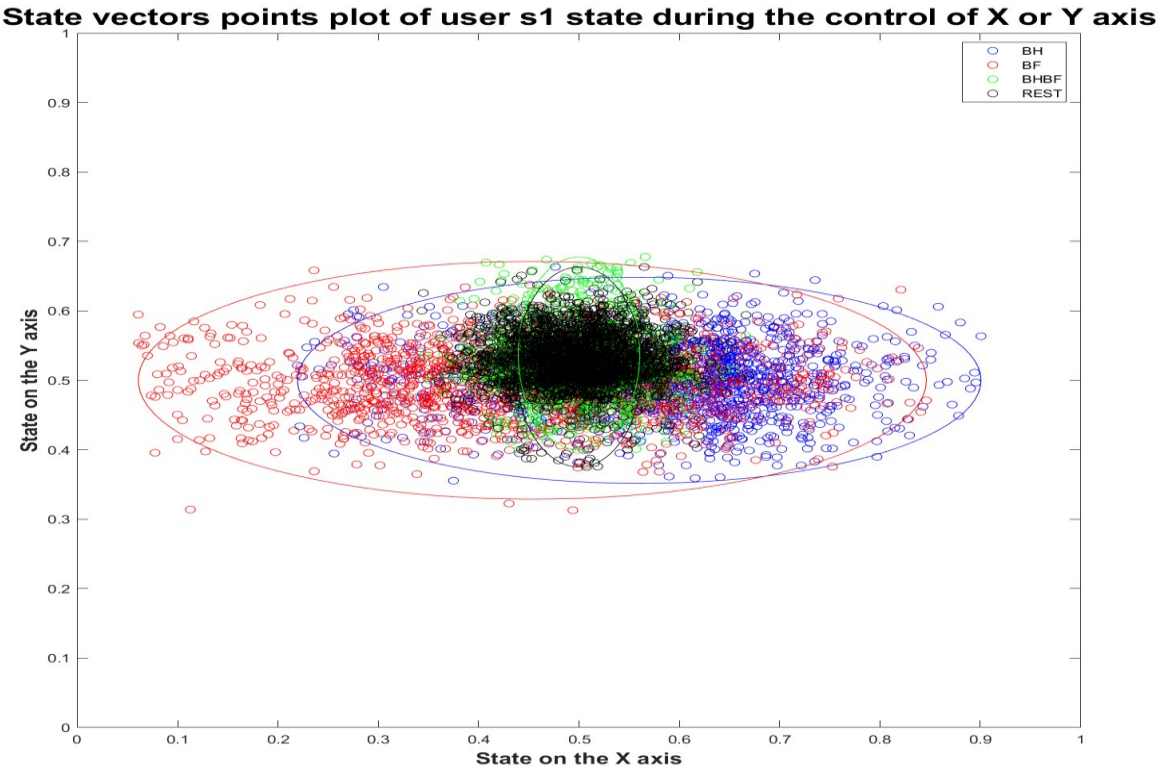

Figure 27: Plot of all the state vector values achieved during the runs with best performances for subject s1. Good differentiation between the horizontal ellipses, but almost an overlap of the vertical ones.

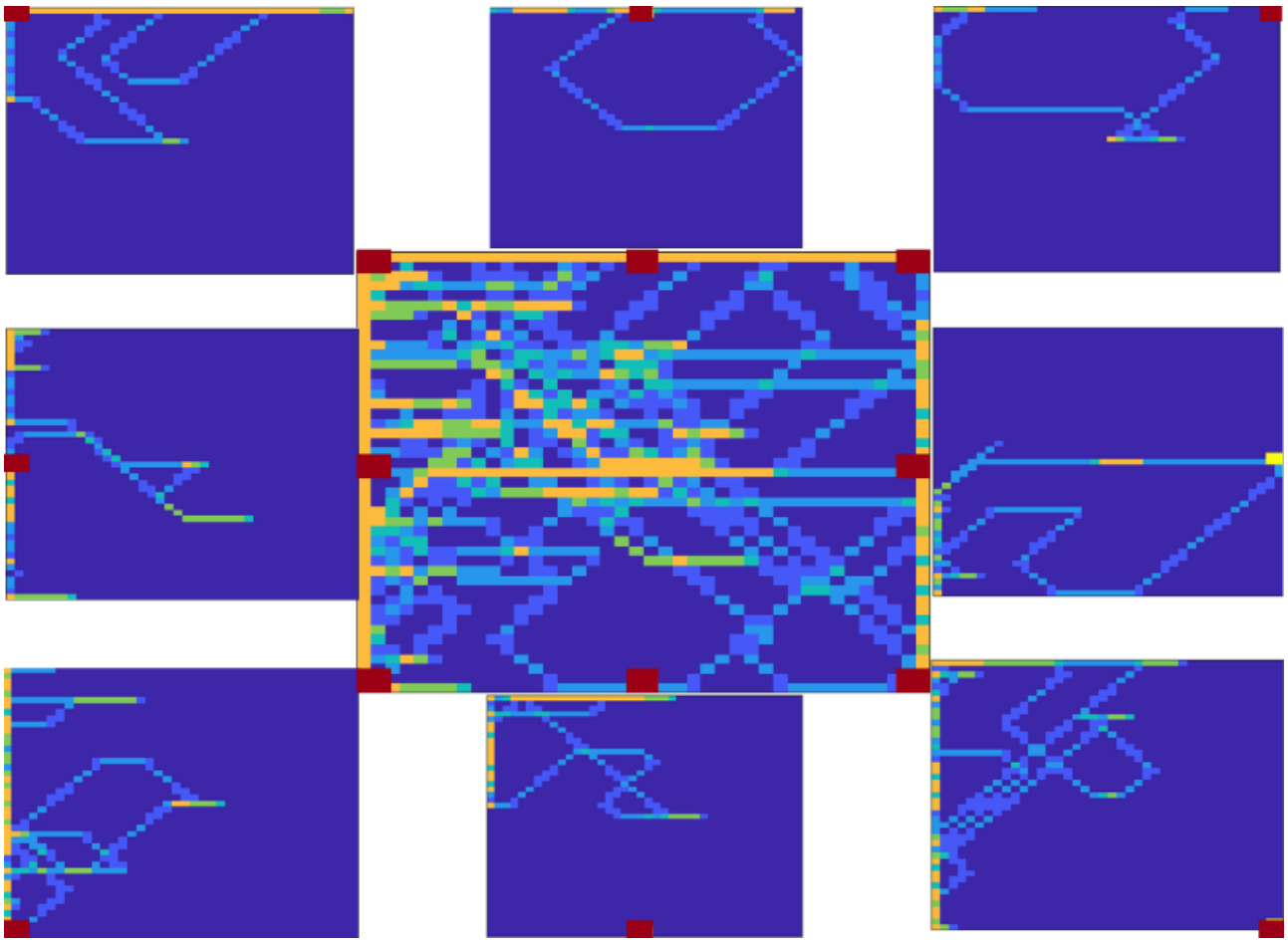

Figure 28: Heat maps of user s1 in the first setup.

User s3 – first setup

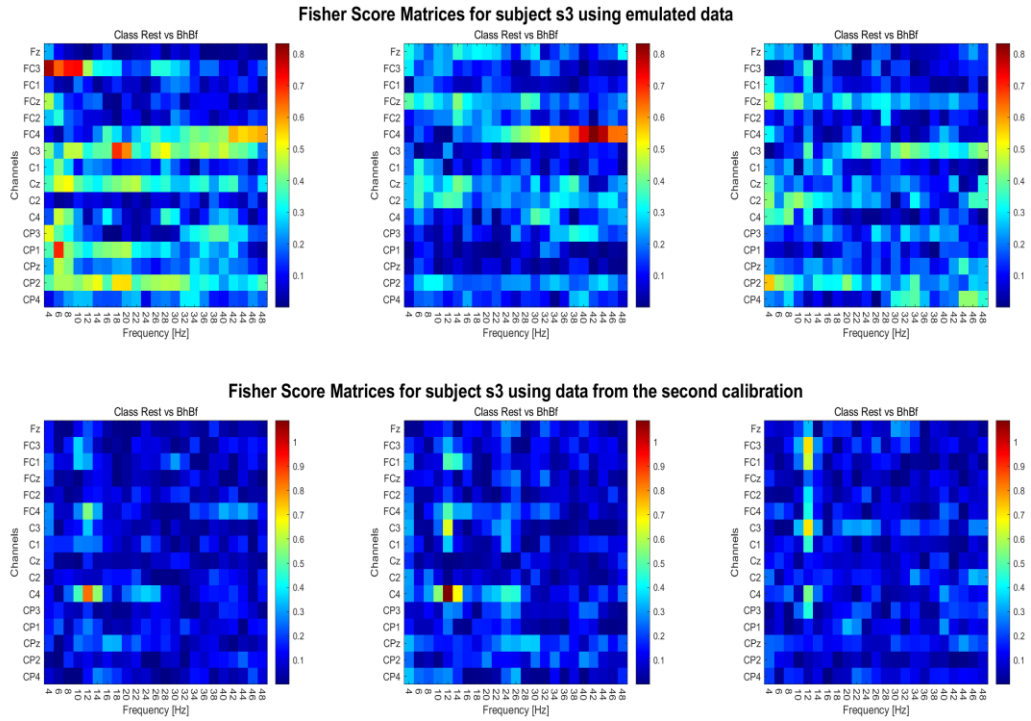

Figure 29: Fisher Score matrices of subject s3 to prove that class Both Hands and Both Feet cannot be derived from class Both Hands and class Both Feet data.

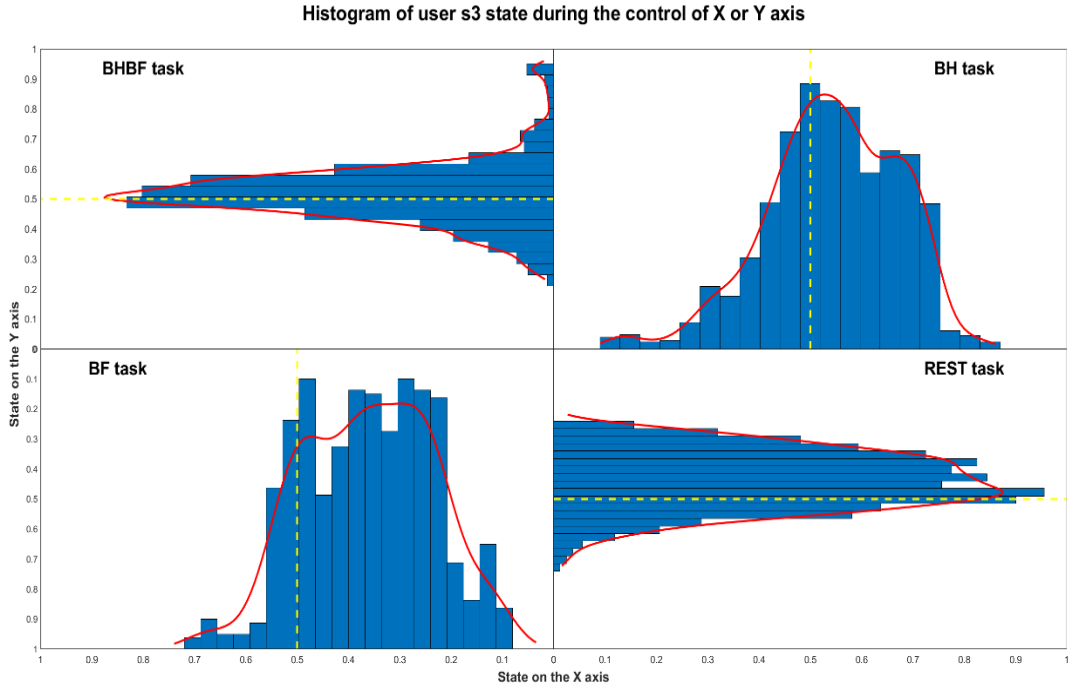

Figure 30: Histograms of all the state vector values achieved during the run with best performance for user s3.

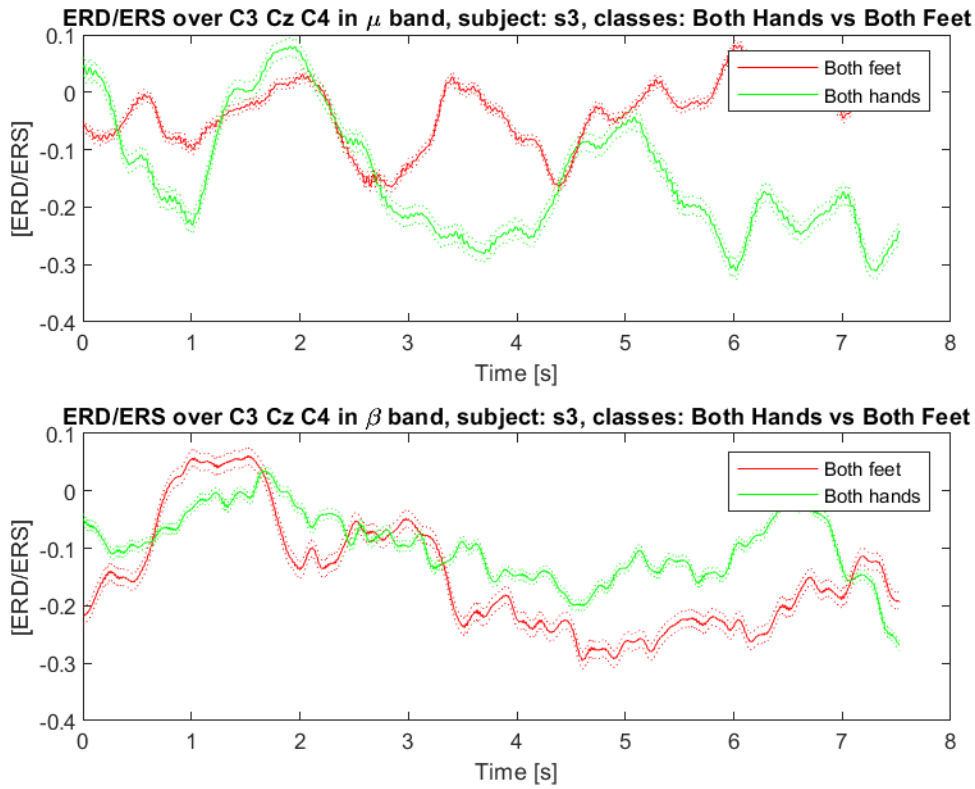

Figure 31: ERD/ERS over main target electrodes in μ and β bands for classes Both Hands and Both Feet, user s3.

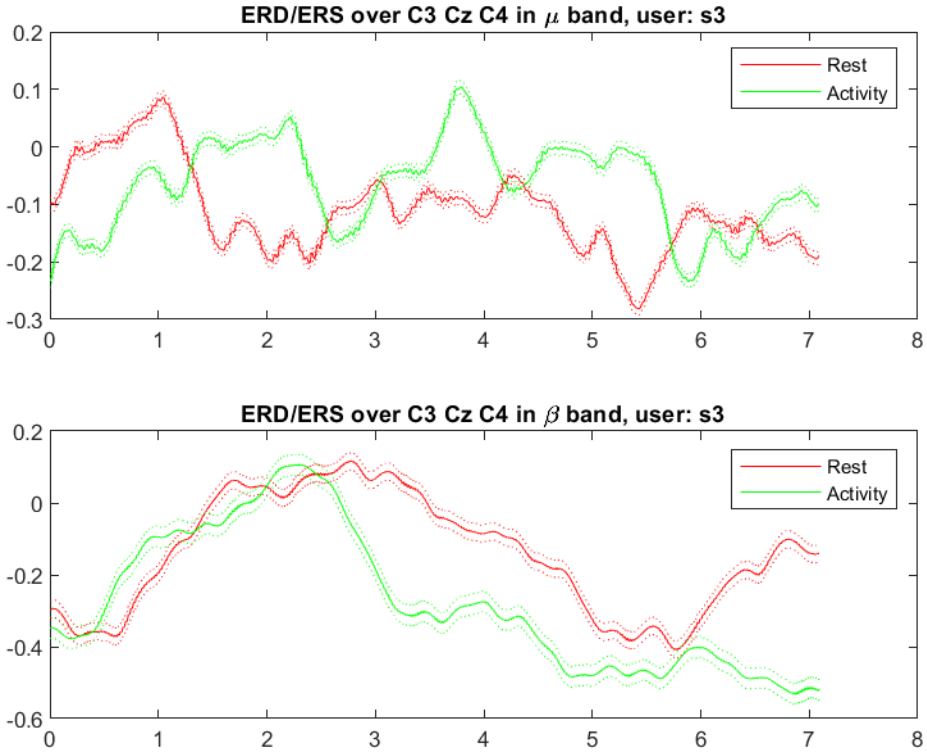

Figure 32: ERD/ERS over main target electrodes in μ and β bands for classes Activity (Both Hands and Both Feet together) and Rest, user s3.

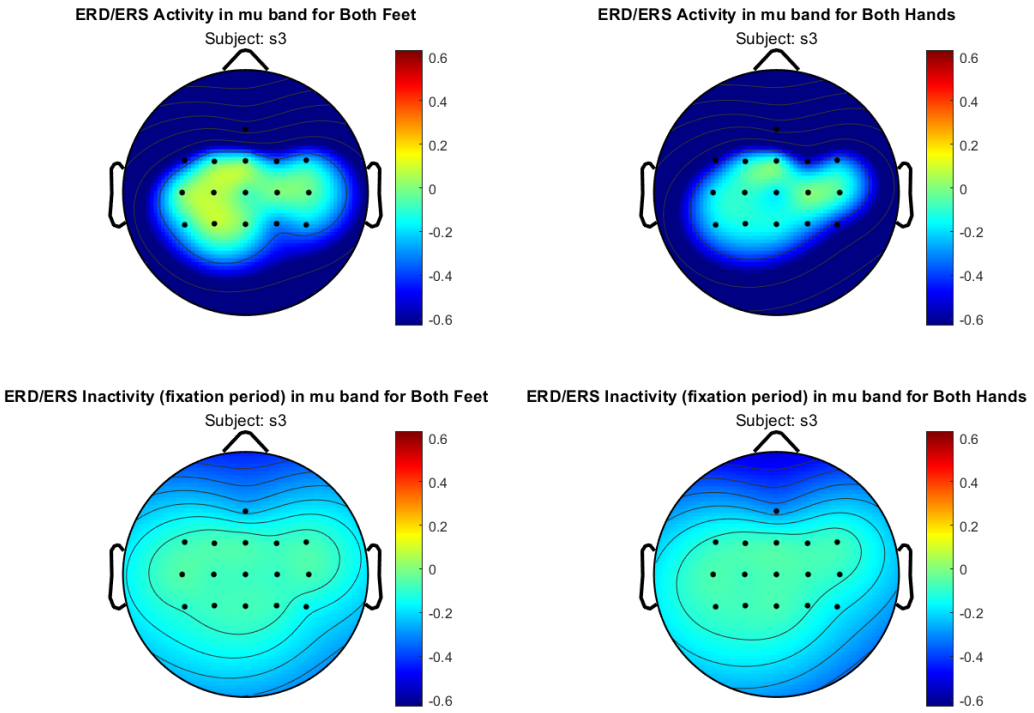

Figure 33: Topomaps related to the ERD/ERS of class Hands and Both Feet, user s3.

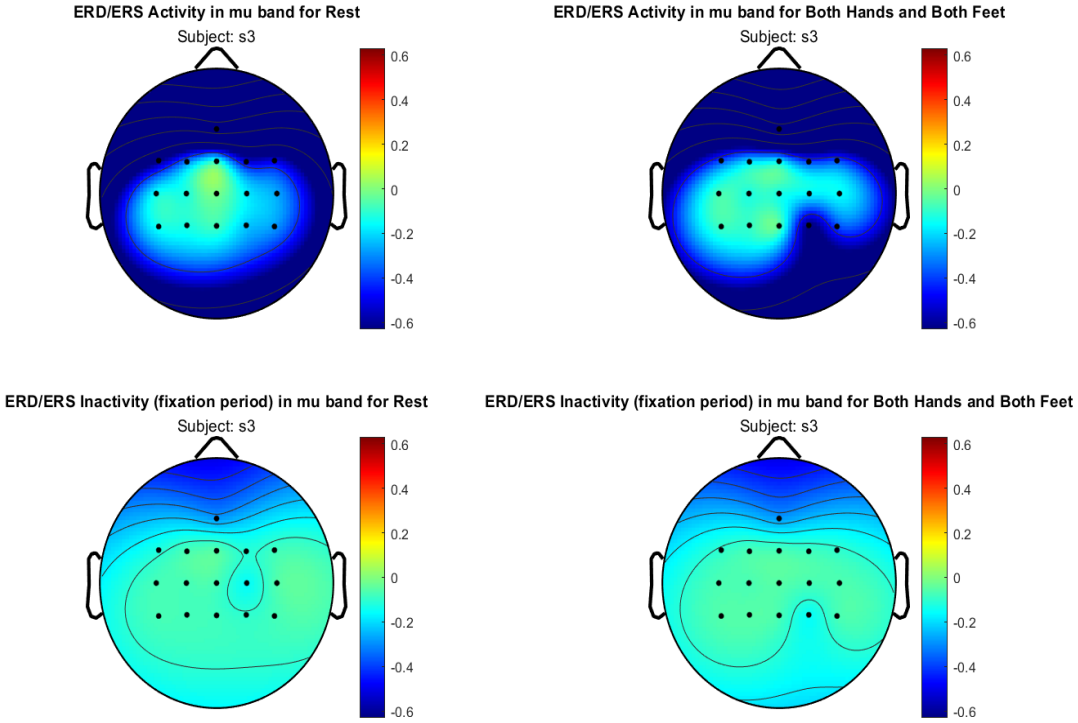

Figure 44: Topomaps related to the ERD/ERS of classes Activity (Both Hands and Both Feet) and Rest (respirarion), user s3

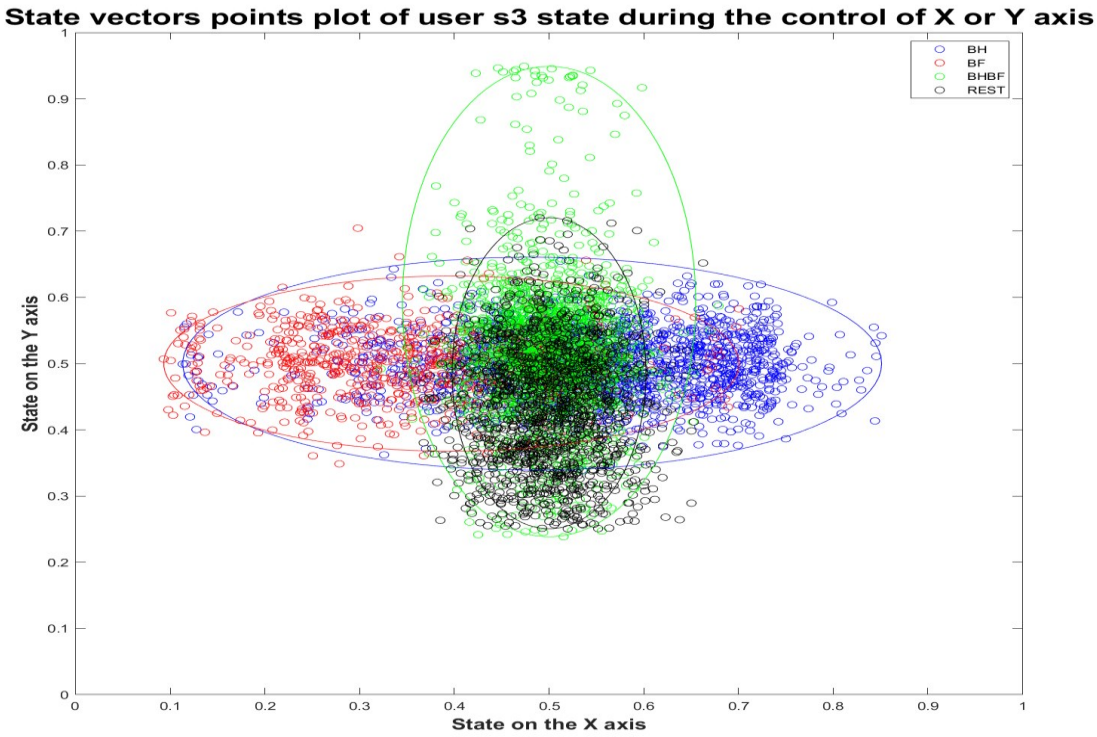

Figure 35: Plot of all the state vector values achieved during the runs with best performances for subject s3. Good differentiation between the horizontal ellipses, lost among the vertical ones.

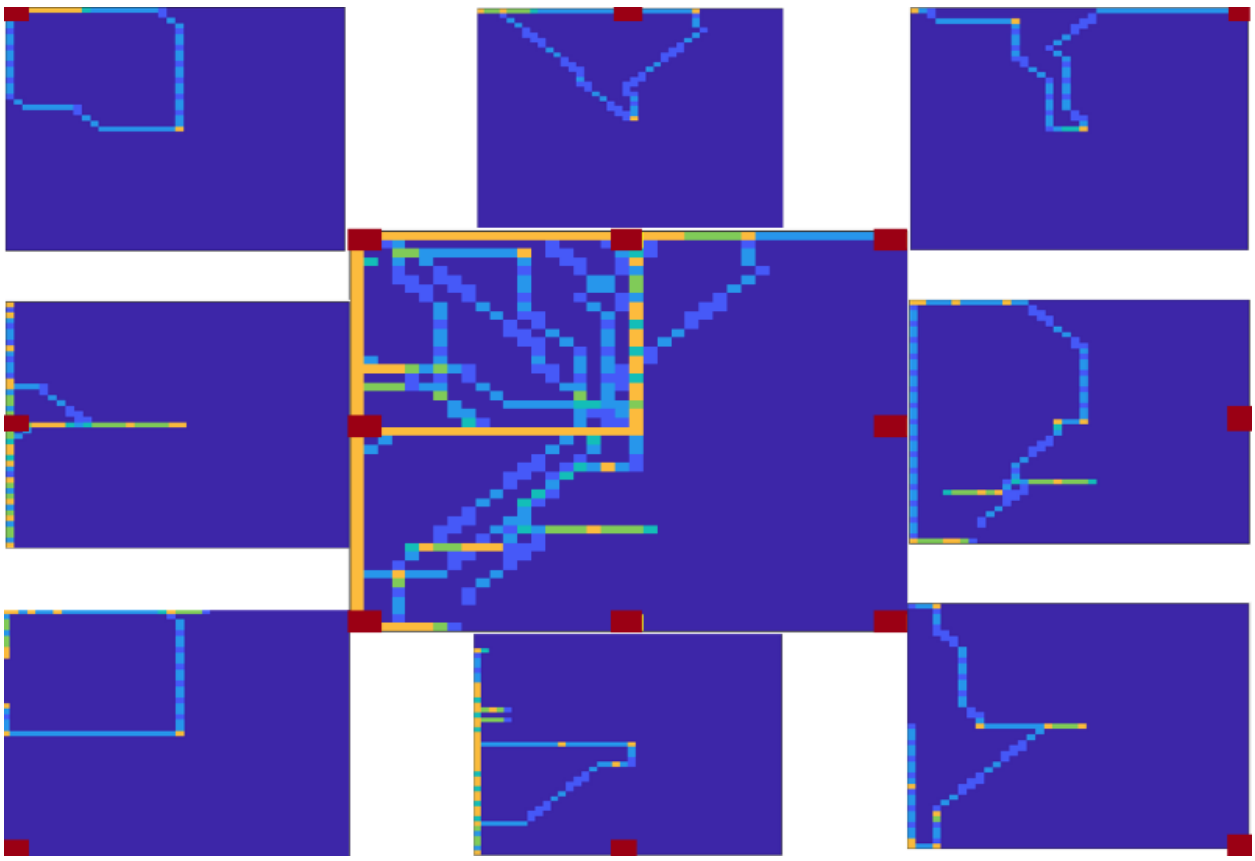

Figure 36: Heat maps of user s1 in the first setup.

User s5 – first setup

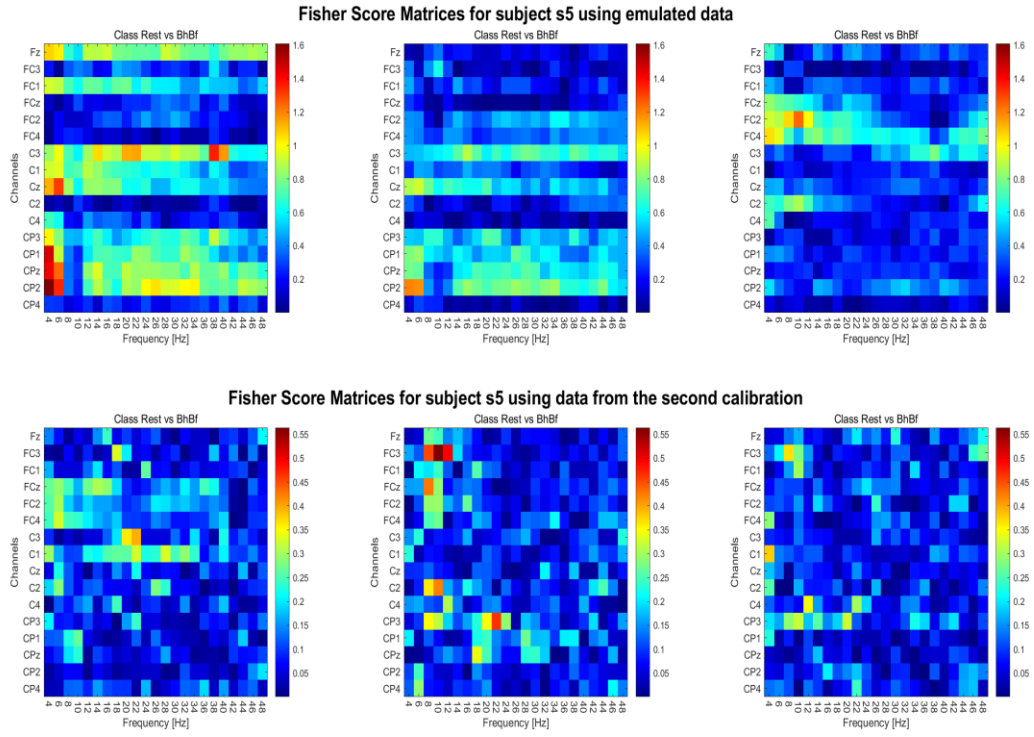

Figure 37: Fisher Score matrices of subject s5 to prove that class Both Hands and Both Feet cannot be derived from class Both Hands and class Both Feet data.

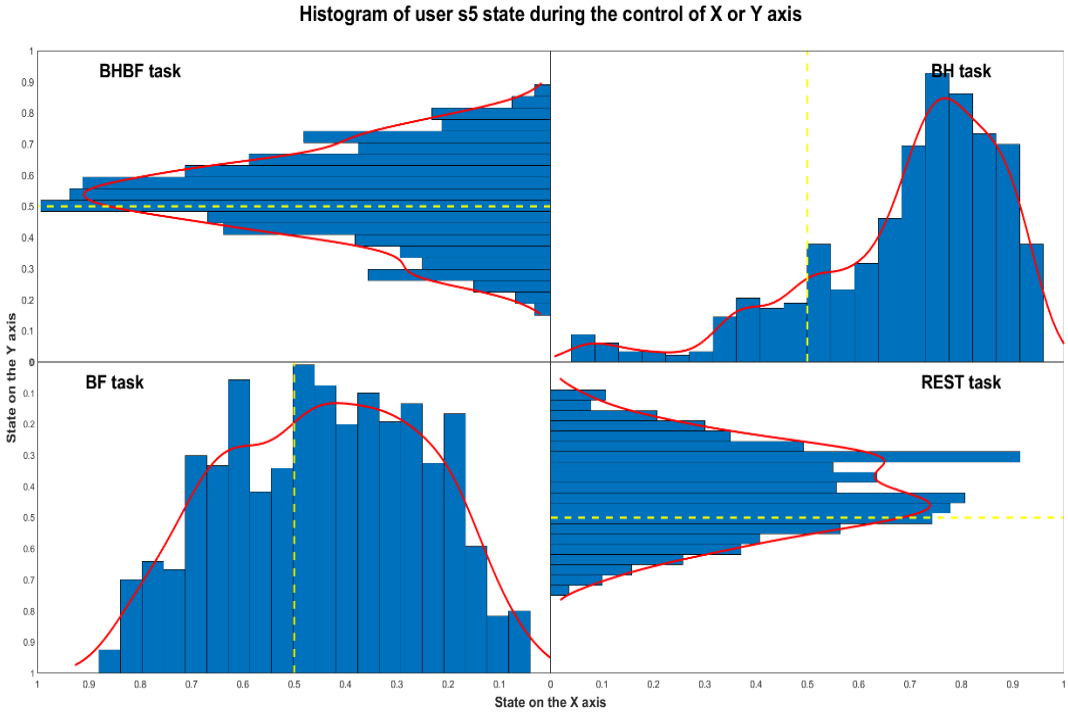

Figure 38: Histograms of all the state vector values achieved during the run with best performance for user s5.

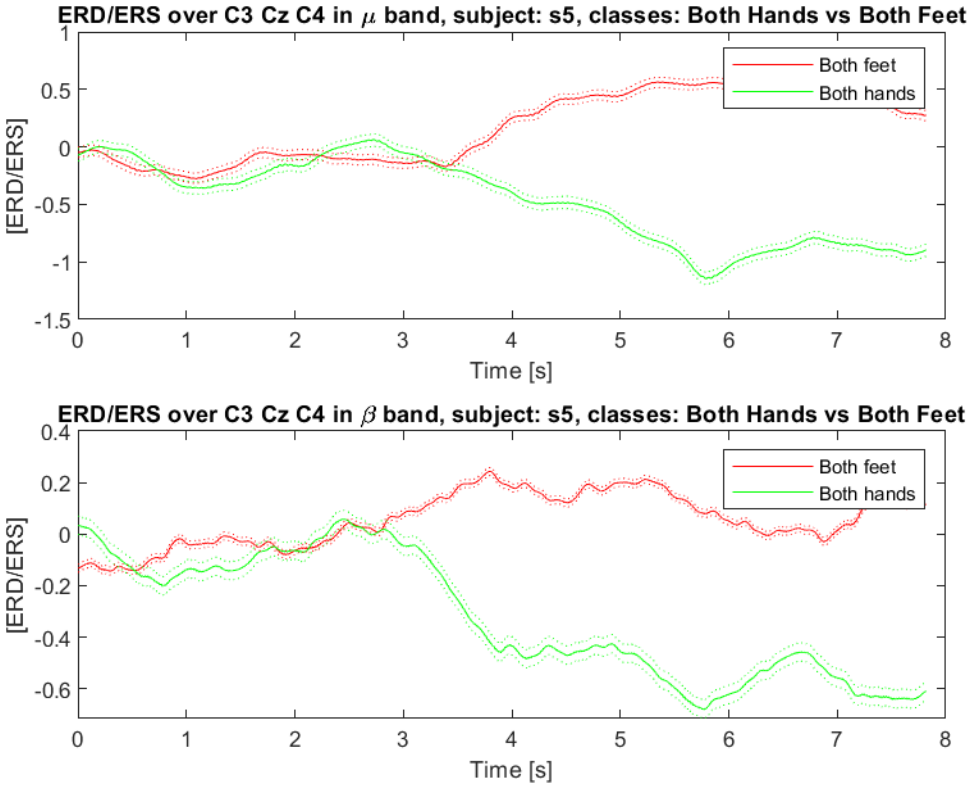

Figure 39: ERD/ERS over main target electrodes in μ and β bands for classes Both Hands and Both Feet, user s5.

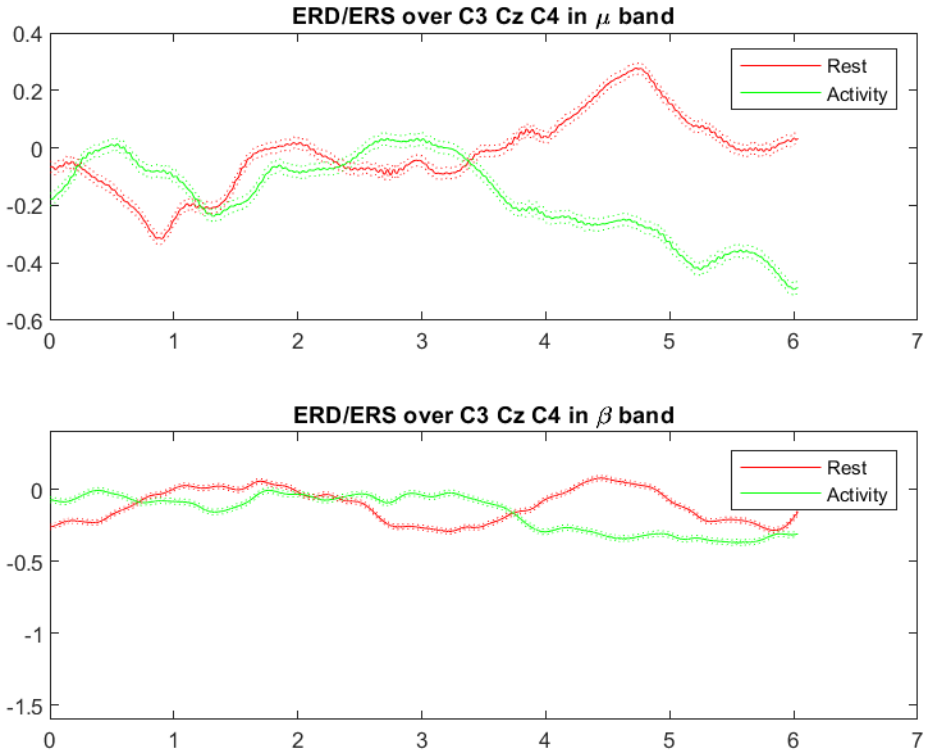

Figure 40: ERD/ERS over main target electrodes in μ and β bands for classes Activity (Both Hands and Both Feet together) and Rest, user s5.

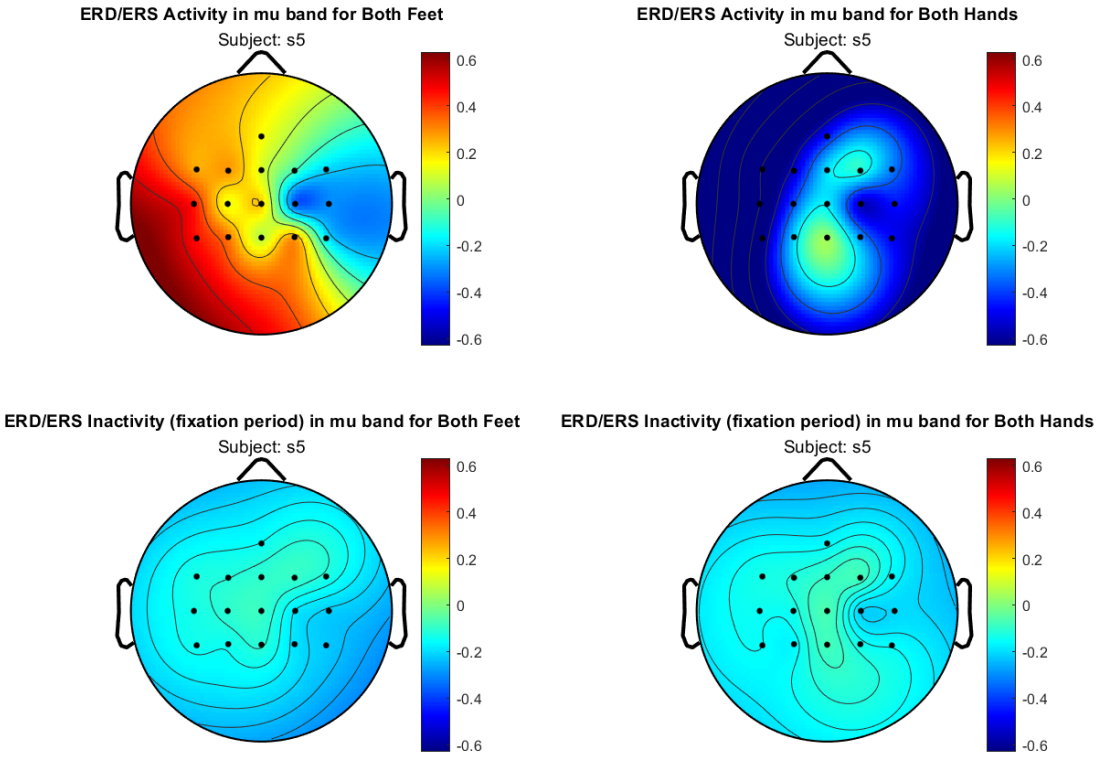

Figure 41: Topomaps related to the ERD/ERS of classes Both Hands and Both Feet, user s5.

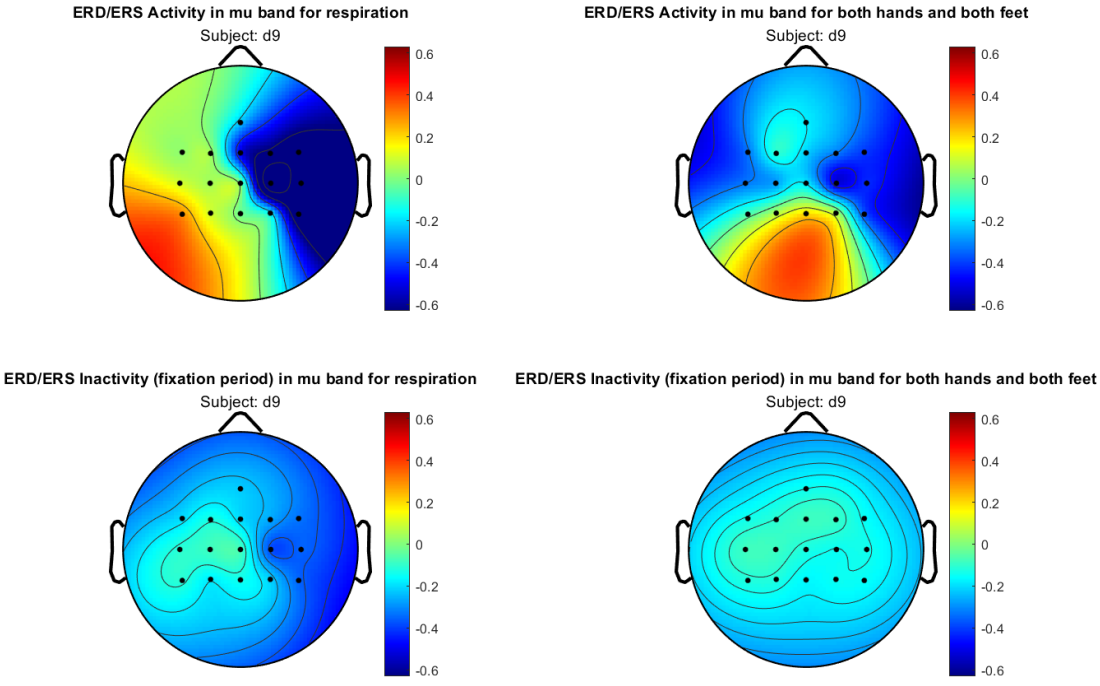

Figure 42: Topomaps related to the ERD/ERS of classes Activity (Both Hands and Both Feet) and Rest (respiration), user s5

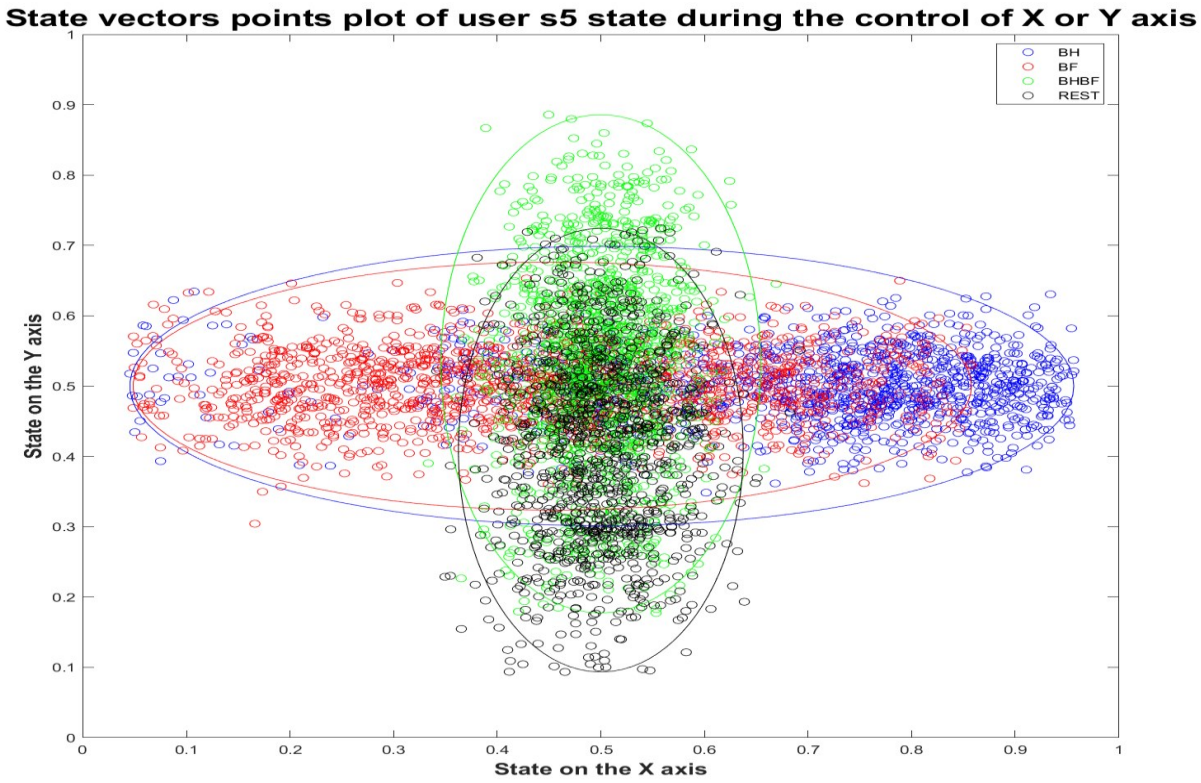

Figure 43: Plot of all the state vector values achieved during the runs with best performances for subject s5. Good differentiation in both the horizontal and vertical ellipses

.

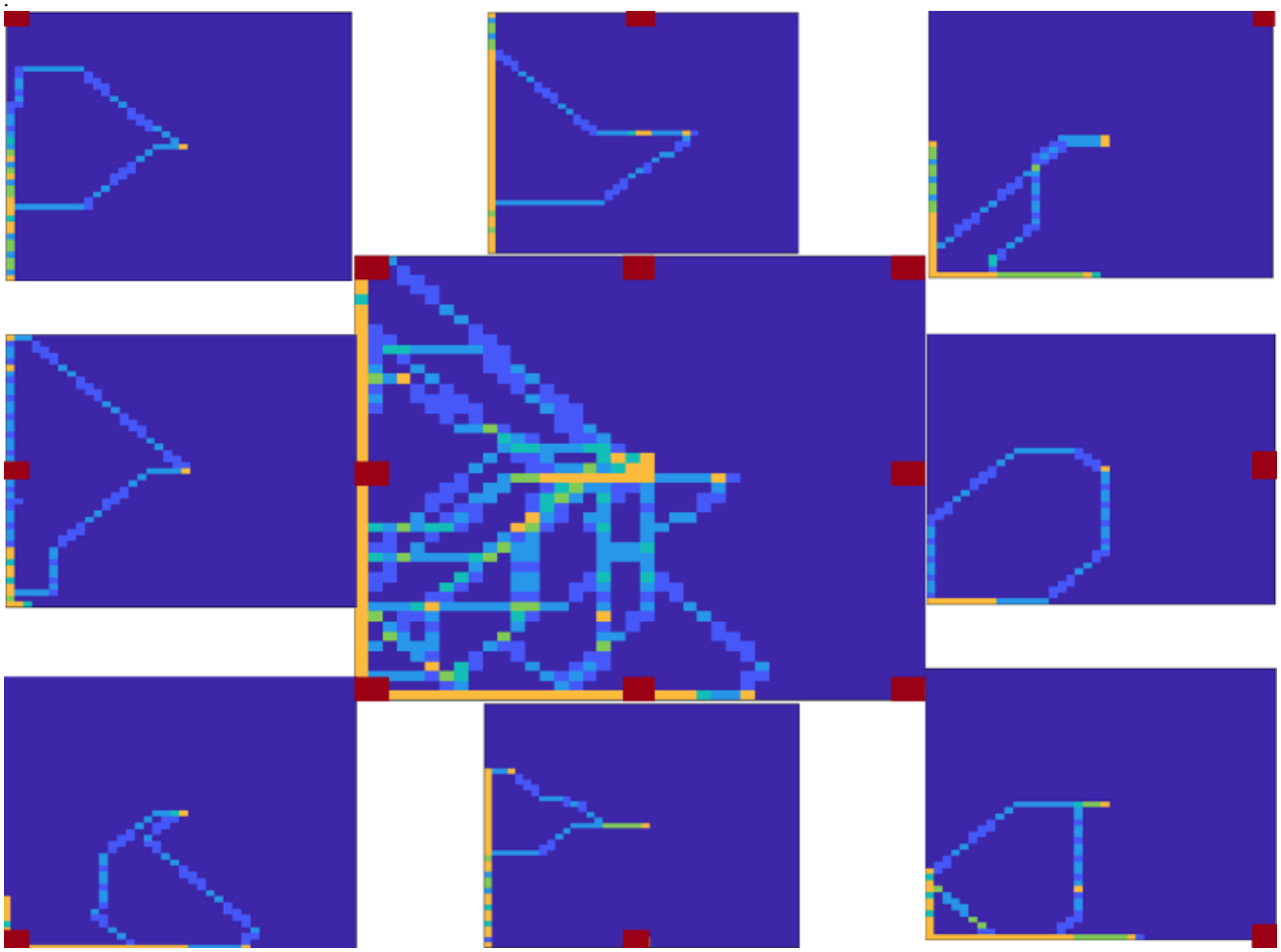

Figure 44: Heat maps of user s5

User s6 – first setup

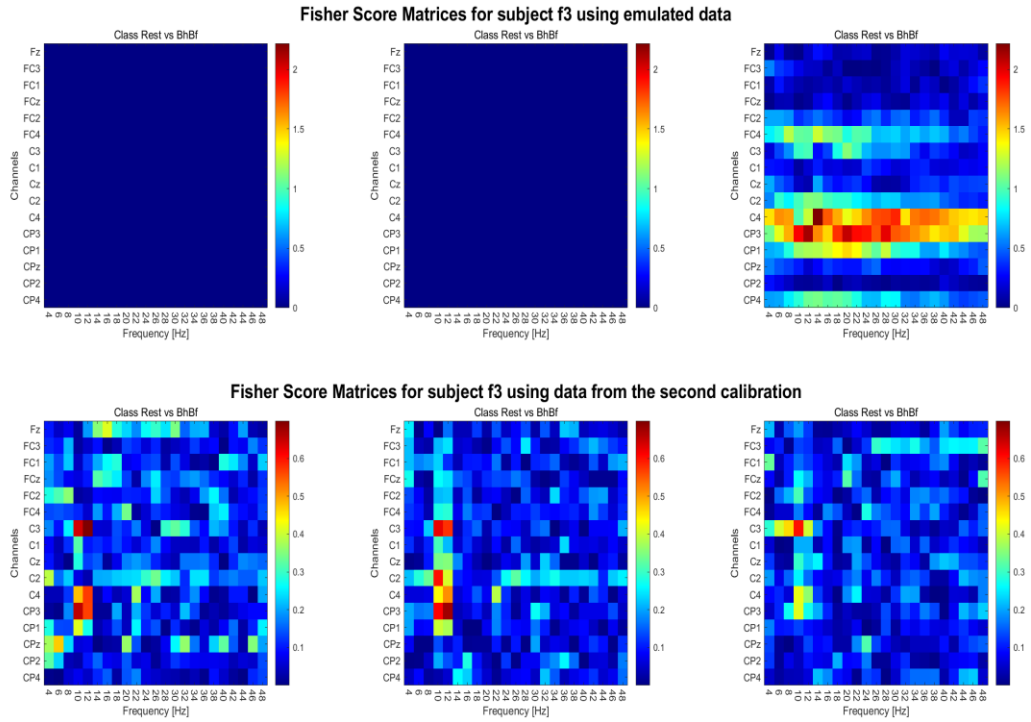

Figure 45: Fisher Score matrices of subject s6 to prove that class Both Hands and Both Feet cannot be derived from class Both Hands and class Both Feet data.

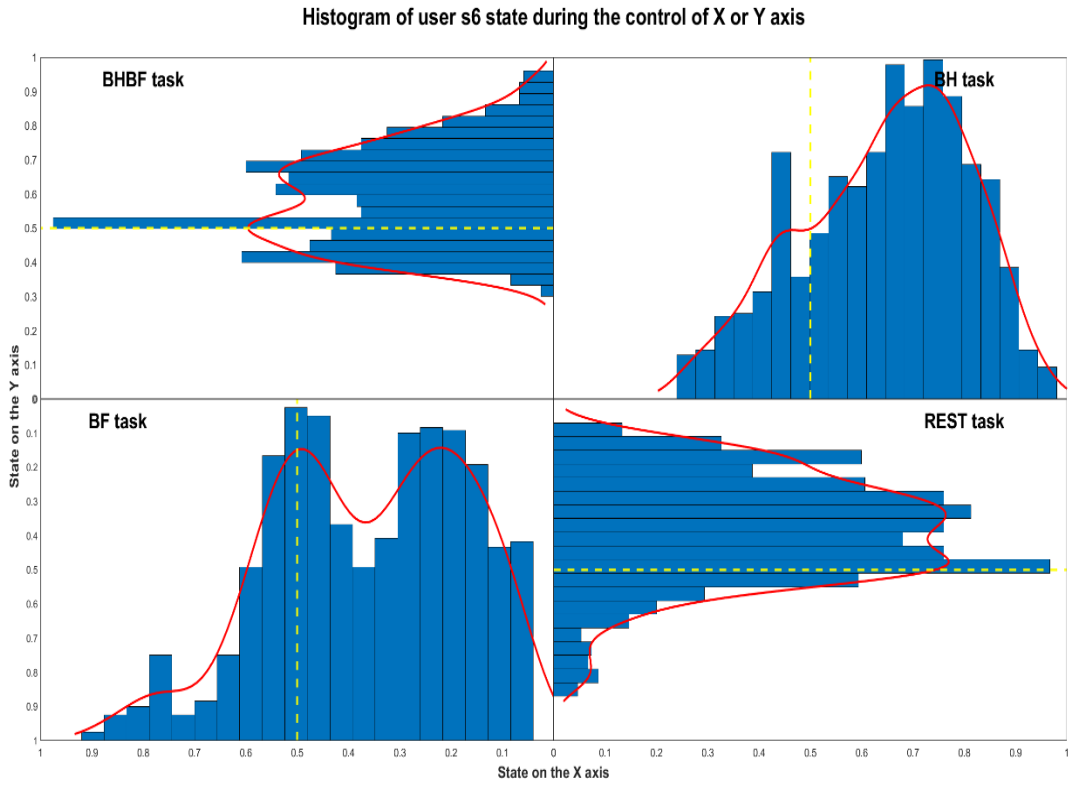

Figure 46: Histograms of all the state vector values achieved during the run with best performance for user s6.

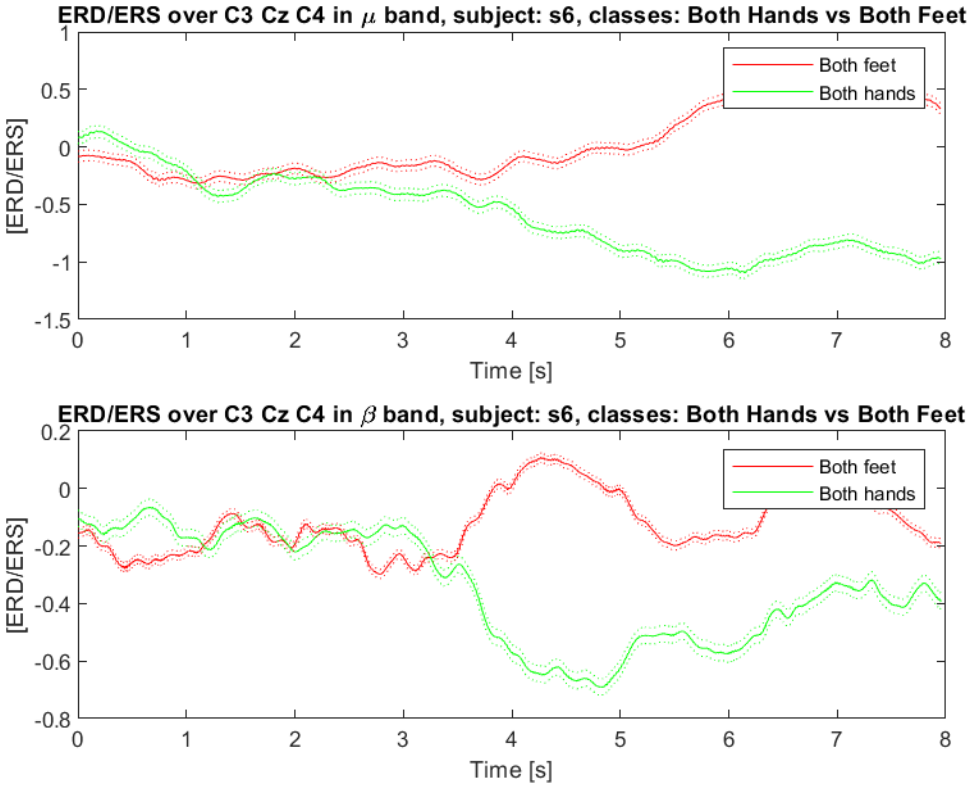

Figure 47: ERD/ERS over main target electrodes in μ and β bands for classes Both Hands and Both Feet, user s6.

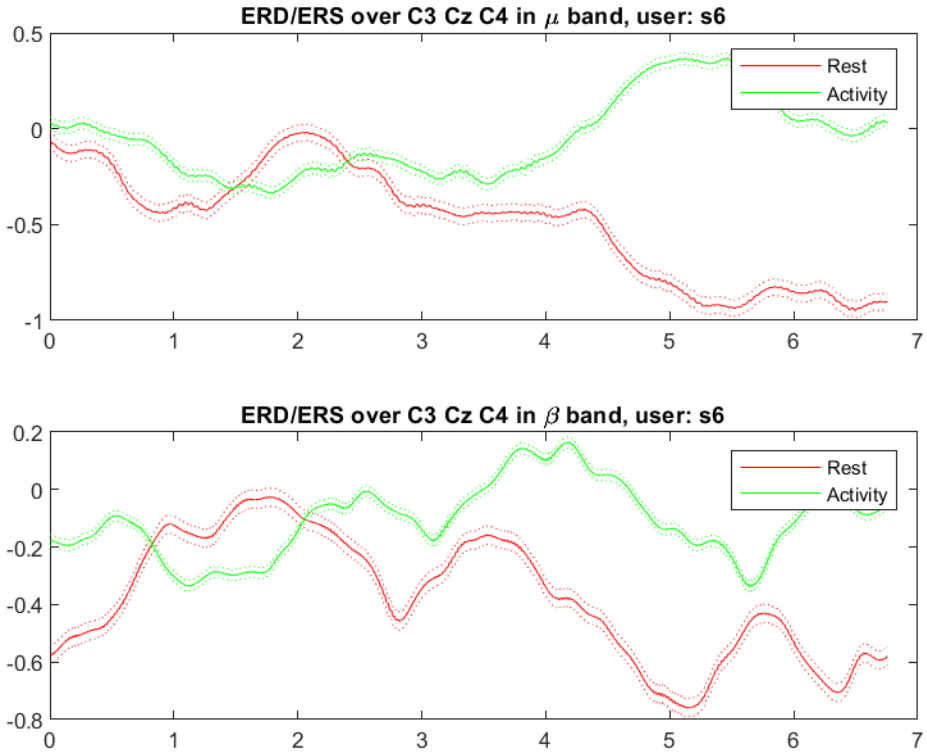

Figure 48: ERD/ERS over main target electrodes in μ and β bands for classes Activity (Both Hands and Both Feet together) and Rest, user s6.

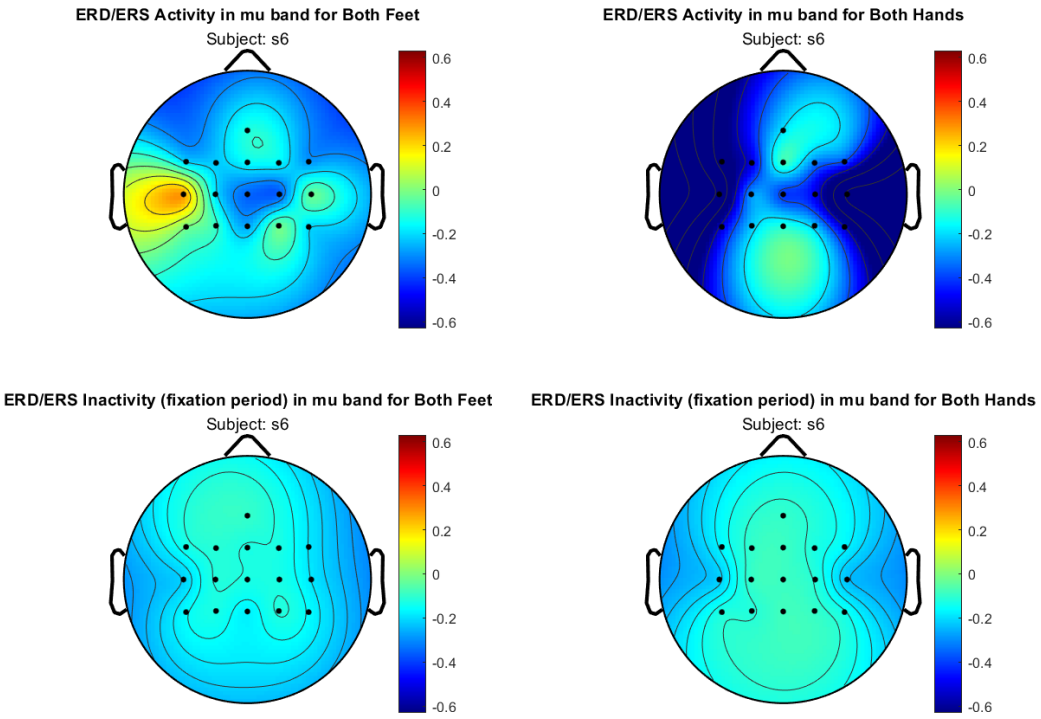

Figure 49: Topomaps related to the ER D/ERS of classes Both Hands and Both Feet, user s6.

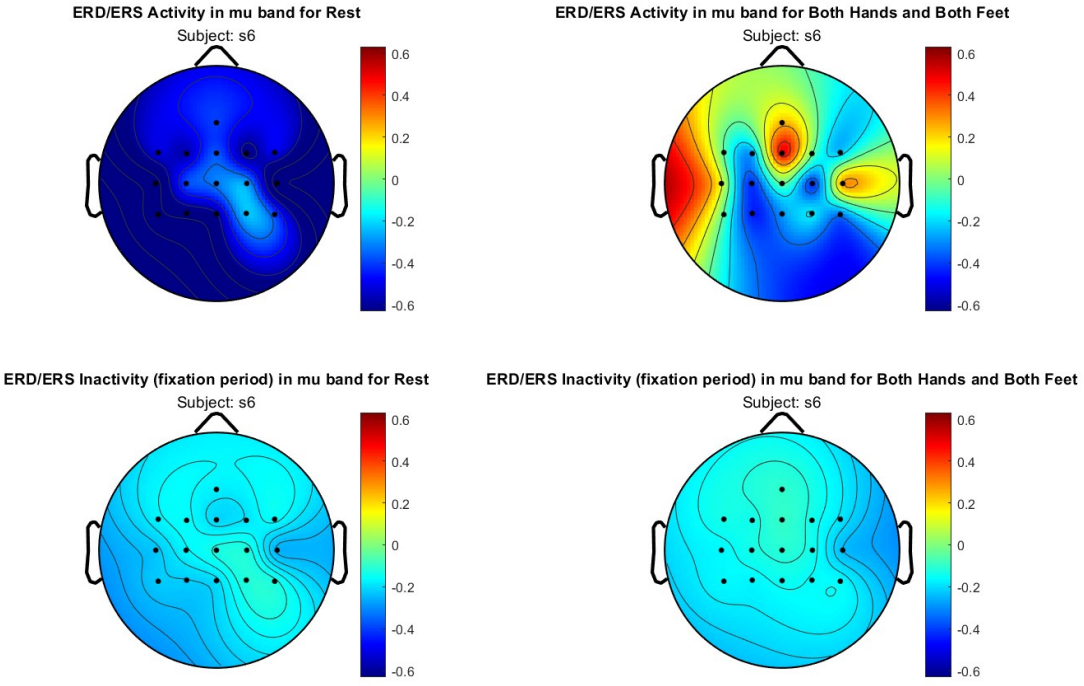

Figure 50: Topomaps related to the ERD/ERS of classes Activity (Both Hands and Both Feet) and Rest (respiration), user s6

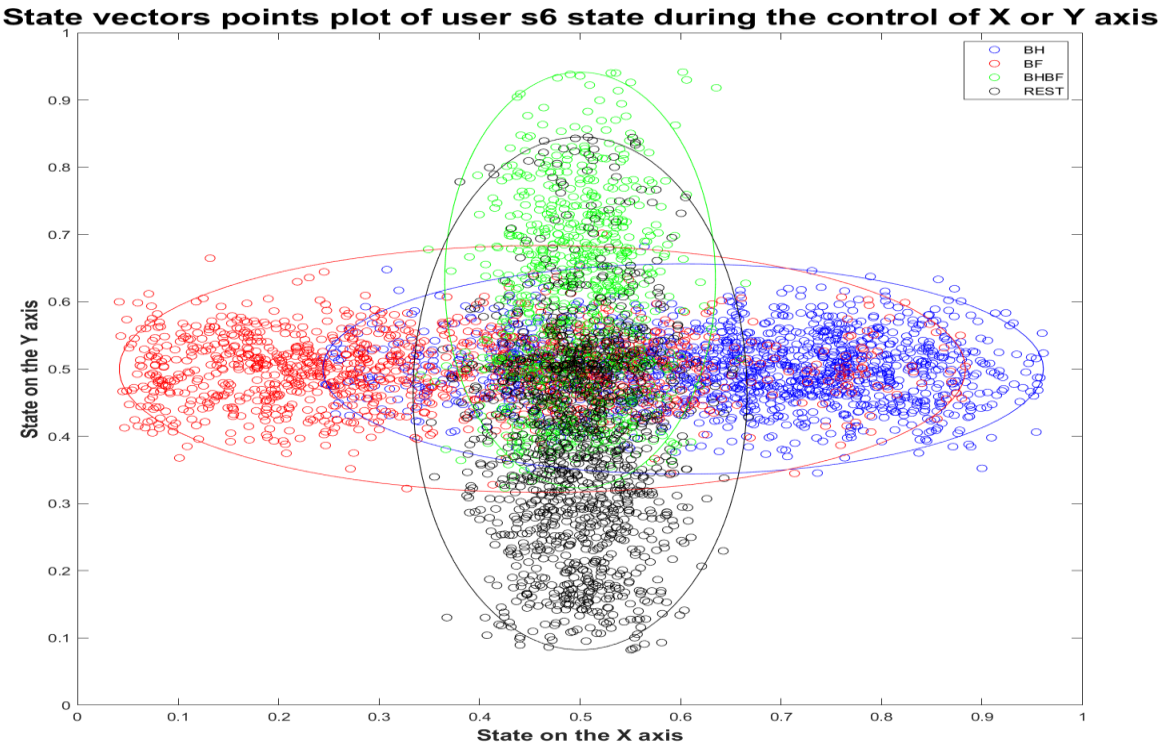

Figure 51: Plot of all the state vector values achieved during the runs with best performances for subject s6. Good differentiation for both the horizontal and vertical ellipse.

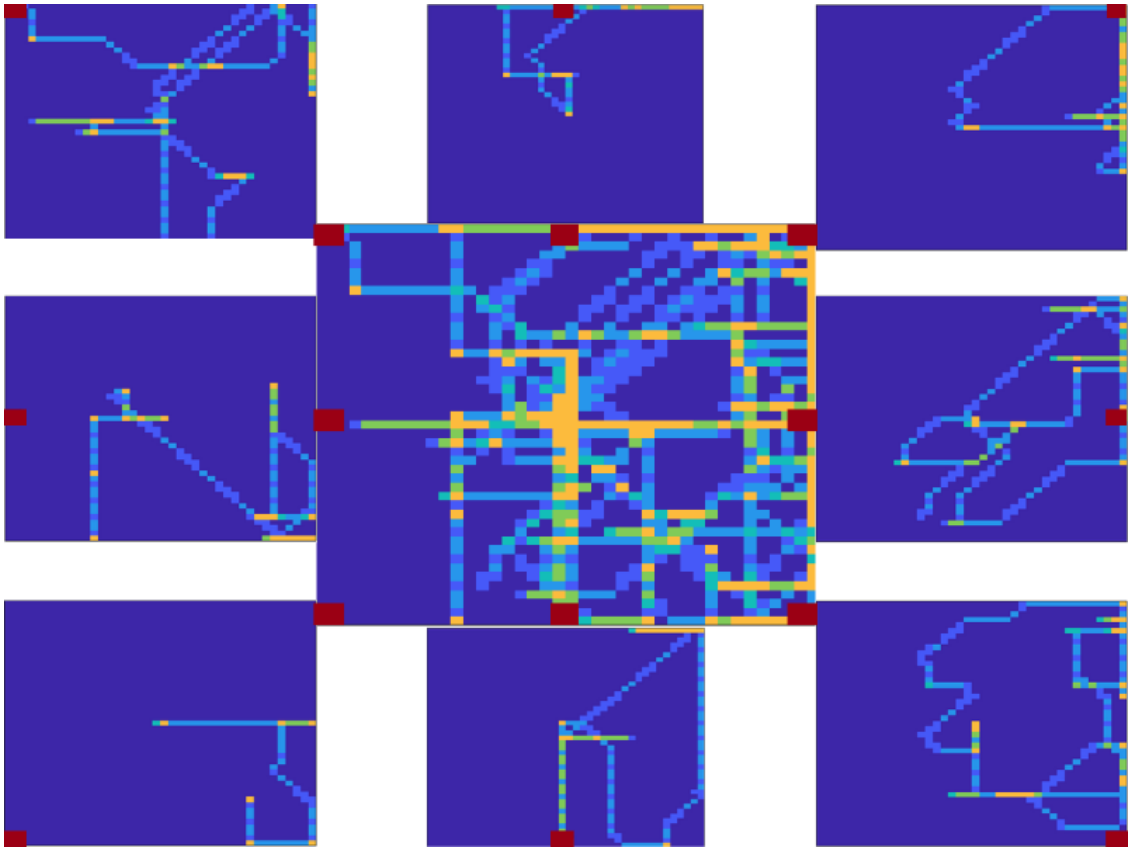

Figure 52: Heat maps of user s6.

User s7 – first setup

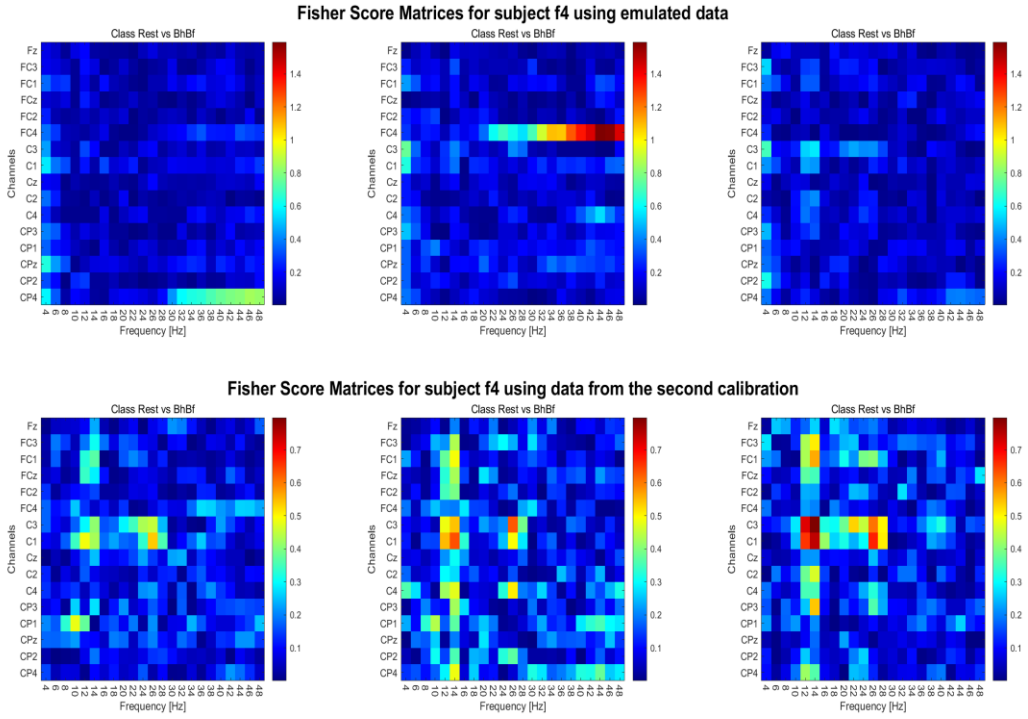

Figure 53: Fisher Score matrices of subject s7 to prove that class Both Hands and Both Feet cannot be derived from class Both Hands and class Both Feet data.

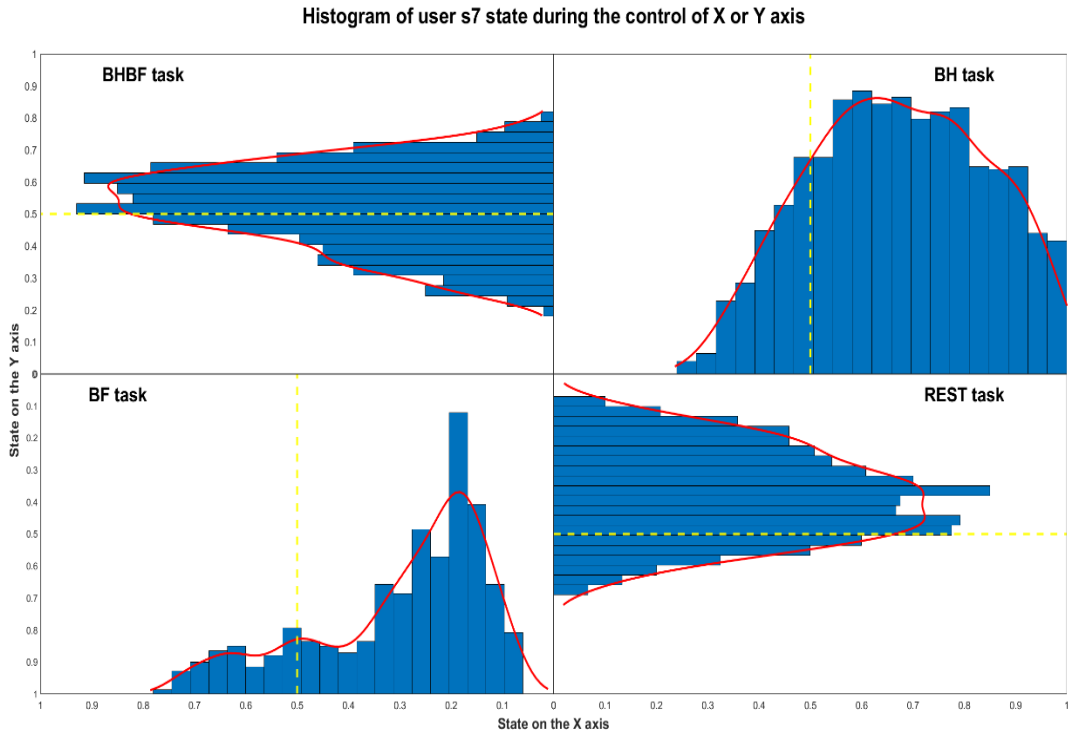

Figure 54: Histograms of all the state vector values achieved during the run with best performance for user s7.

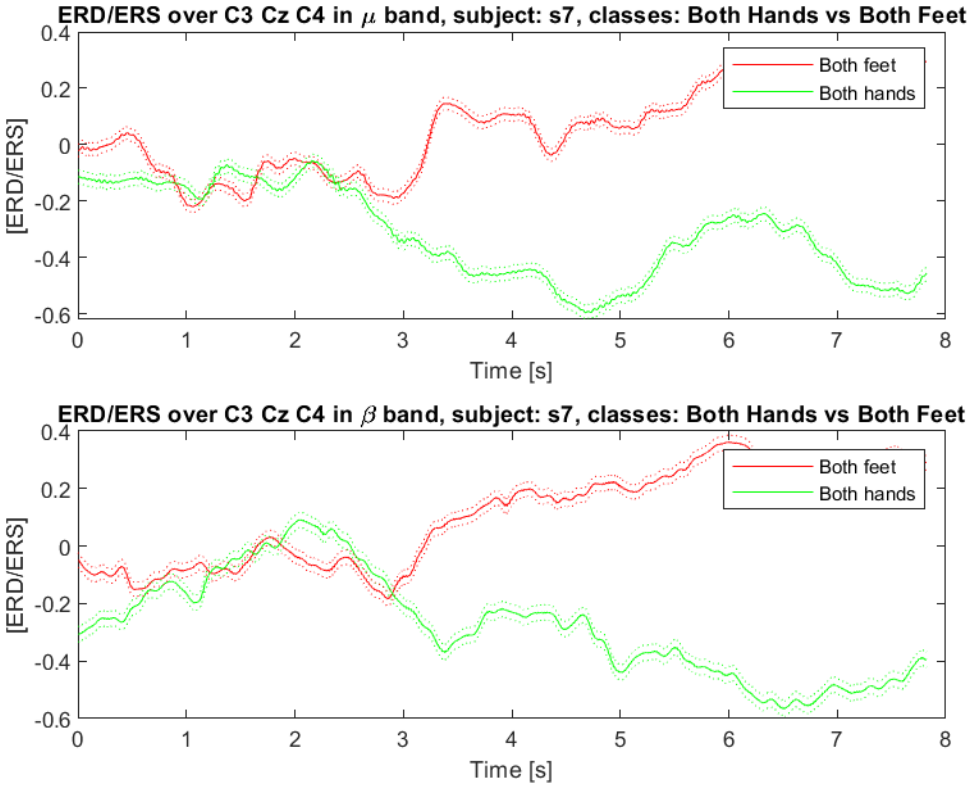

Figure 55: ERD/ERS over main target electrodes in μ and β bands for classes Both Hands and Both Feet, user s7.

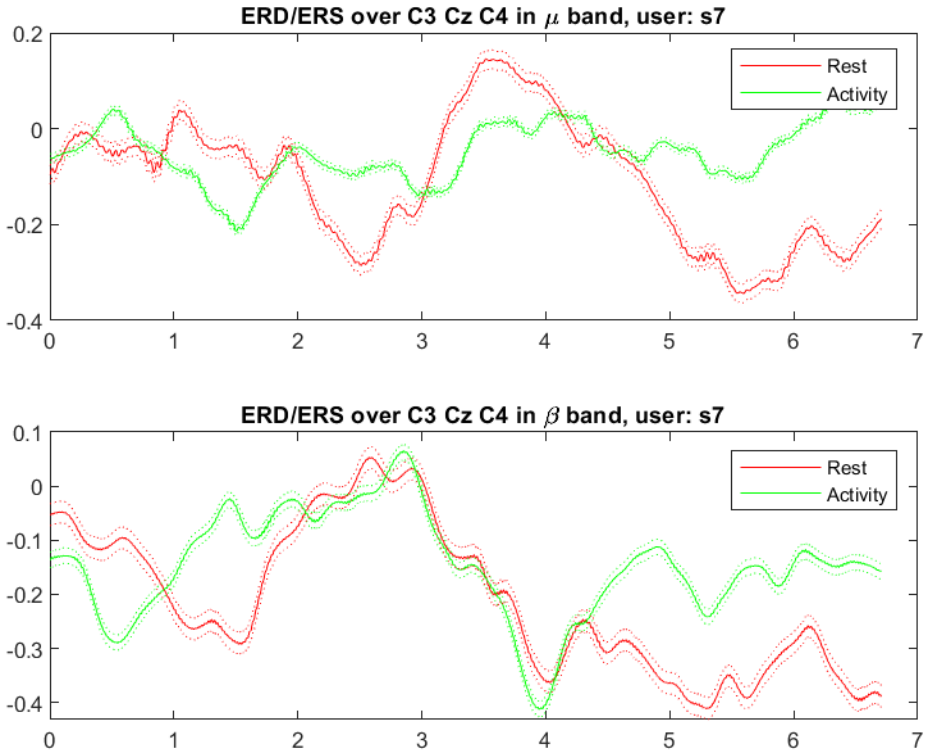

Figure 66: ERD/ERS over main target electrodes in μ and β bands for classes Activity (Both Hands and Both Feet together) and Rest, user s7.

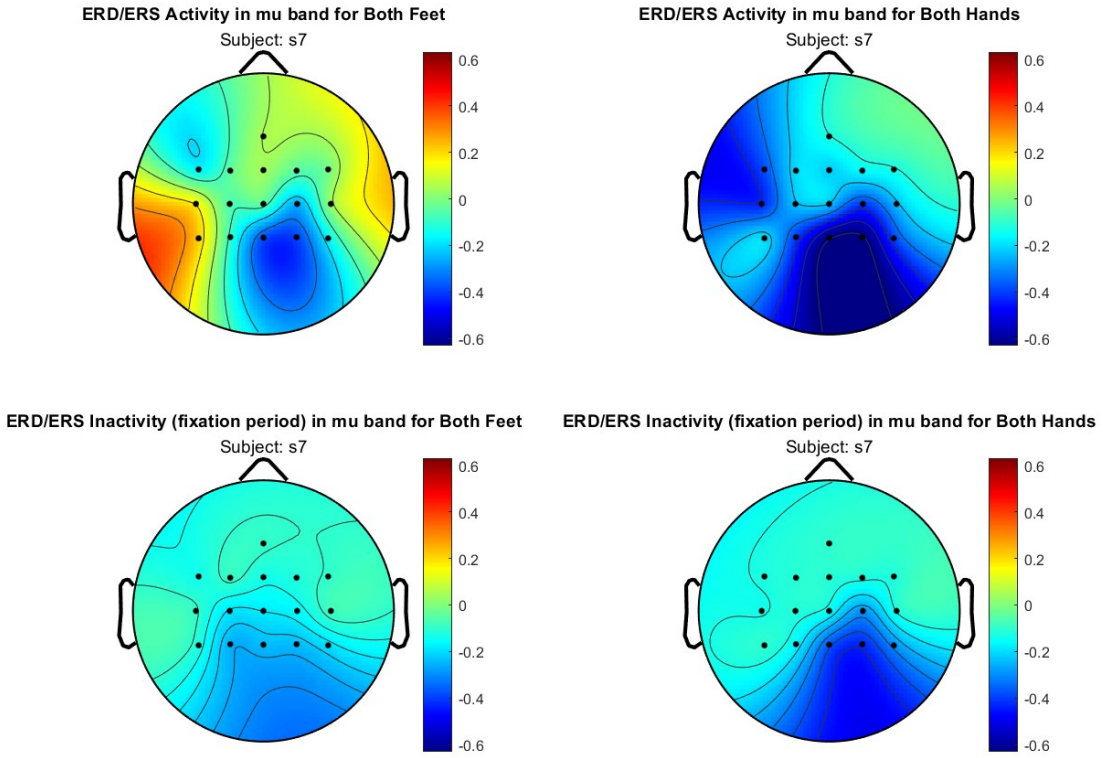

Figure 57: Topomaps related to the ERD/ERS of classes Both Hands and Both Feet, user s7.

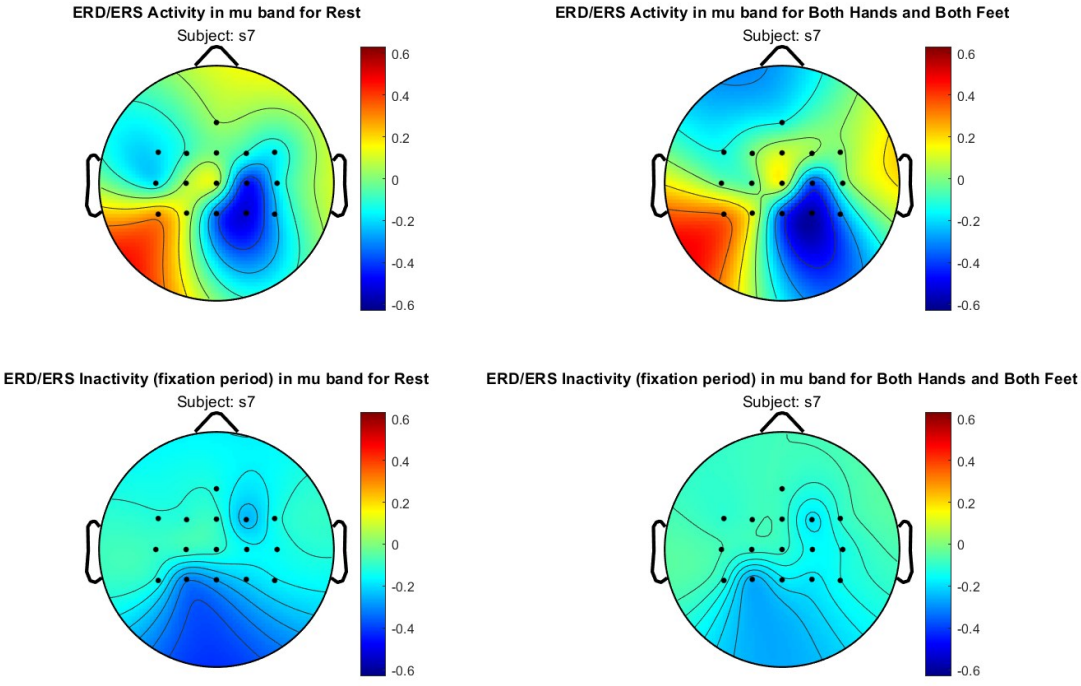

Figure 58: Topomaps related to the ERD/ERS of classes Activity (Both Hands and Both Feet) and Rest (respiration), user s7

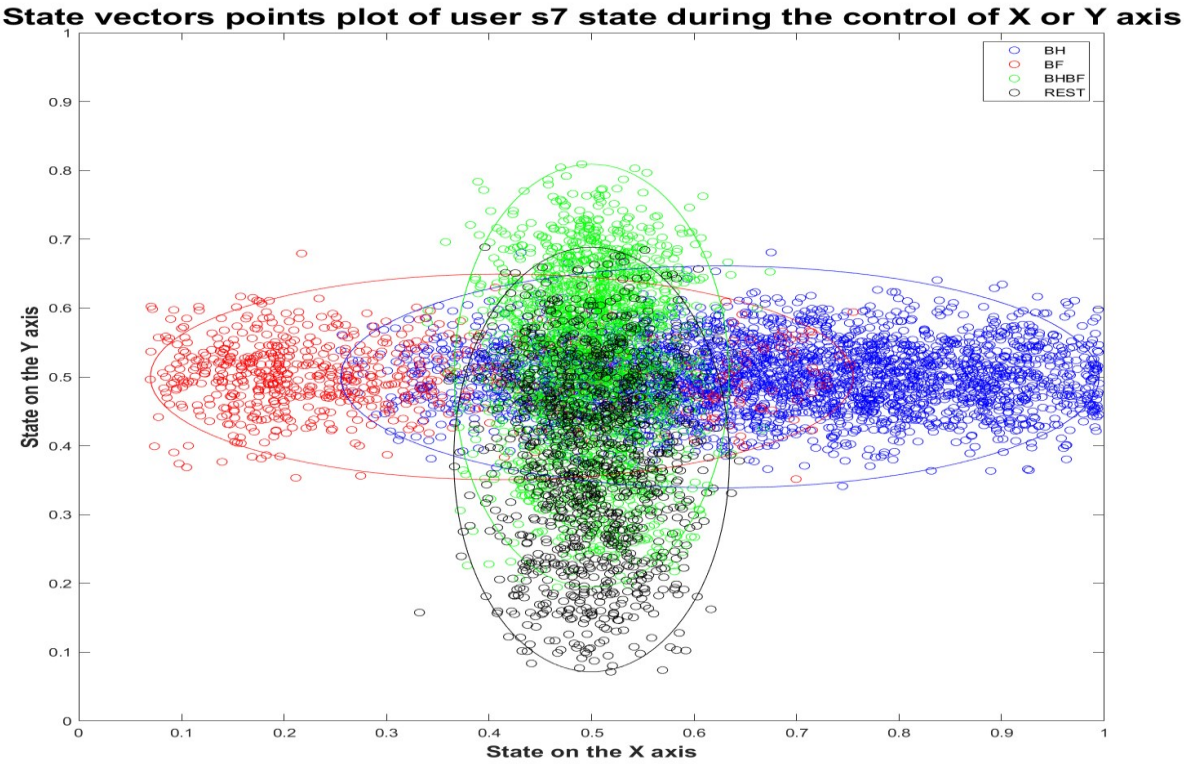

Figure 59: Plot of all the state vector values achieved during the runs with best performances for subject s7. Very good differentiation between the horizontal ellipses, good among the vertical ones.

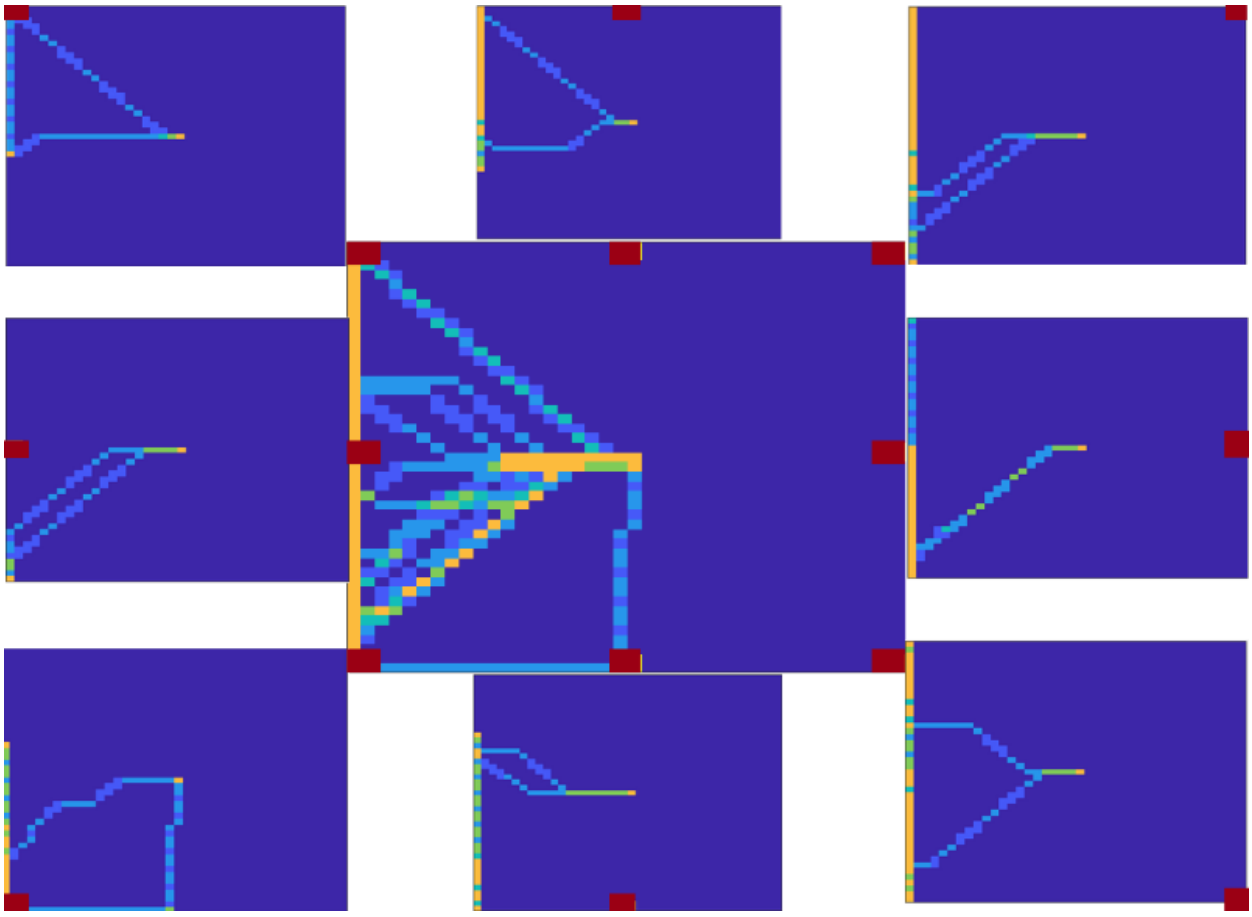

Figure 60: Heat maps of user s7.

User s8 – first setup

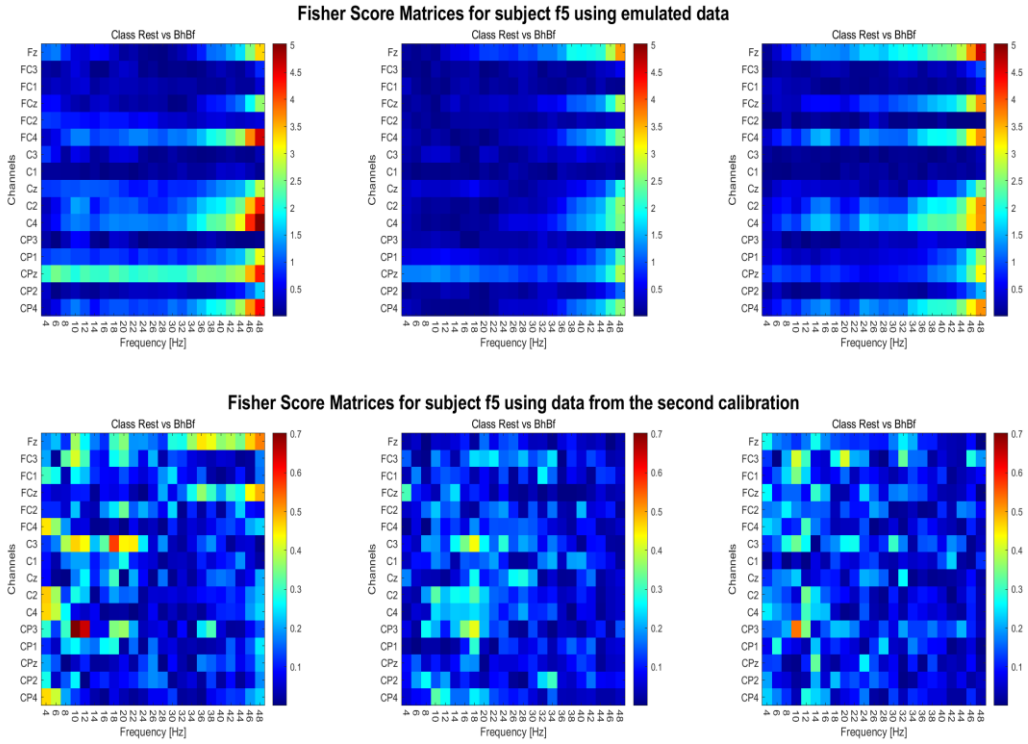

Figure 61: Fisher Score matrices of subject s8 to prove that class Both Hands and Both Feet cannot be derived from class Both Hands and class Both Feet data.

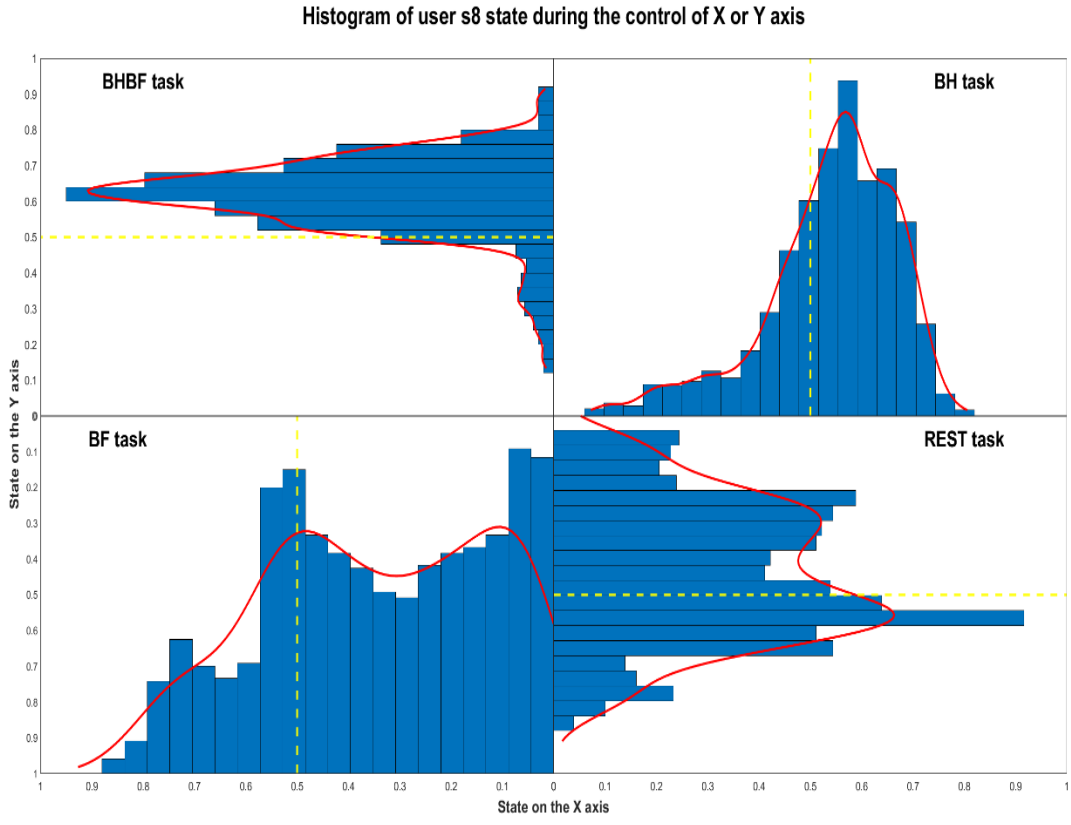

Figure 62: Histograms of all the state vector values achieved during the run with best performance for user s8.

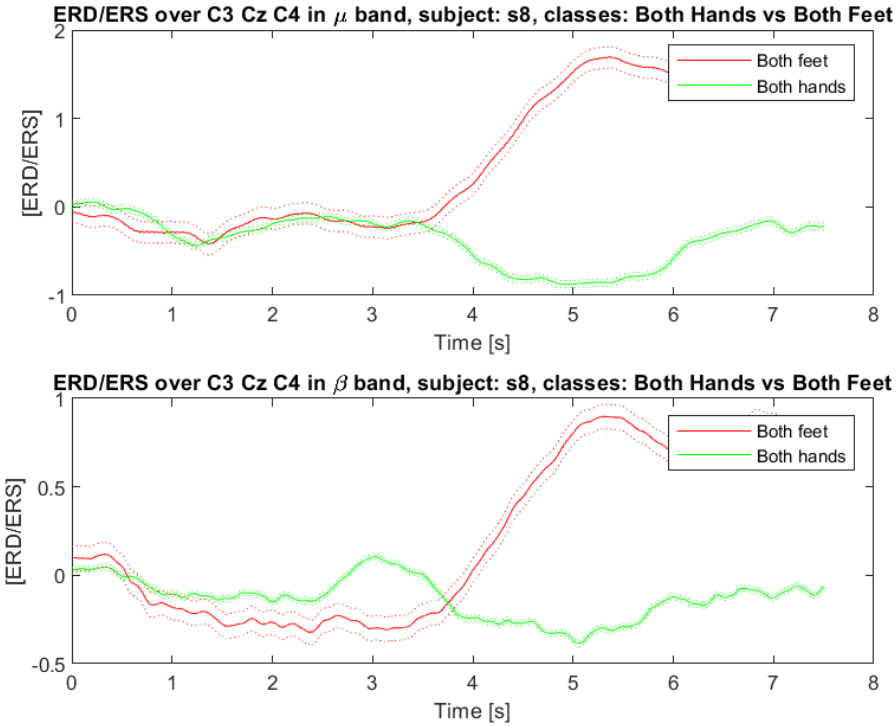

Figure 63: ERD/ERS over main target electrodes in μ and β bands for classes Both Hands and Both Feet, user s8.

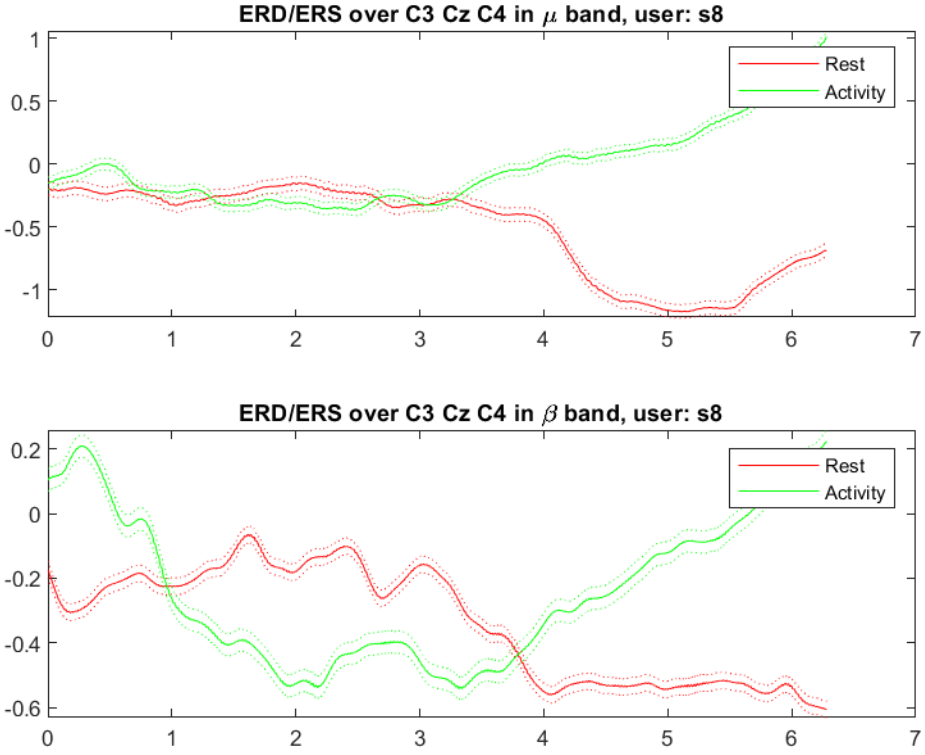

Figure 64: ERD/ERS over main target electrodes in μ and β bands for classes Activity (Both Hands and Both Feet together) and Rest, user s8.

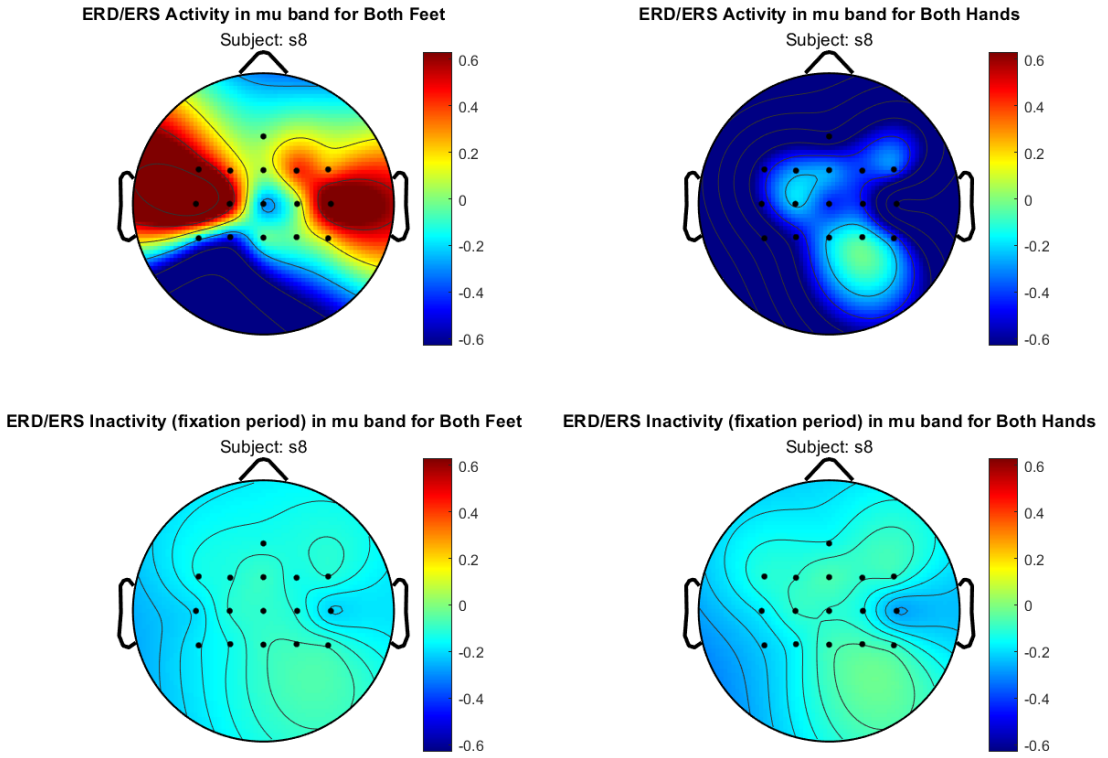

Figure 65: Topomaps related to the ERD/ERS of classes Both Hands and Both Feet, user s8.

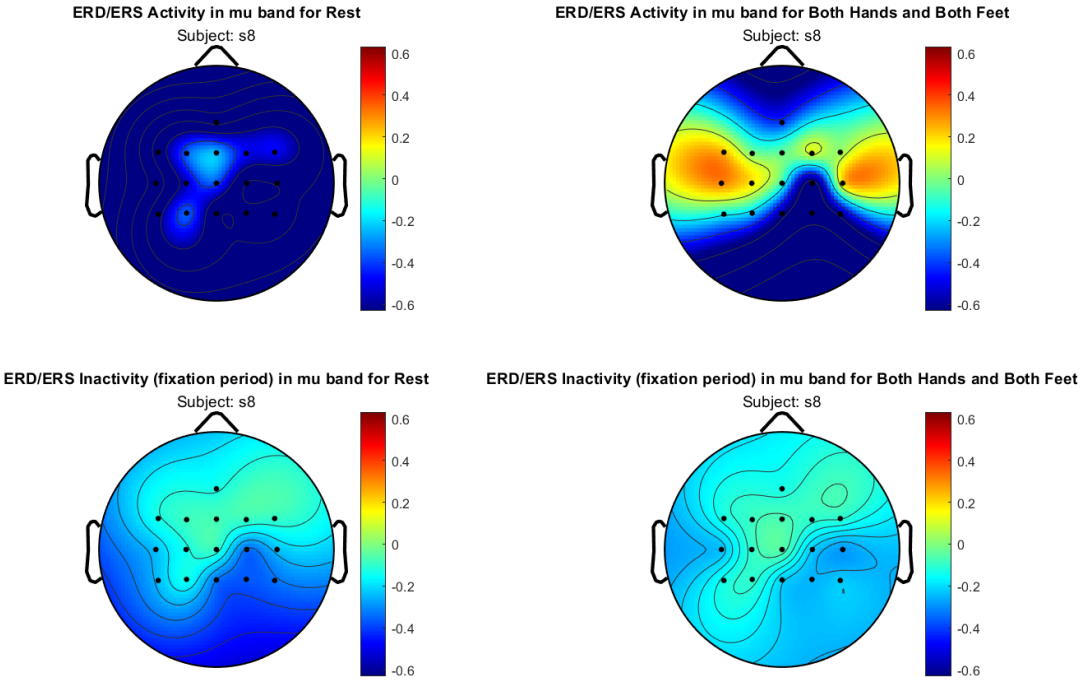

Figure 66: Topomaps related to the ERD/ERS of classes Activity (Both Hands and Both Feet) and Rest (respiration), user s8.

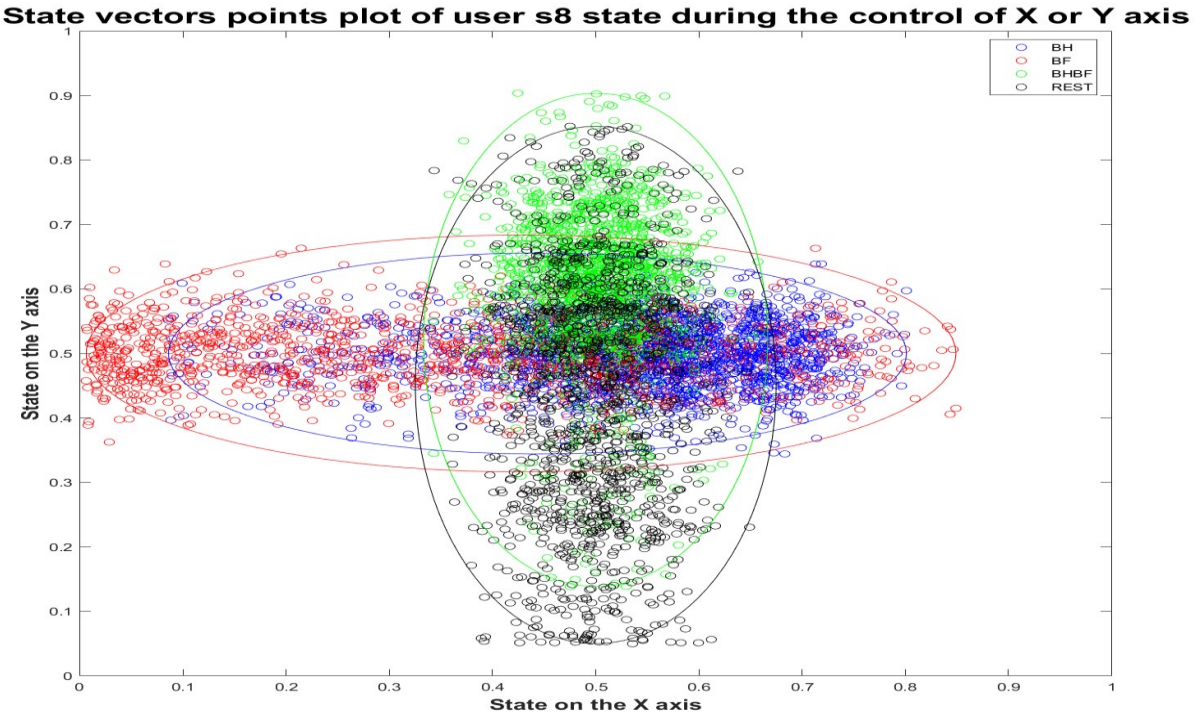

Figure 67: Plot of all the state vector values achieved during the runs with best performances for subject s8Almost a complete overlap among both the horizontal and the vertical ellipses.

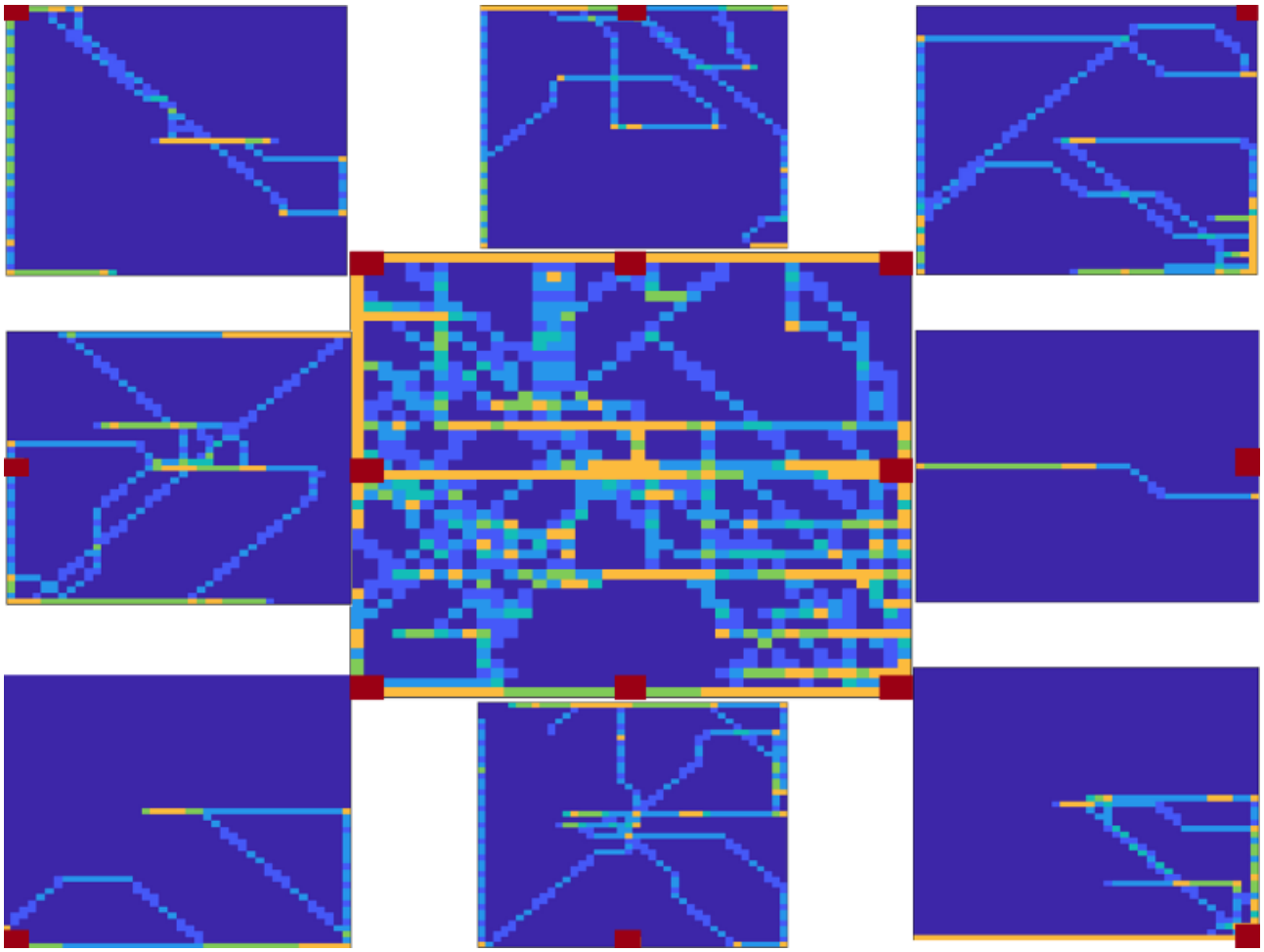

Figure 68: Heat maps of user s10.

User s10 – first setup

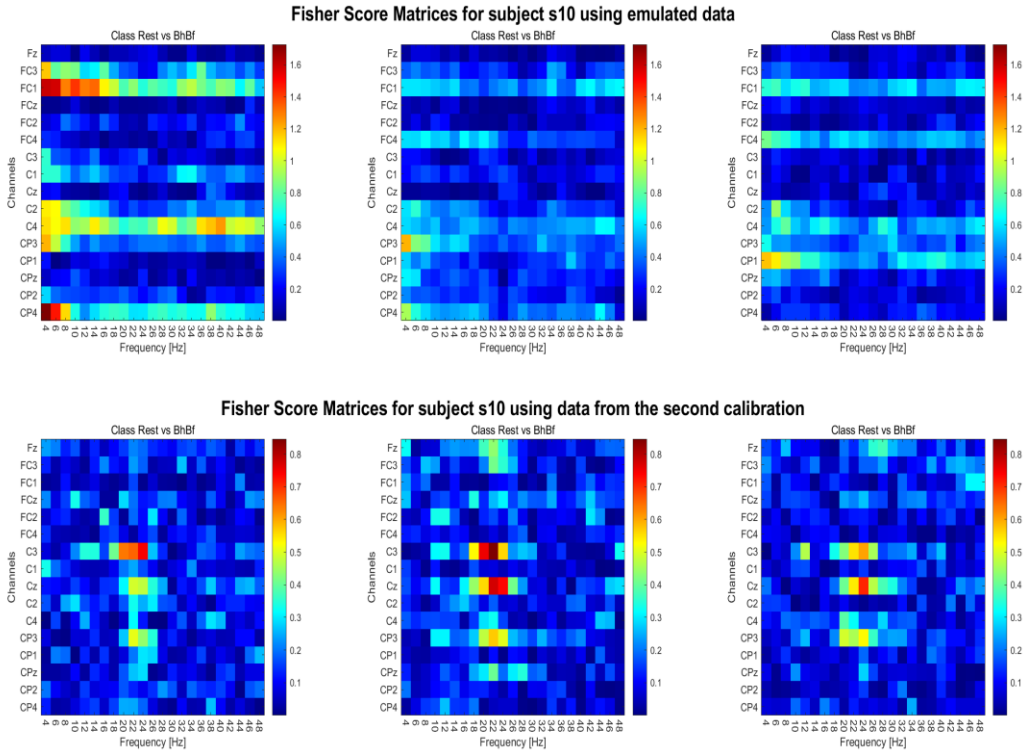

Figure 69: Fisher Score matrices of subject s10 to prove that class Both Hands and Both Feet cannot be derived from class Both Hands and class Both Feet data.

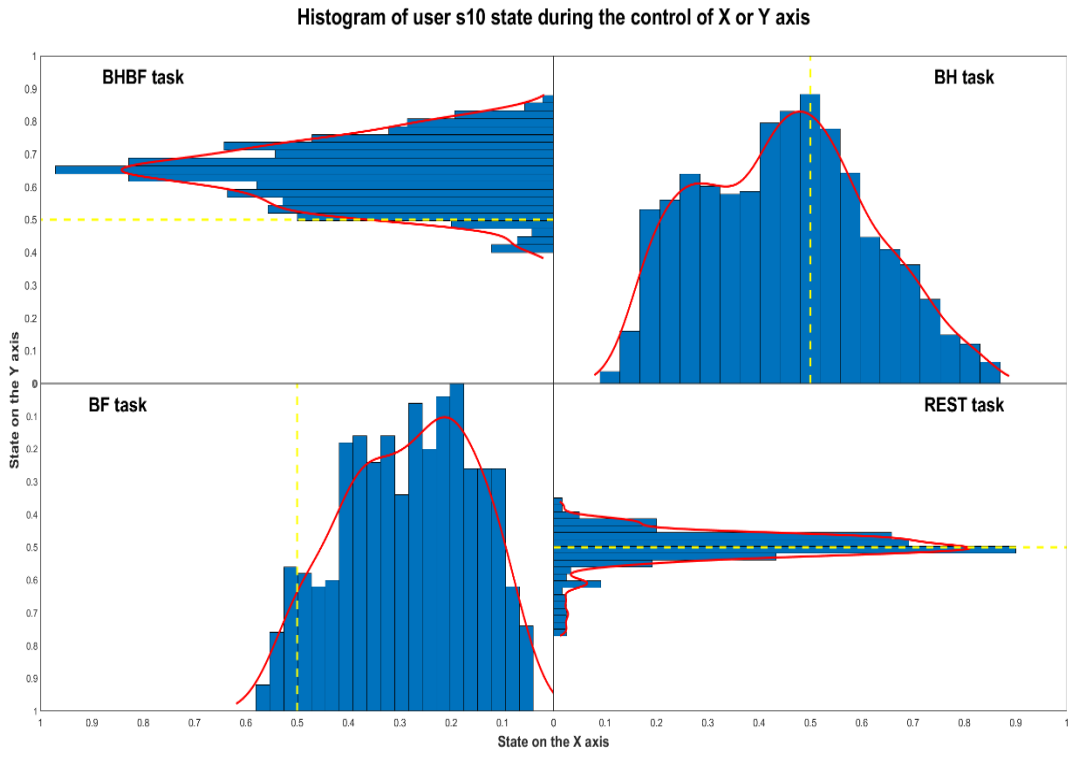

Figure 70: Histograms of all the state vector values achieved during the run with best performance for user s10.

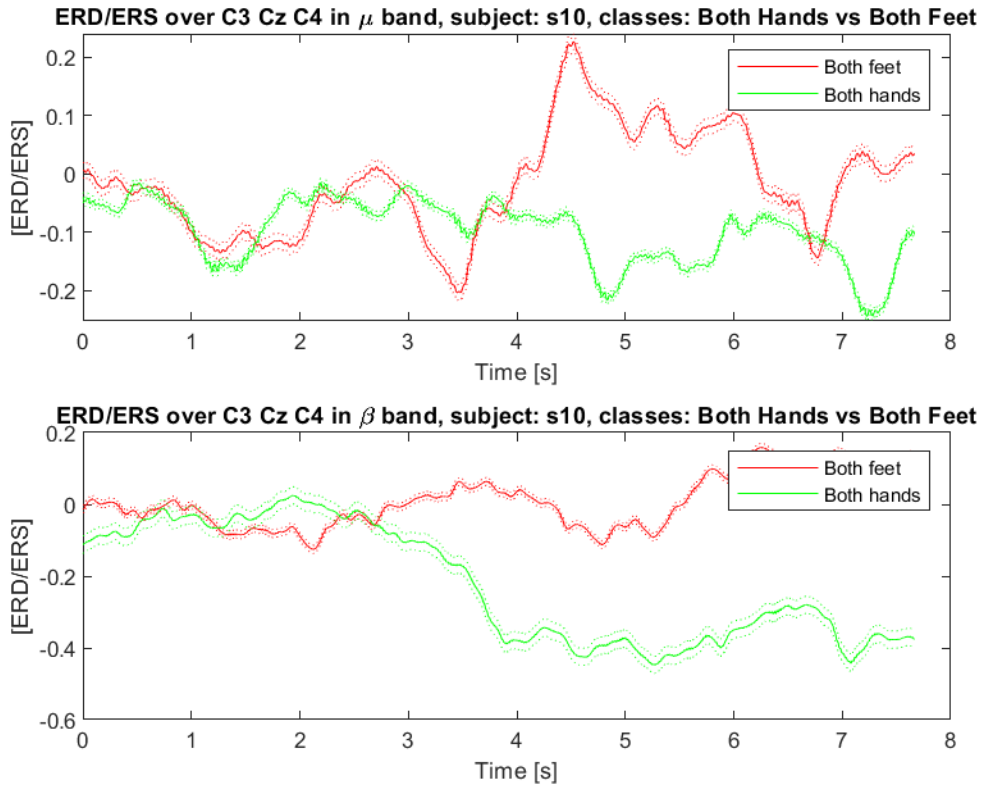

Figure 72: ERD/ERS over main target electrodes in μ and β bands for classes Both Hands and Both Feet, user s10.

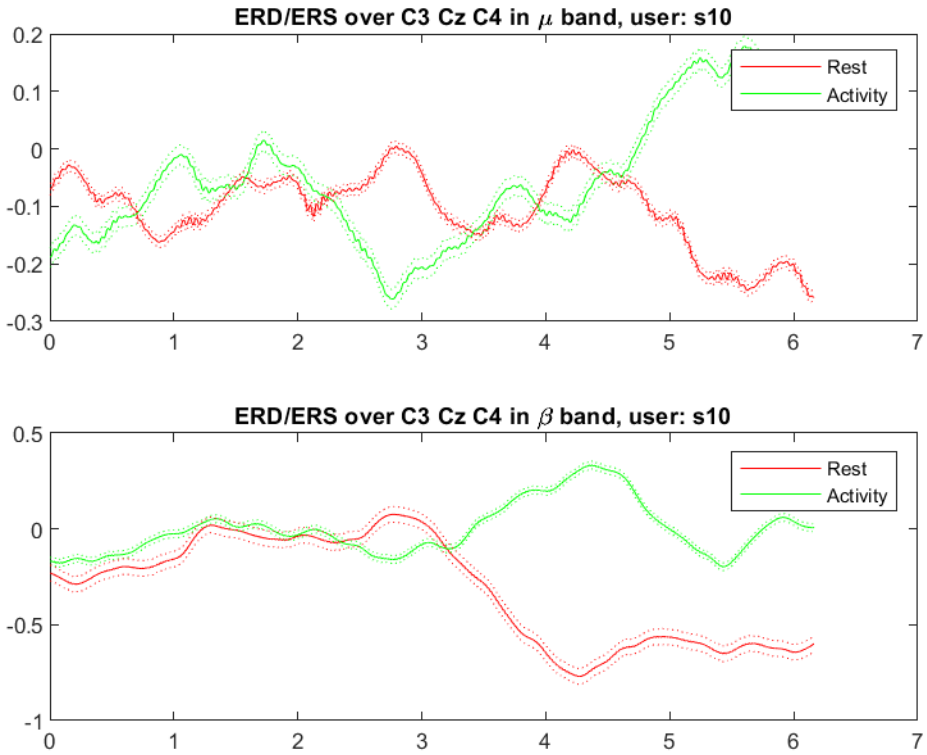

Figure 73: ERD/ERS over main target electrodes in μ and β bands for classes Activity (Both Hands and Both Feet together) and Rest, user s10.

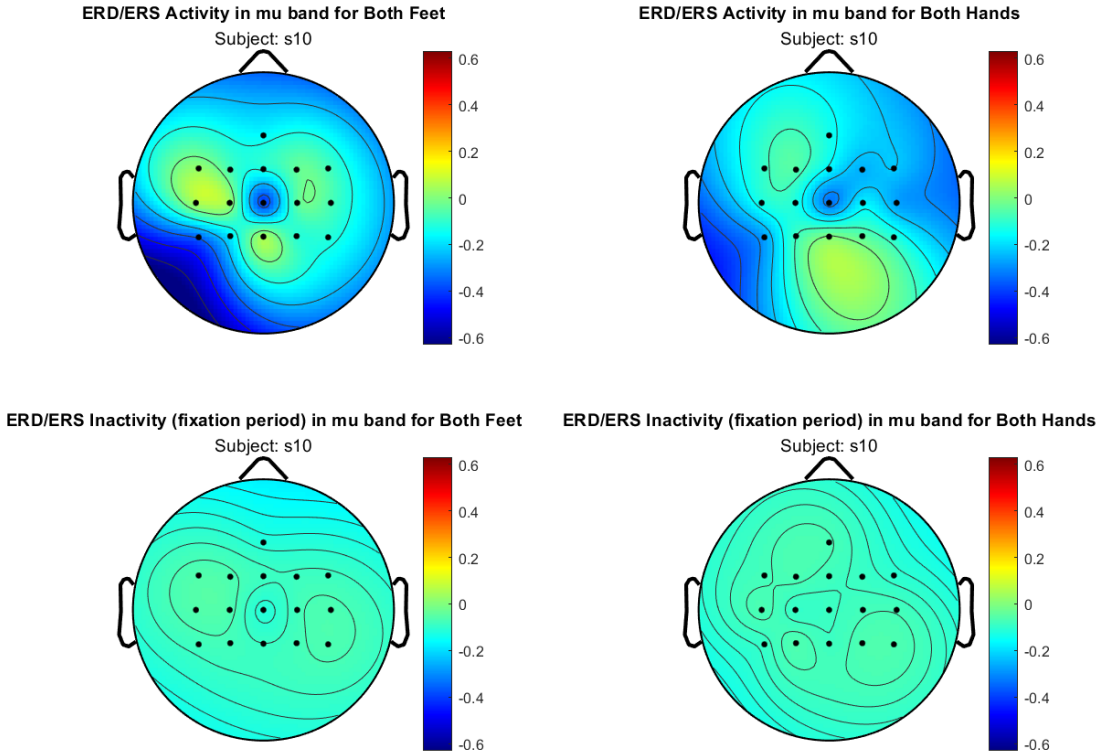

Figure 74: Topomaps related to the ERD/ERS of classes Both Hands and Both Feet, user s10.

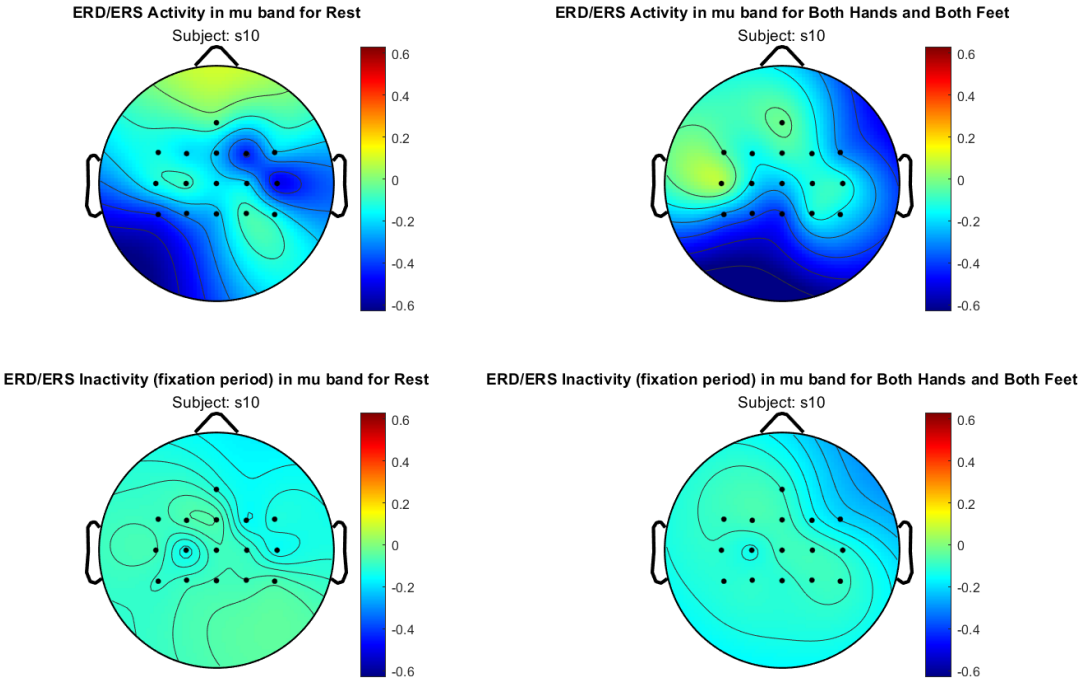

Figure 75: Topomaps related to the ERD/ERS of classes Activity (Both Hands and Both Feet) and Rest (respiration), user s10.

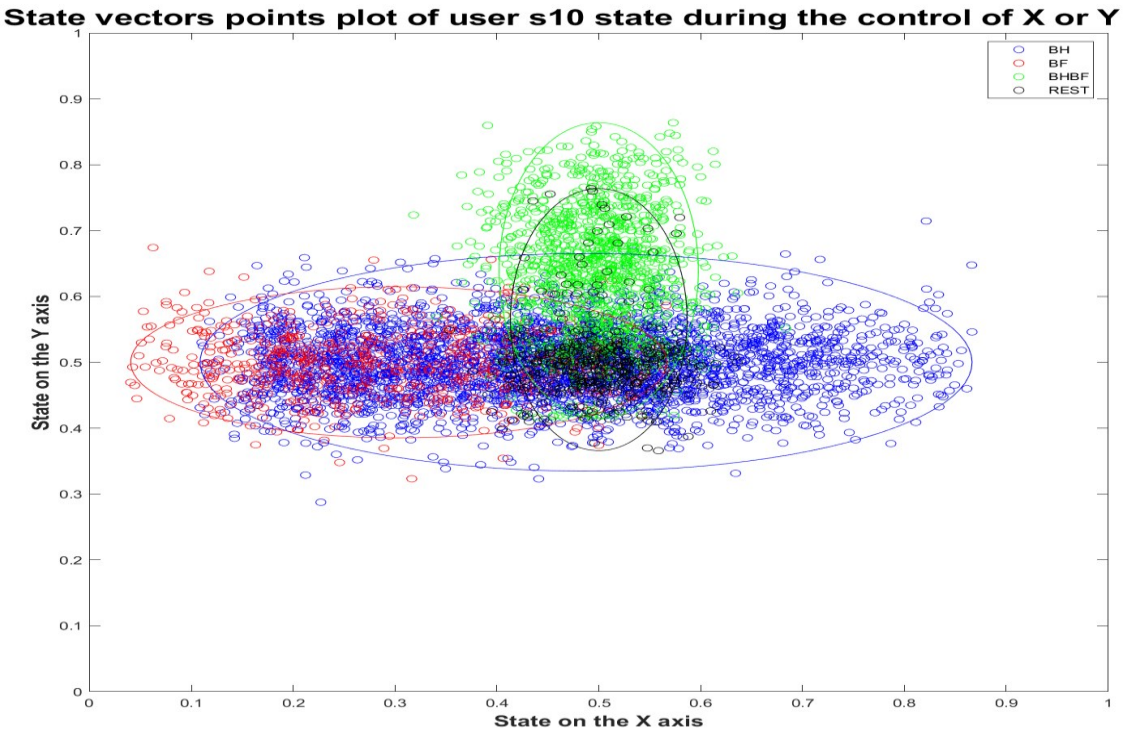

Figure 76: Plot of all the state vector values achieved during the runs with best performances for subject s10. Much overlap among both the horizontal and vertical ellipses.

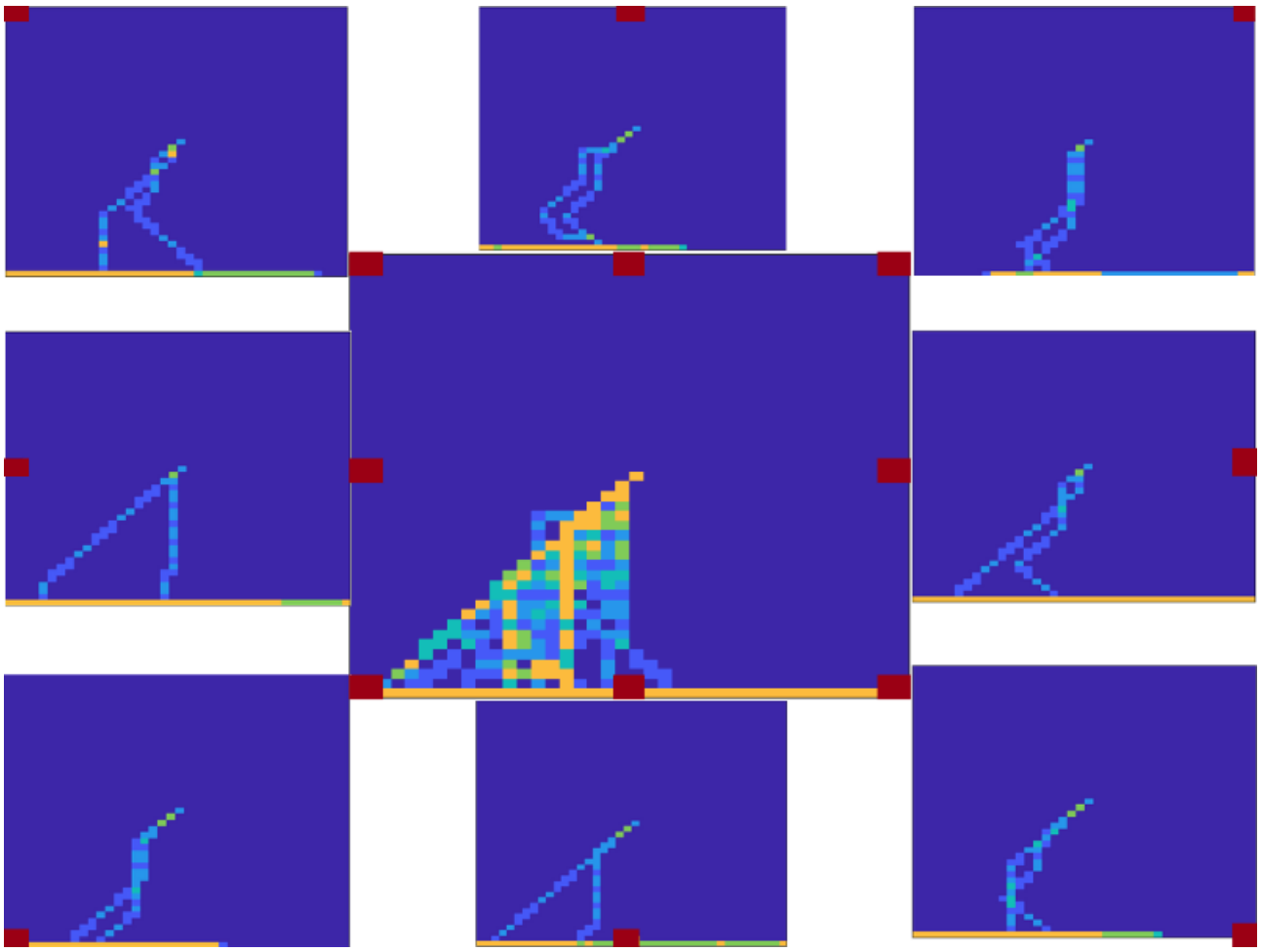

Figure 77: Heat maps of user s10.

User s11 – first setup

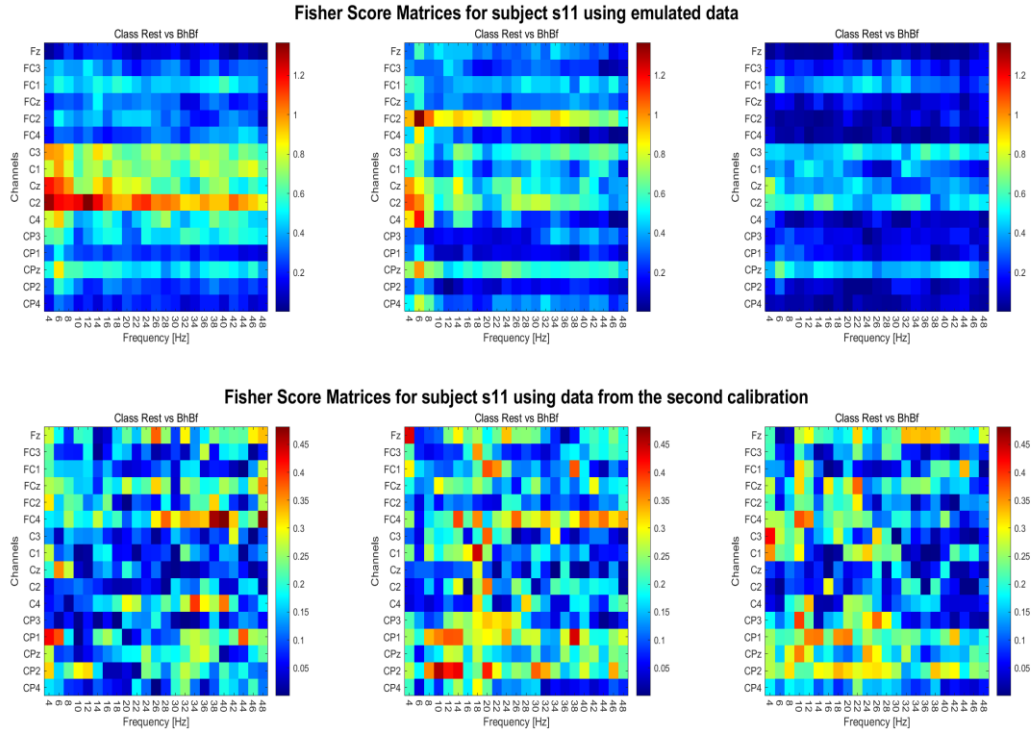

Figure 78: Fisher Score matrices of subject s11 to prove that class Both Hands and Both Feet cannot be derived from class Both Hands and class Both Feet data.

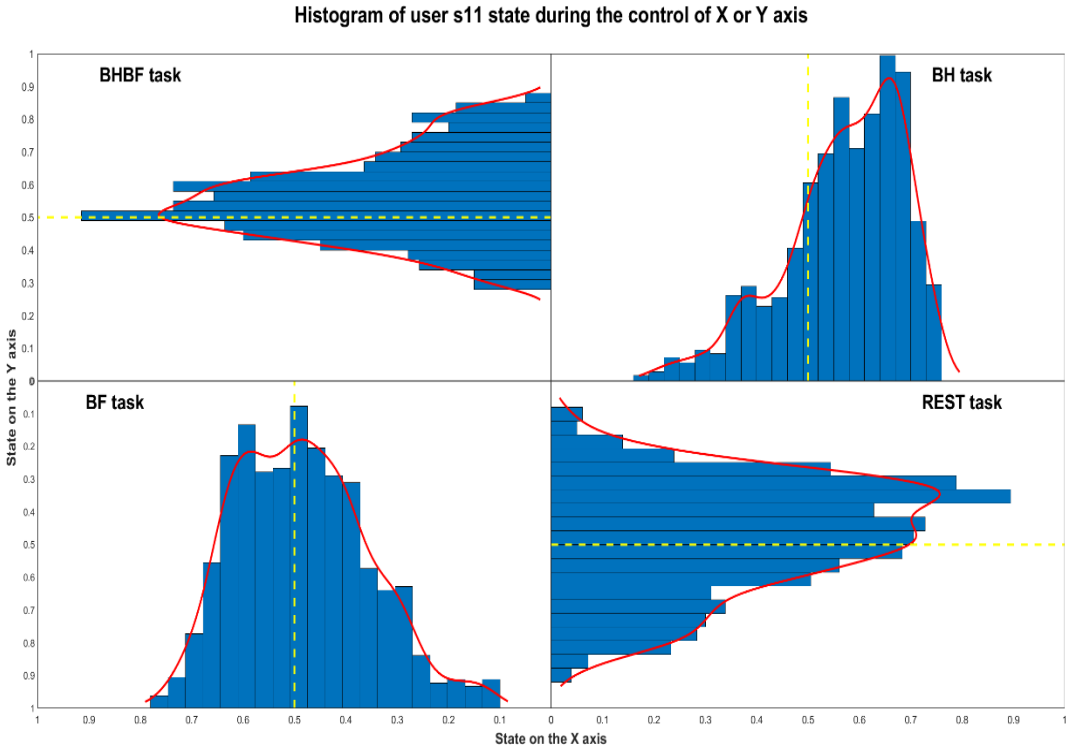

Figure 79: Histograms of all the state vector values achieved during the run with best performance for user s11.

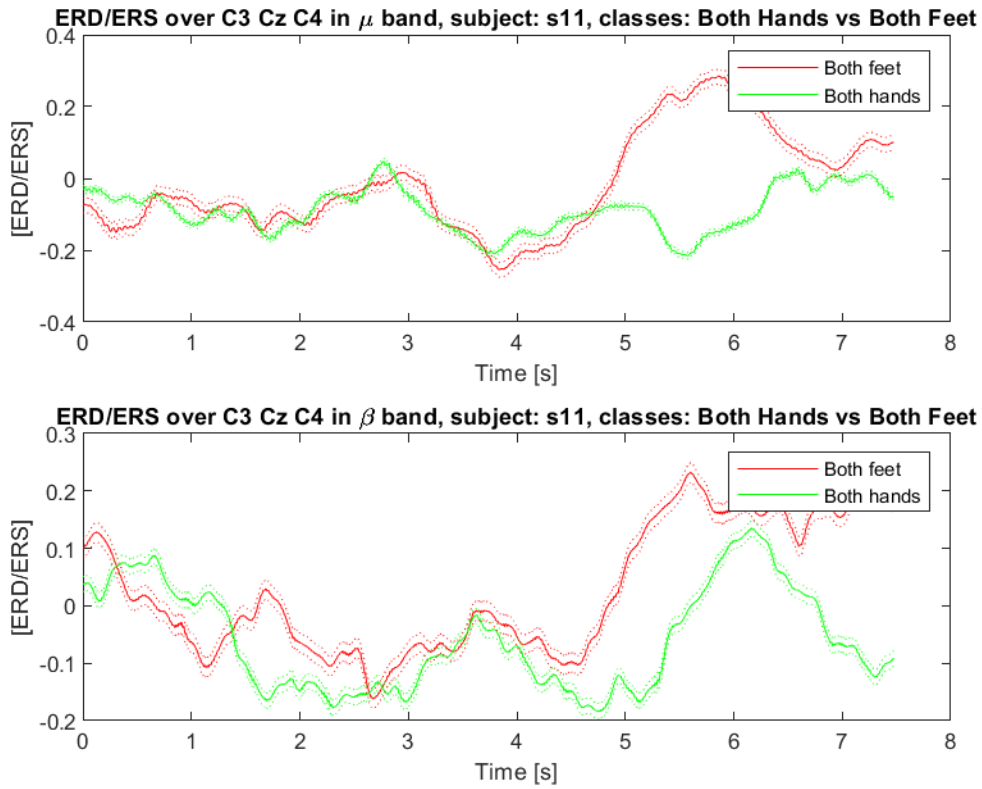

Figure 80: ERD/ERS over main target electrodes in μ and β bands for classes Both Hands and Both Feet, user s11.

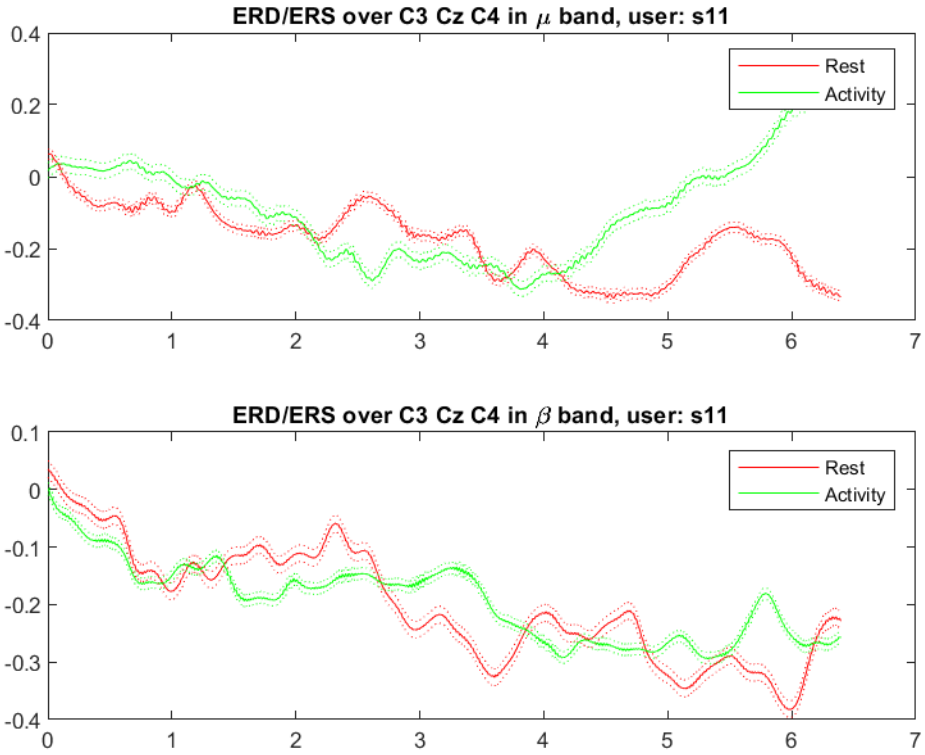

Figure 81: ERD/ERS over main target electrodes in μ and β bands for classes Activity (Both Hands and Both Feet together) and Rest, user s11.

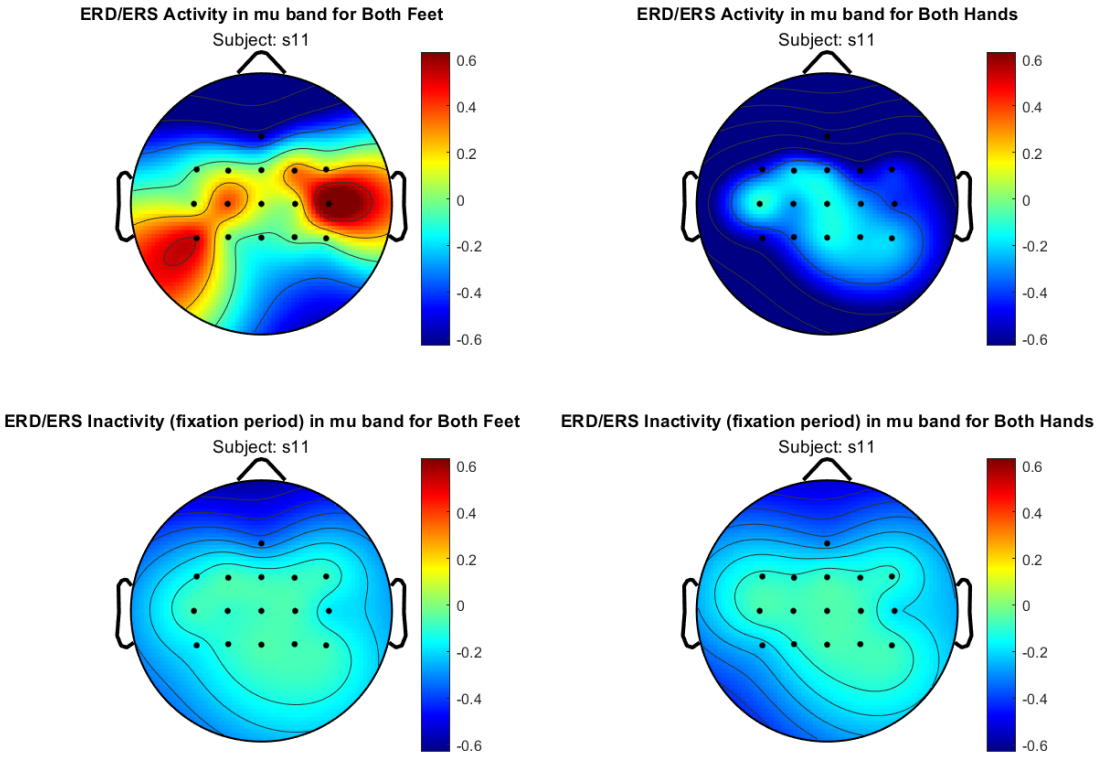

Figure 82: Topomaps related to the ERD/ERS of classes Both Hands and Both Feet, user s11.

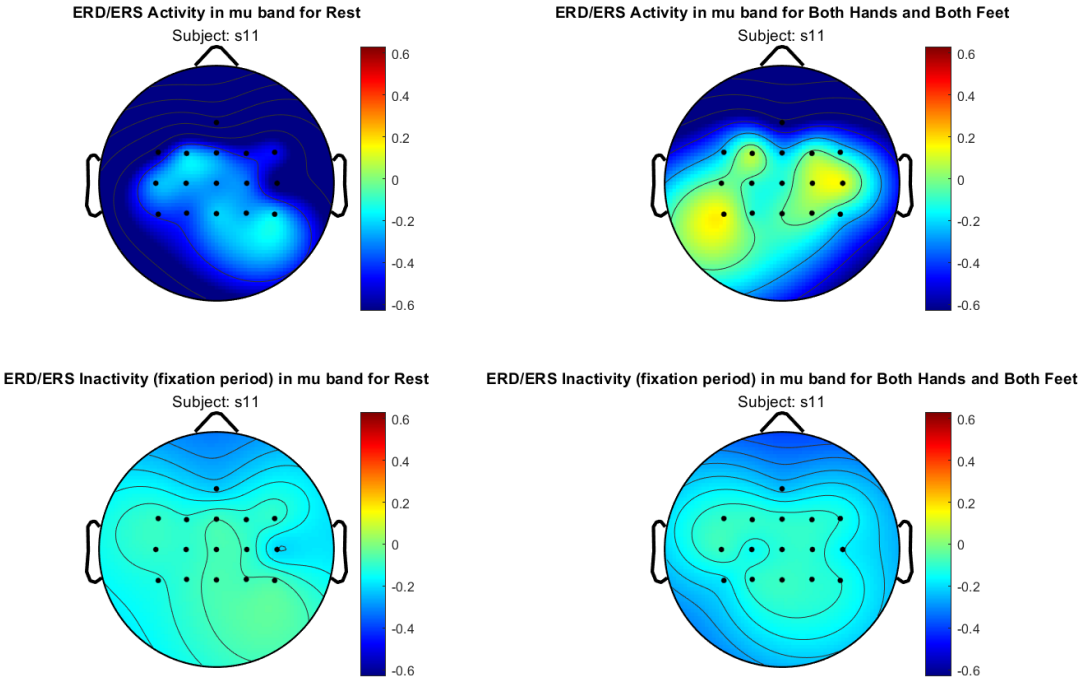

Figure 87: Topomaps related to the ERD/ERS of classes Activity (Both Hands and Both Feet) and Rest (respiration), user s11.

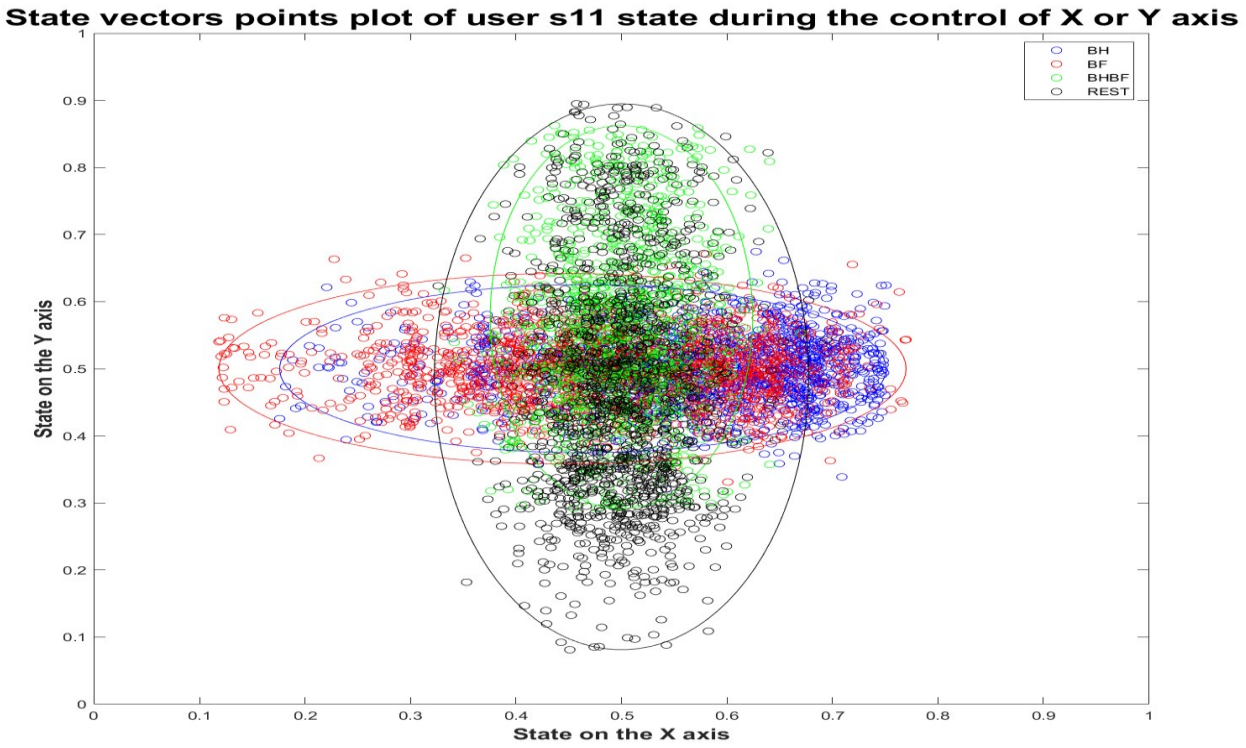

Figure 84: Plot of all the state vector values achieved during the runs with best performances for subject s11. Great overlap between the horizontal ellipses, while on the vertical side the black ellipse completely incorporates the green one.

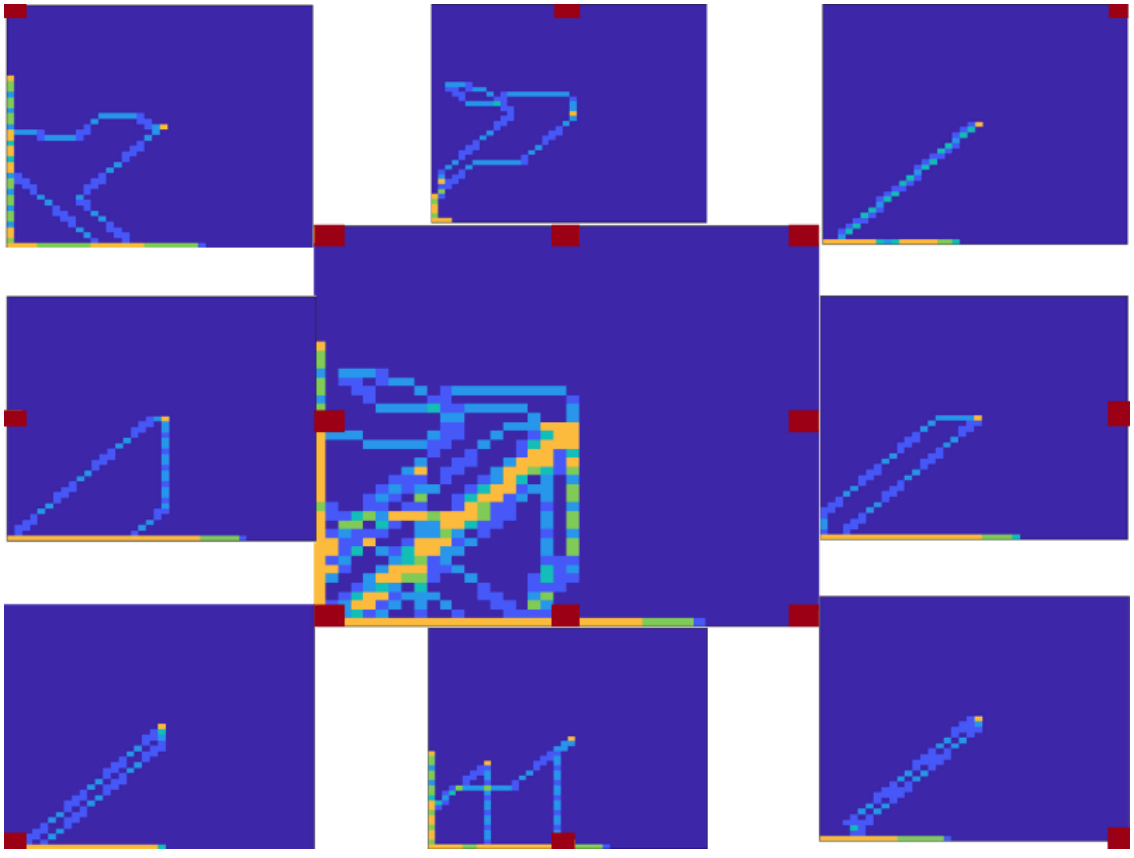

Figure 85: Heat maps of user s11.

User s1 – second setup

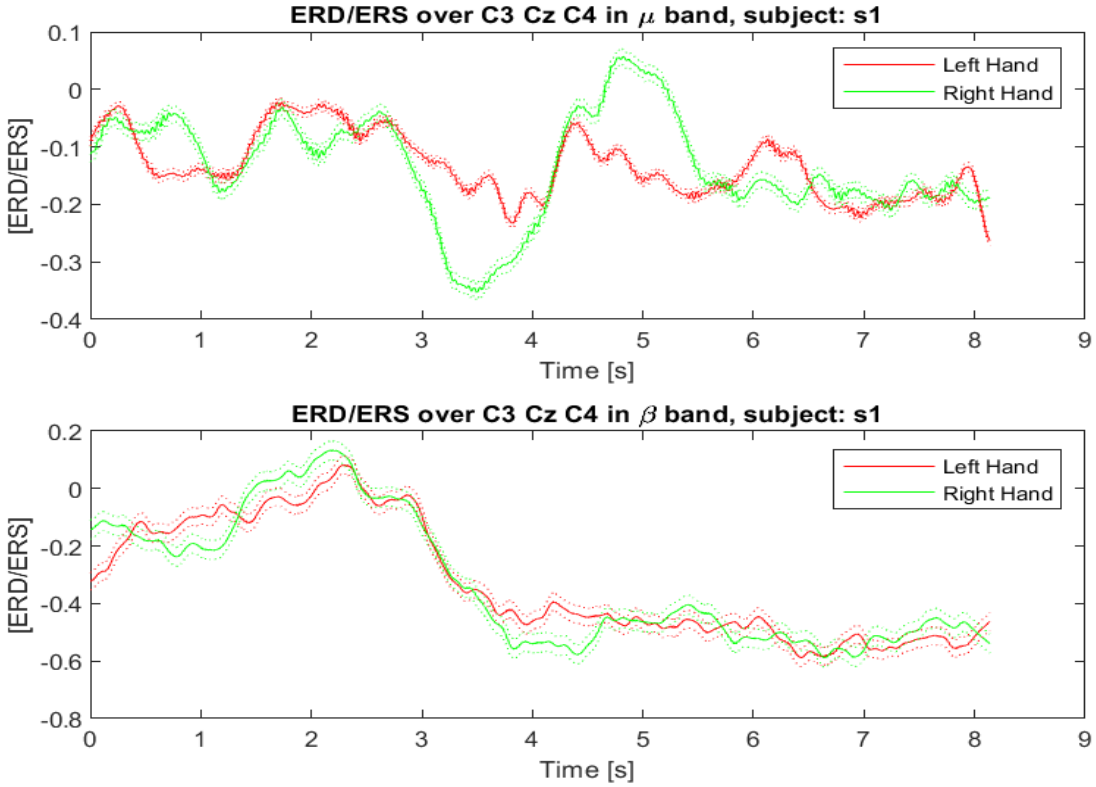

Figure 86: ERD/ERS over main target electrodes in μ and β bands for classes Right Hand and Left Hand, user s1.

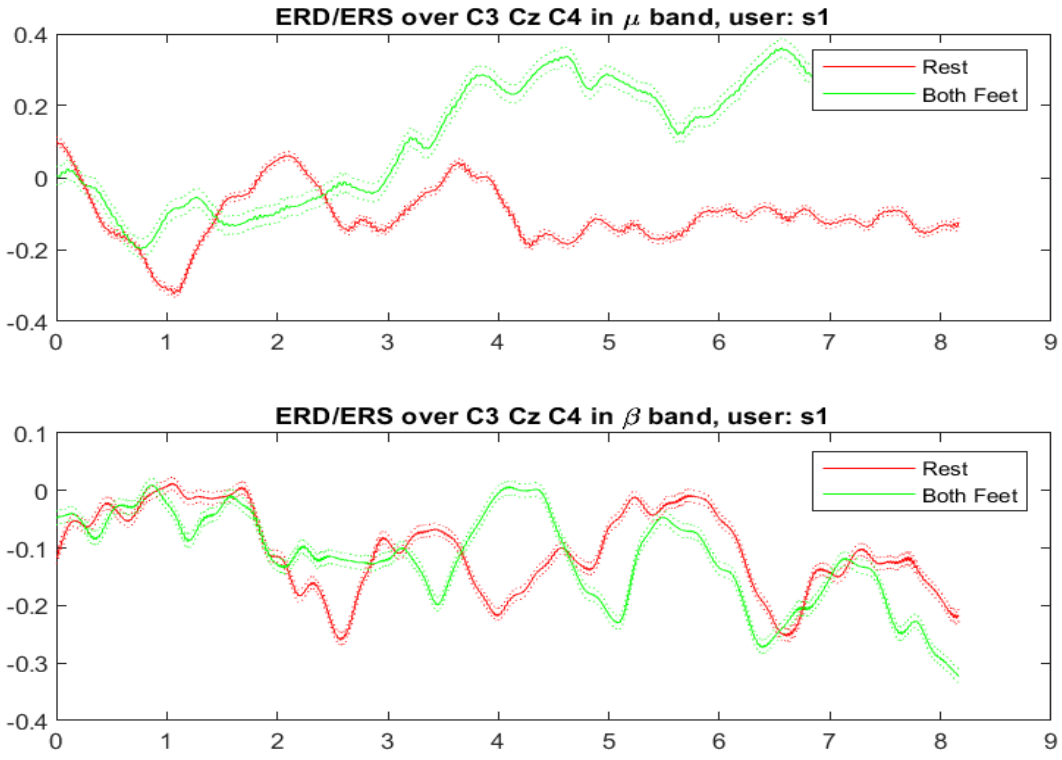

Figure 87: ERD/ERS over main target electrodes in μ and β bands for classes Both Feet and Rest, user s1.

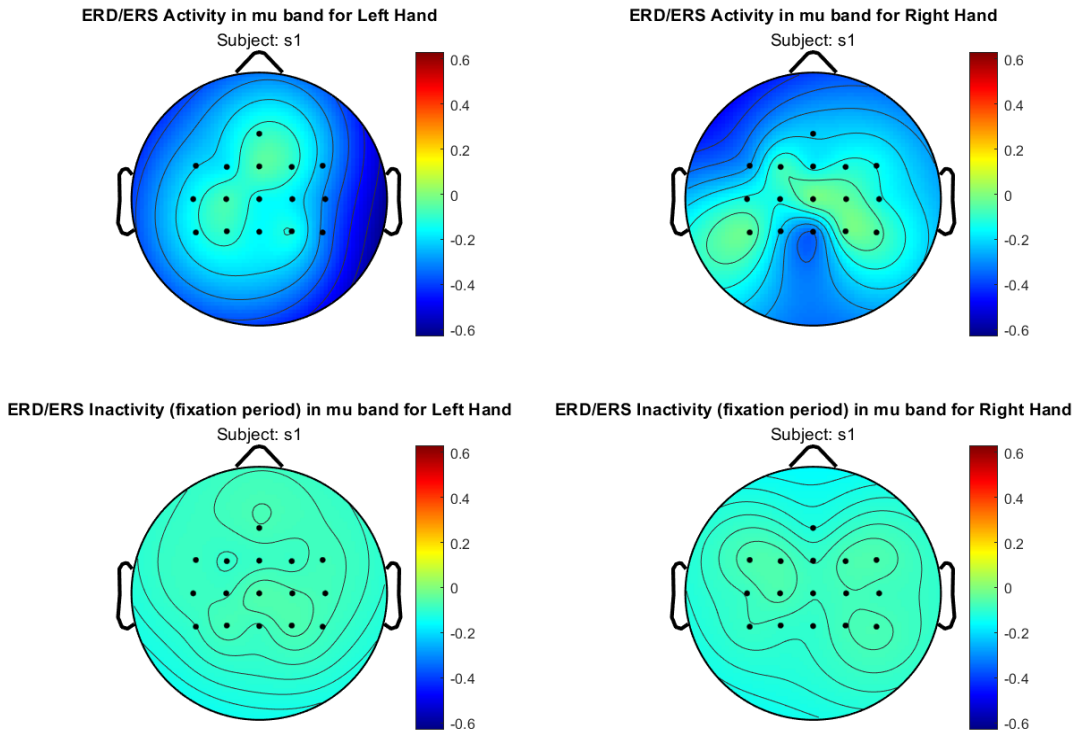

Figure 88: Topomaps related to the ERD/ERS of classes Right Hand and Left Hand, user s1.

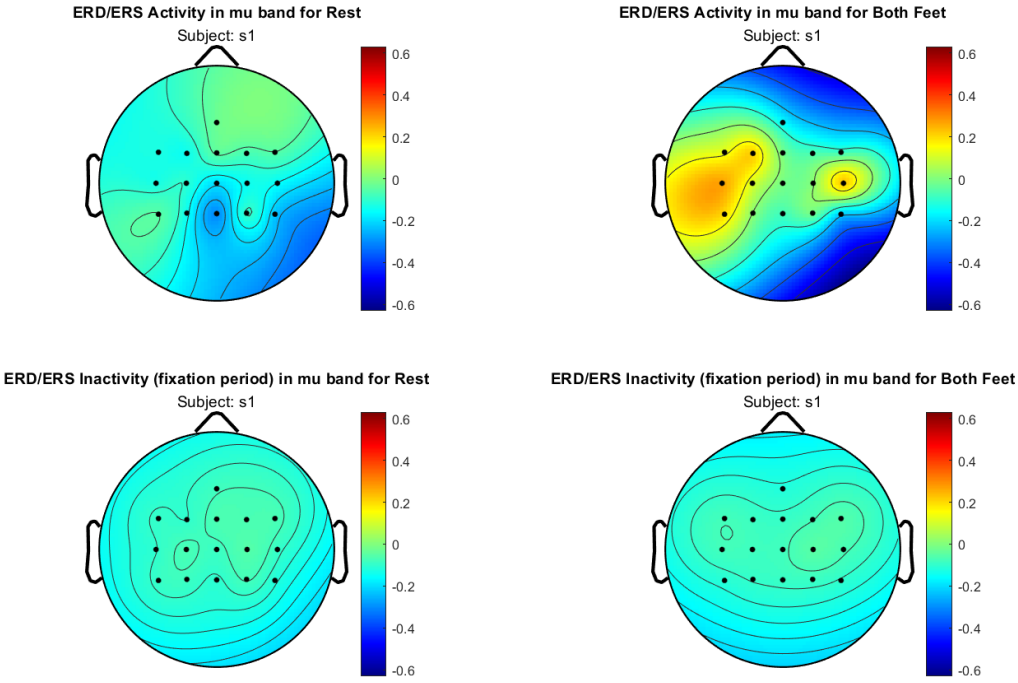

Figure 89: Topomaps related to the ERD/ERS of classes Both Feet and Rest, user s1.

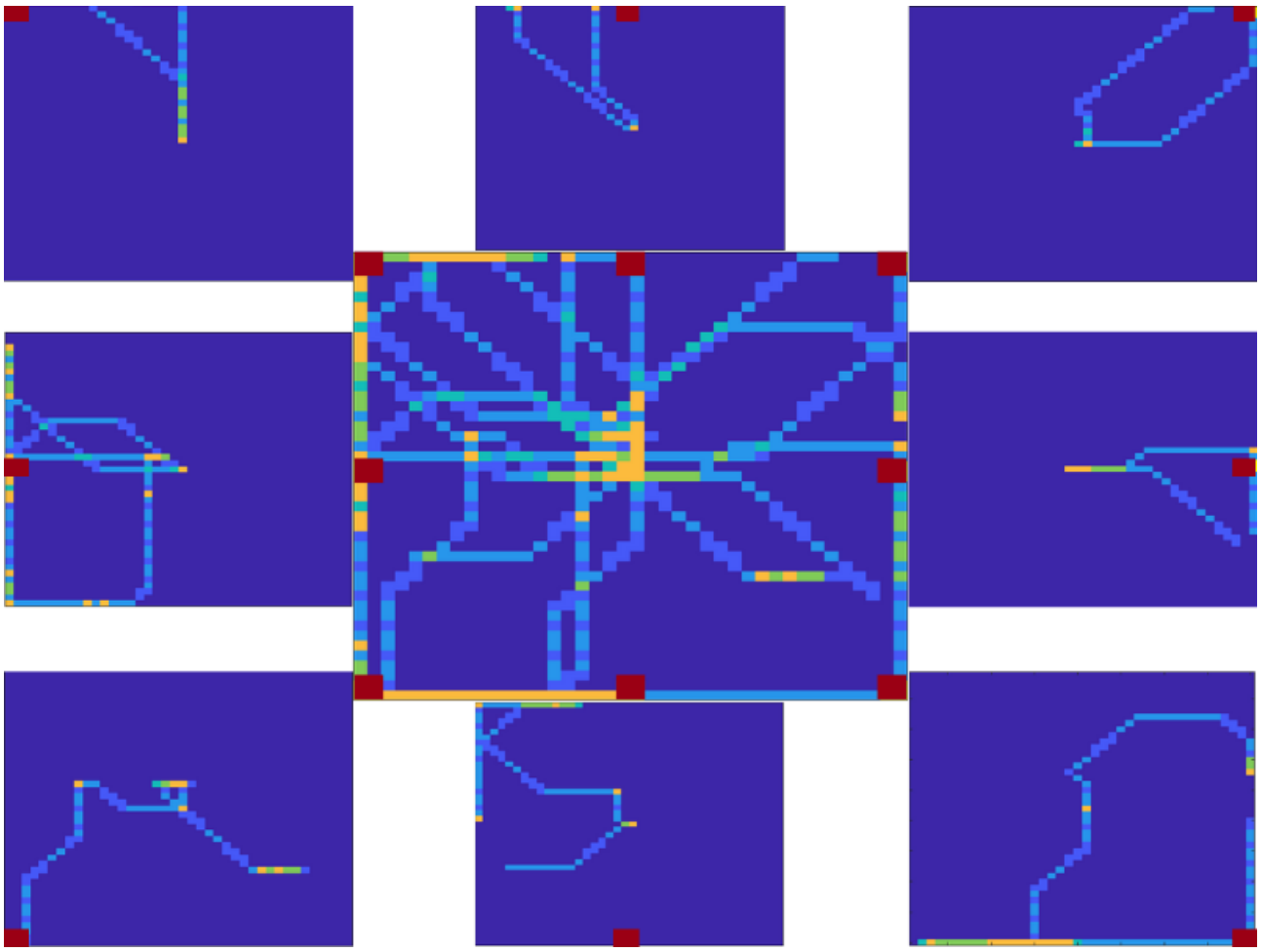

Figure 8: Heat maps of user s1, second setup.

User s3 – second setup

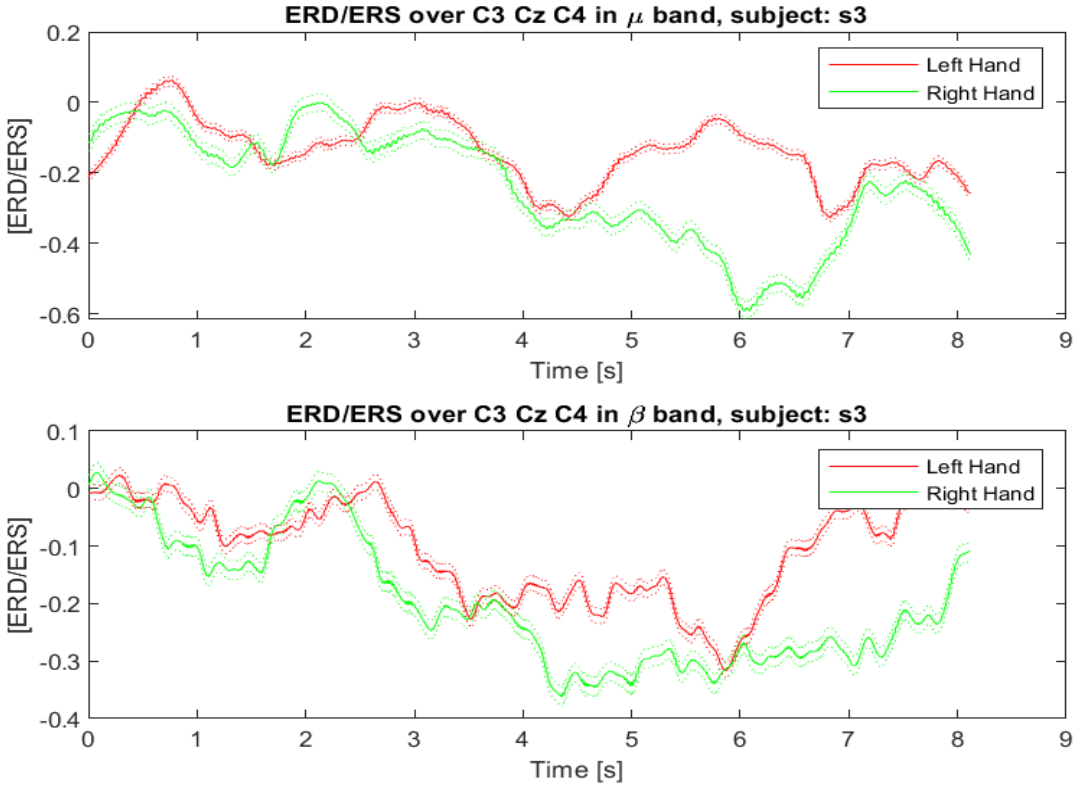

Figure 91: ERD/ERS over main target electrodes in μ and β bands for classes Right Hand and Left Hand, user s3.

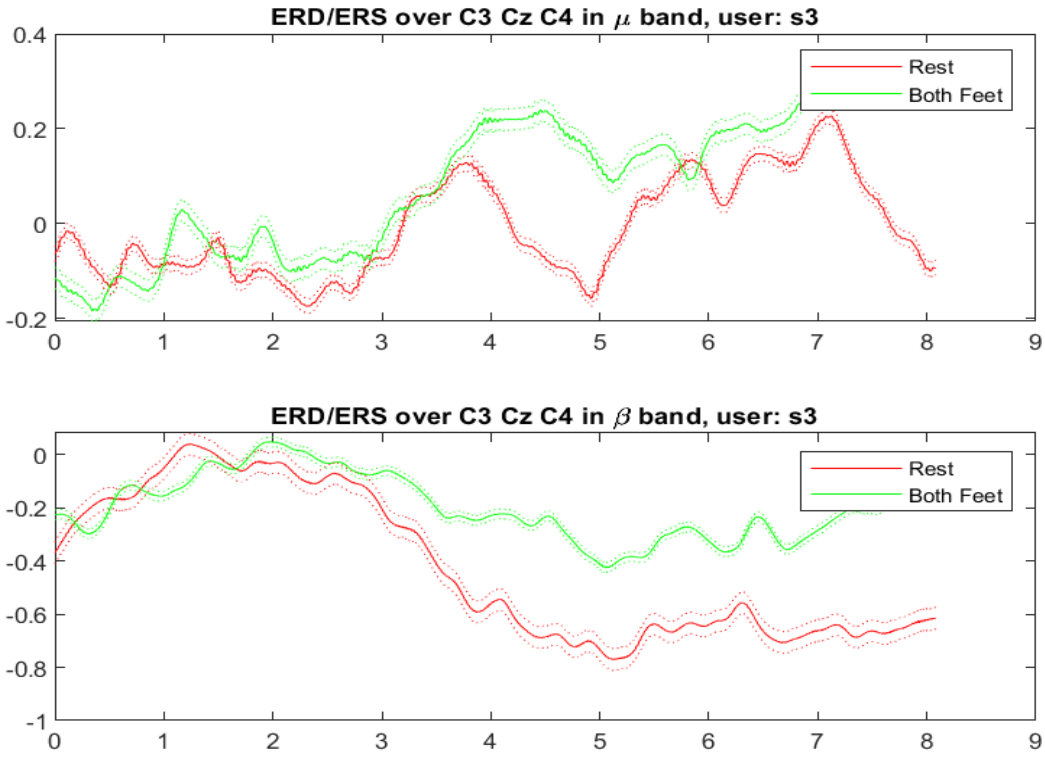

Figure 92: ERD/ERS over main target electrodes in μ and β bands for classes Both Feet and Rest, user s3.

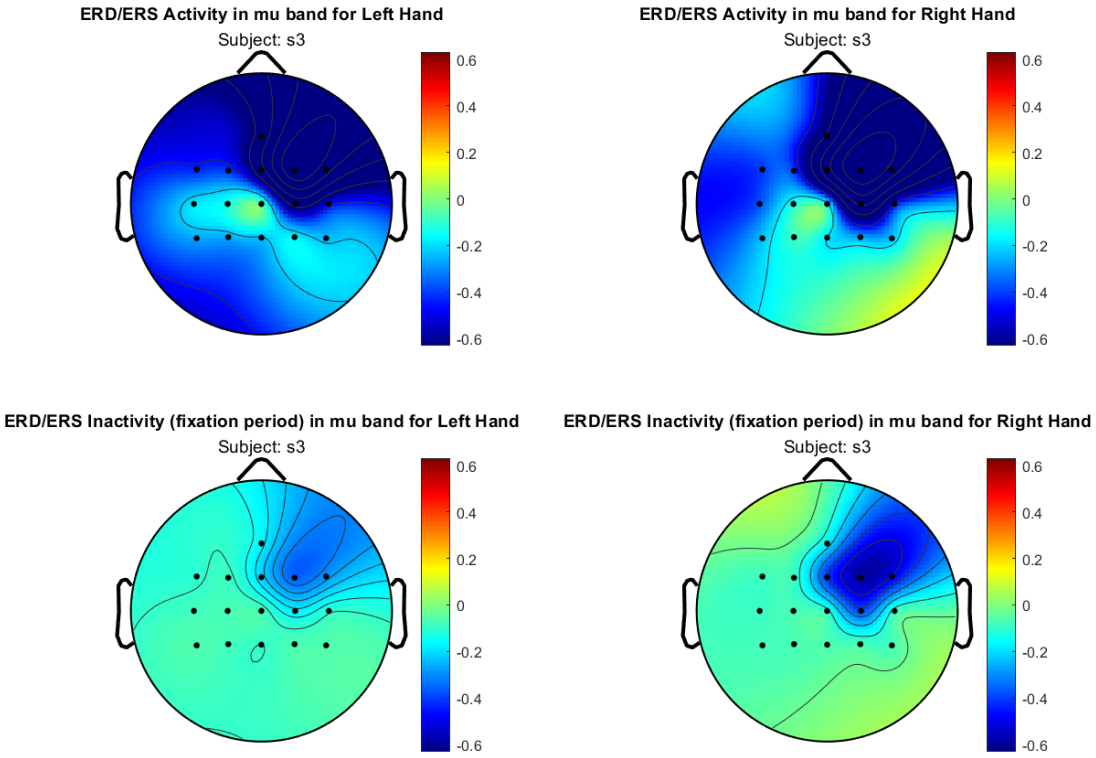

Figure 93: Topomaps related to the ERD/ERS of classes Right Hand and Left Hand, user s3.

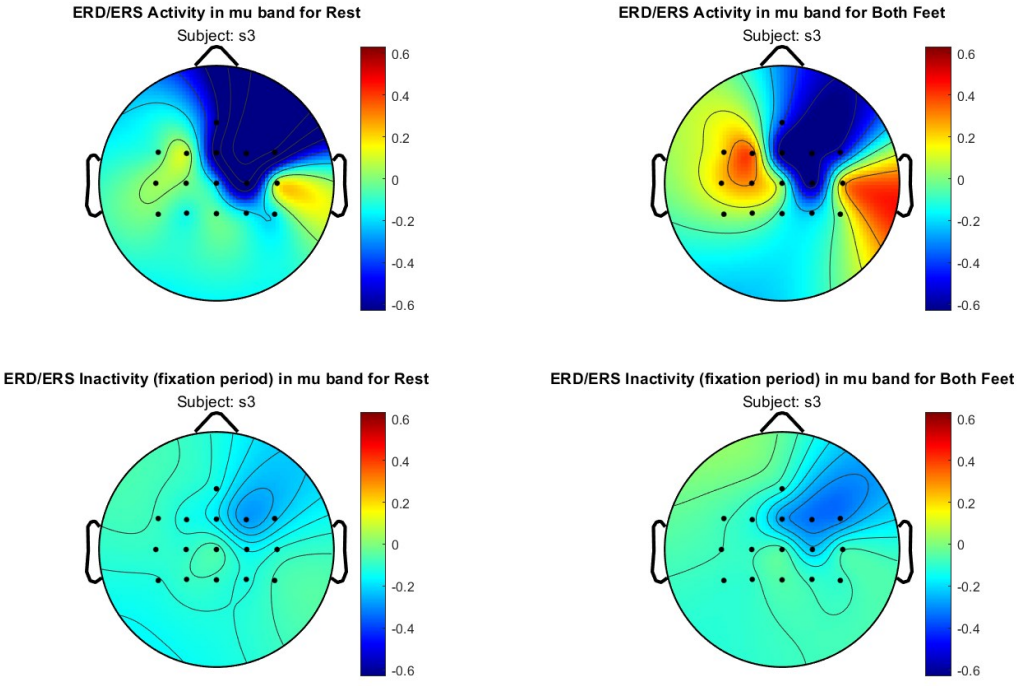

Figure 94: Topomaps related to the ERD/ERS of classes Both Feet and Rest, user s3.

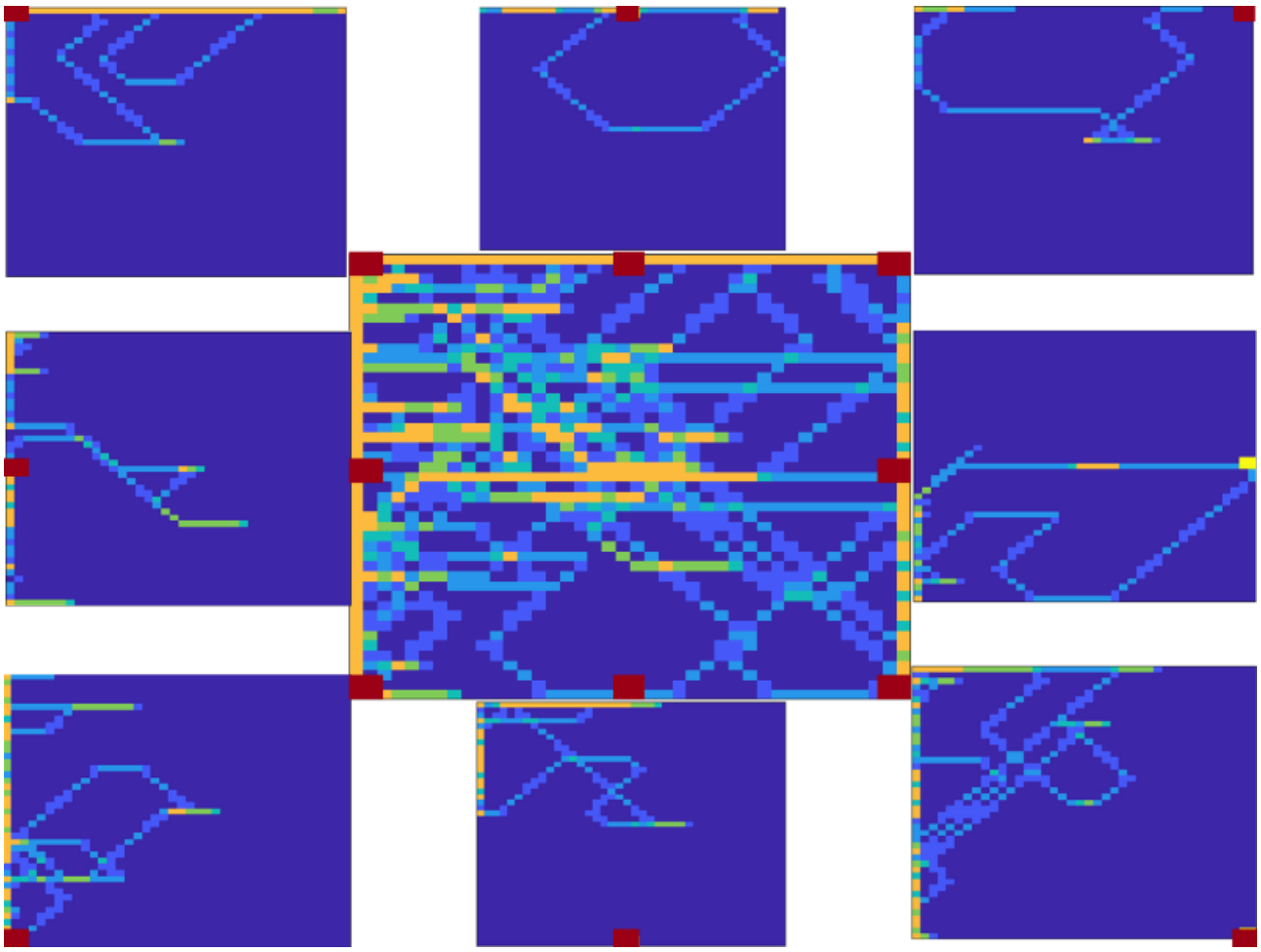

Figure 95: Heat maps of user s3, second setup.

User s5 – second setup

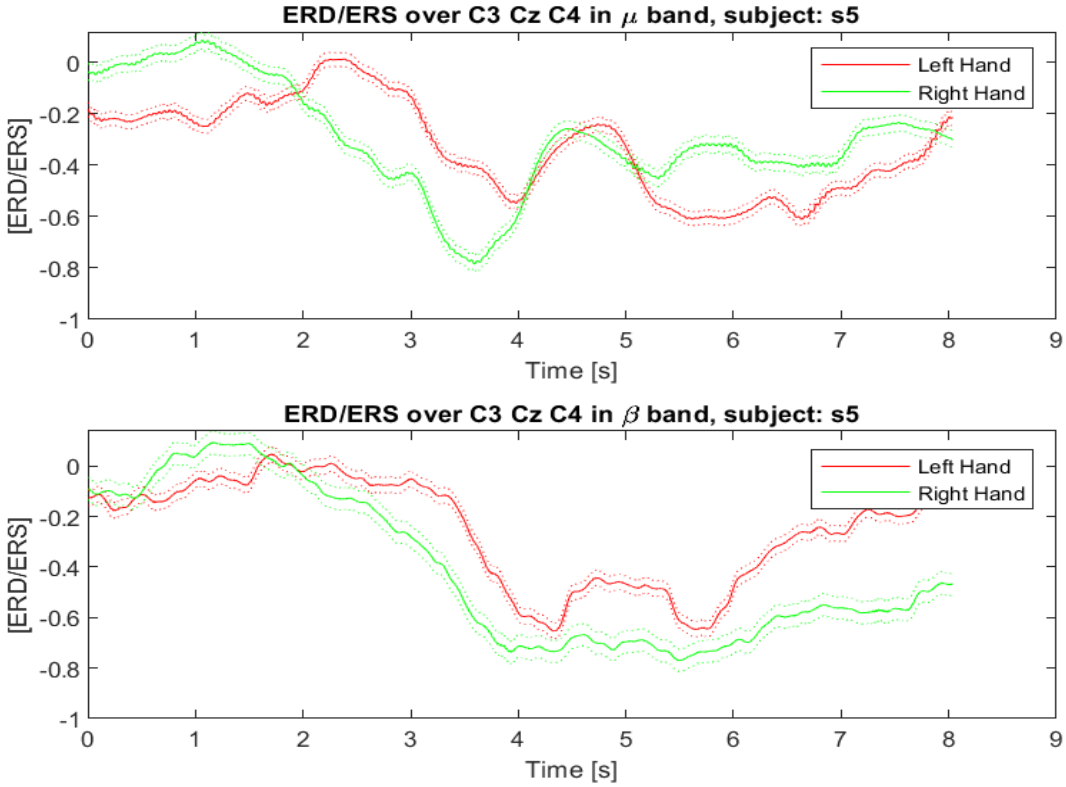

Figure 96: ERD/ERS over main target electrodes in μ and β bands for classes Right Hand and Left Hand, user s5.

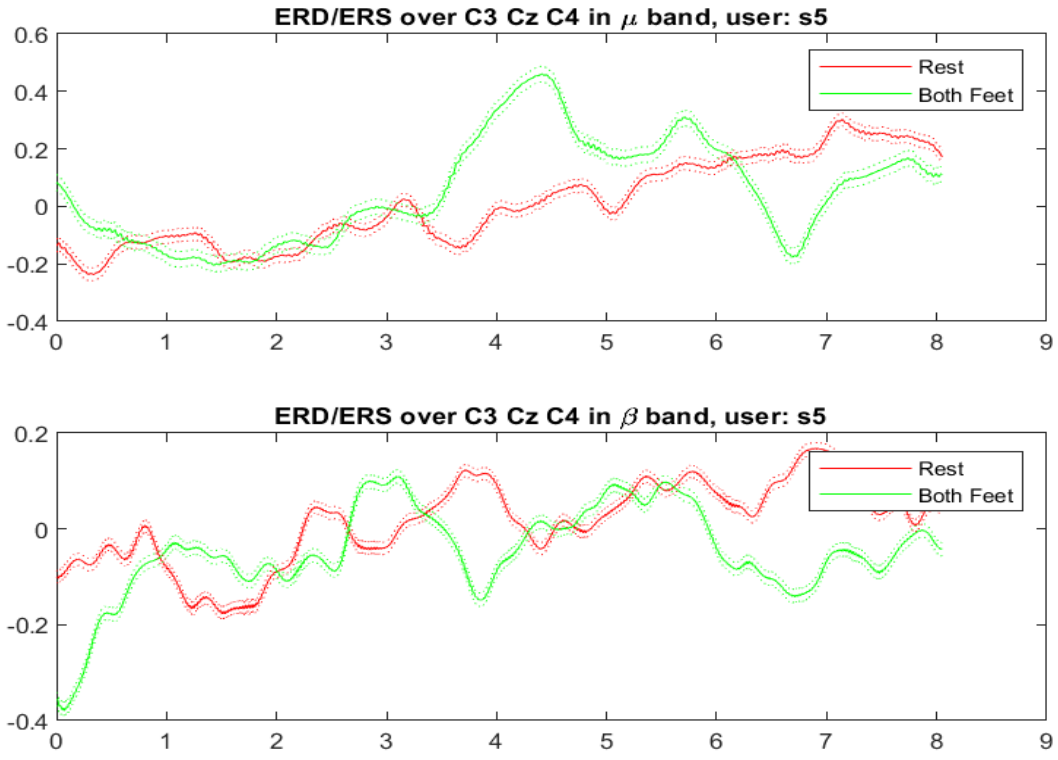

Figure 97: ERD/ERS over main target electrodes in μ and β bands for classes Both Feet and Rest, user s5.

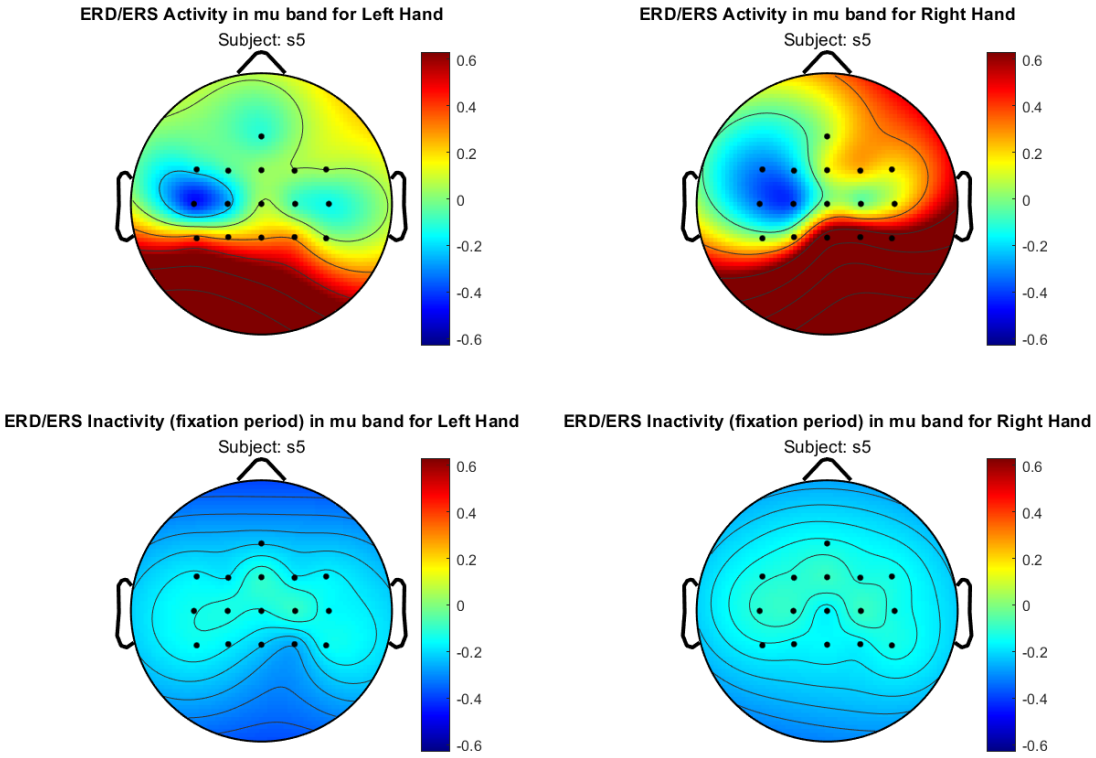

Figure 98: Topomaps related to the ERD/ERS of classes Right Hand and Left Hand, user s5.

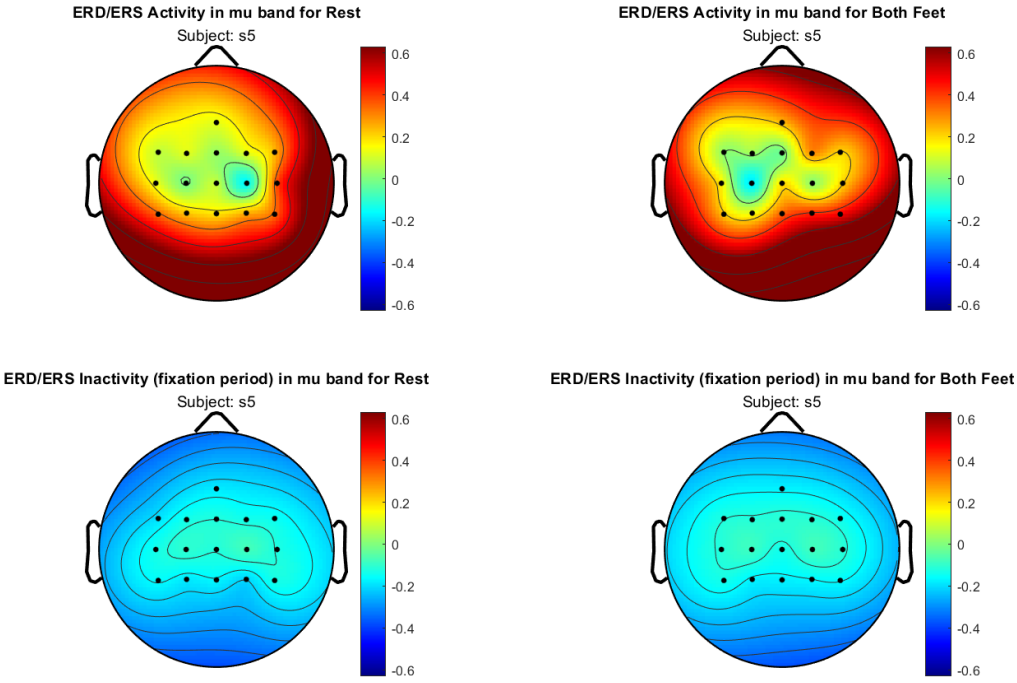

Figure 99: Topomaps related to the ERD/ERS of classes Both Feet and Rest, user s5.

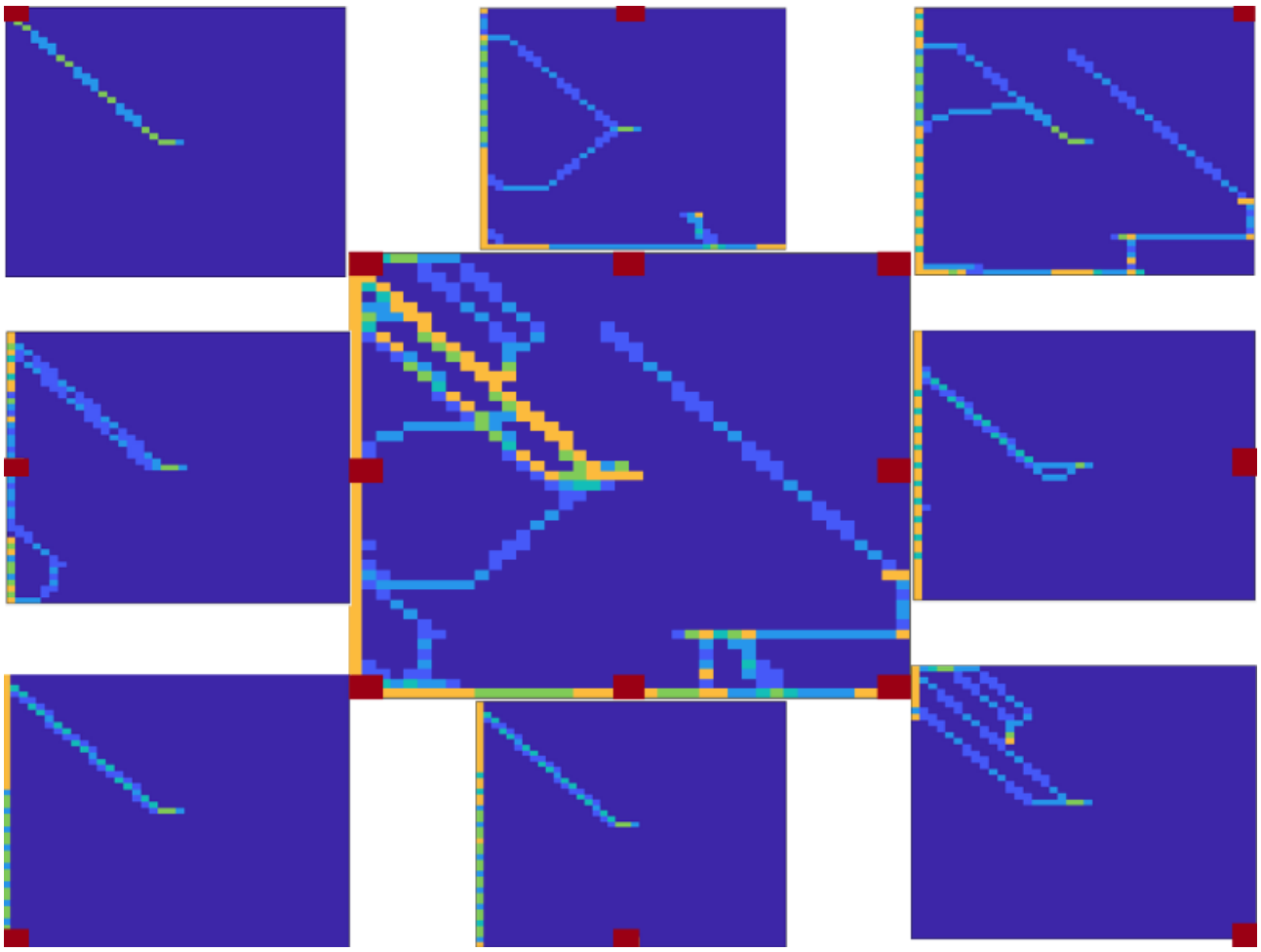

Figure 100: Heat maps of user s5, second setup.

User s12 – second setup

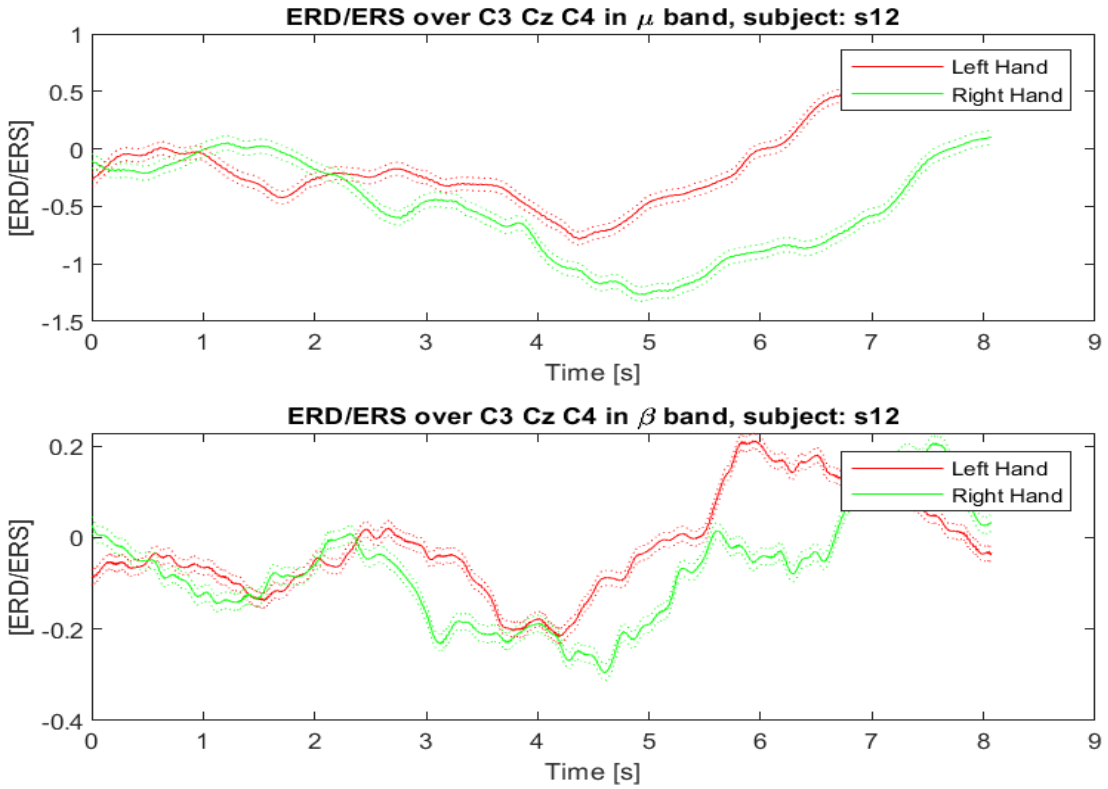

Figure 101: ERD/ERS over main target electrodes in μ and β bands for classes Right Hand and Left Hand, user s12.

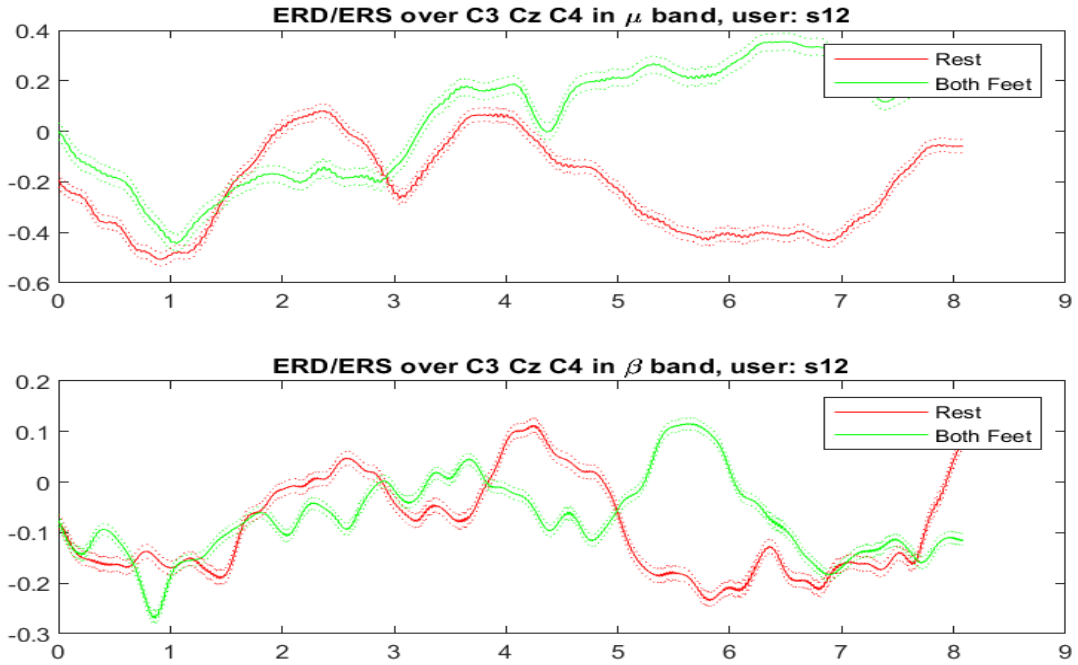

Figure 102: ERD/ERS over main target electrodes in μ and β bands for classes Both Feet and Rest, user s11.

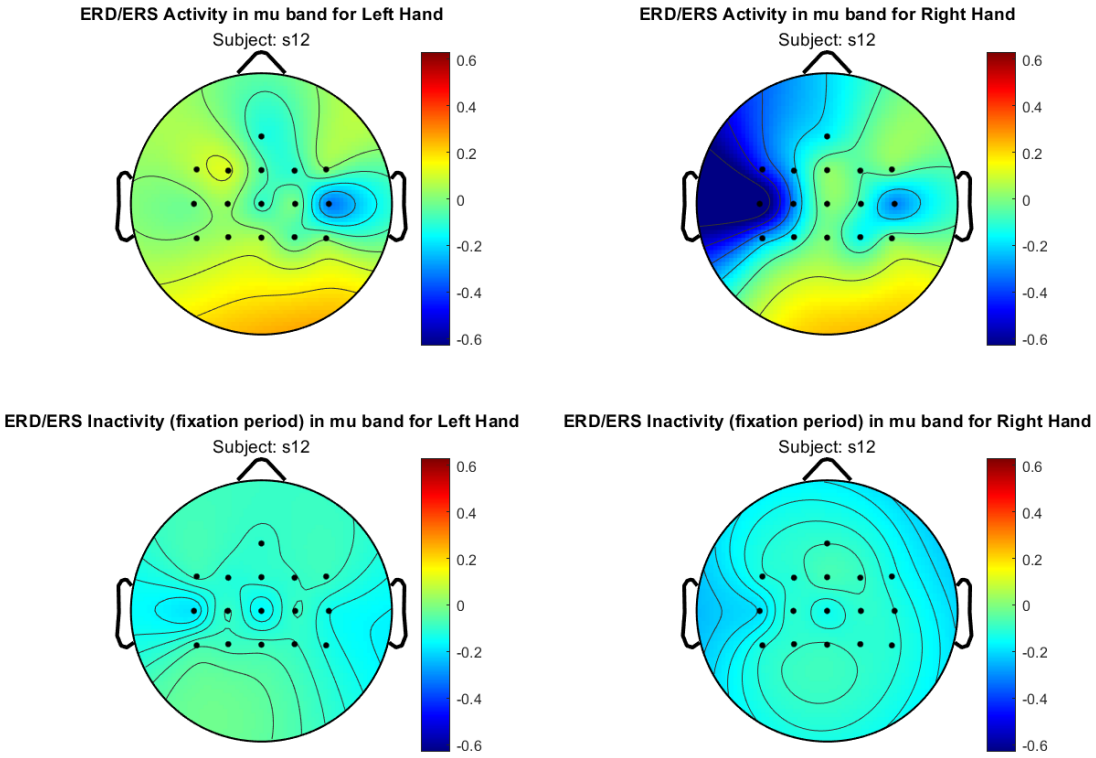

Figure 103: Topomaps related to the ERD/ERS of classes Right Hand and Left Hand, user s11.

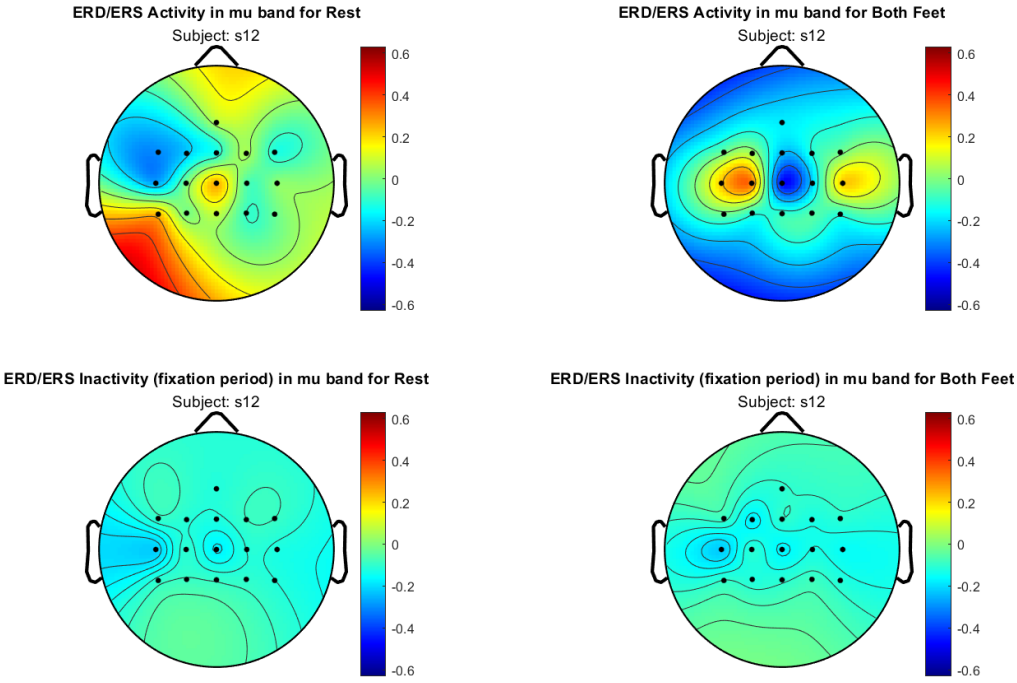

Figure 104: Topomaps related to the ERD/ERS of classes Both Feet and Rest, user s12.

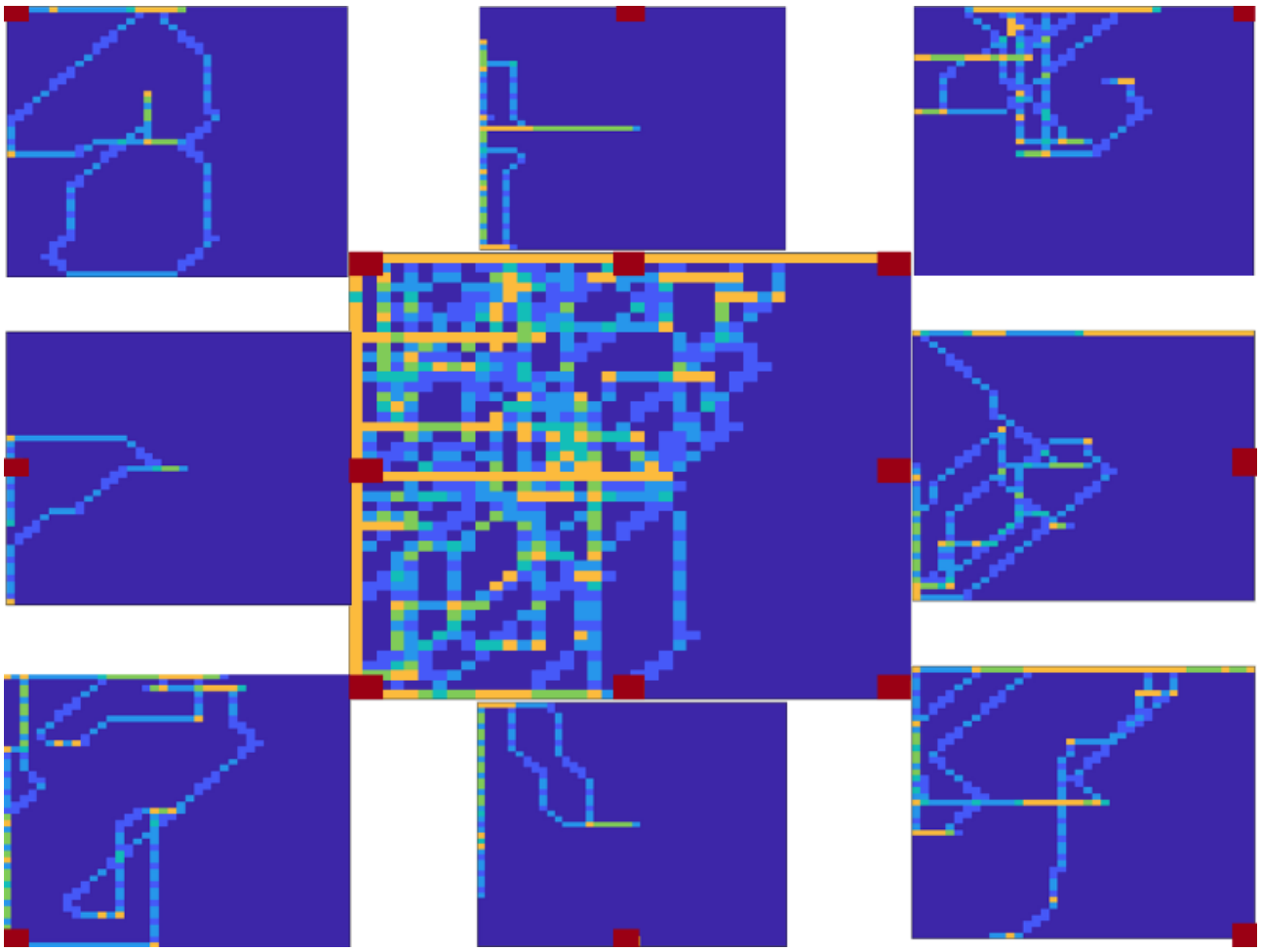

Figure 105: Heat maps of user s12, second setup.

User s13 – second setup

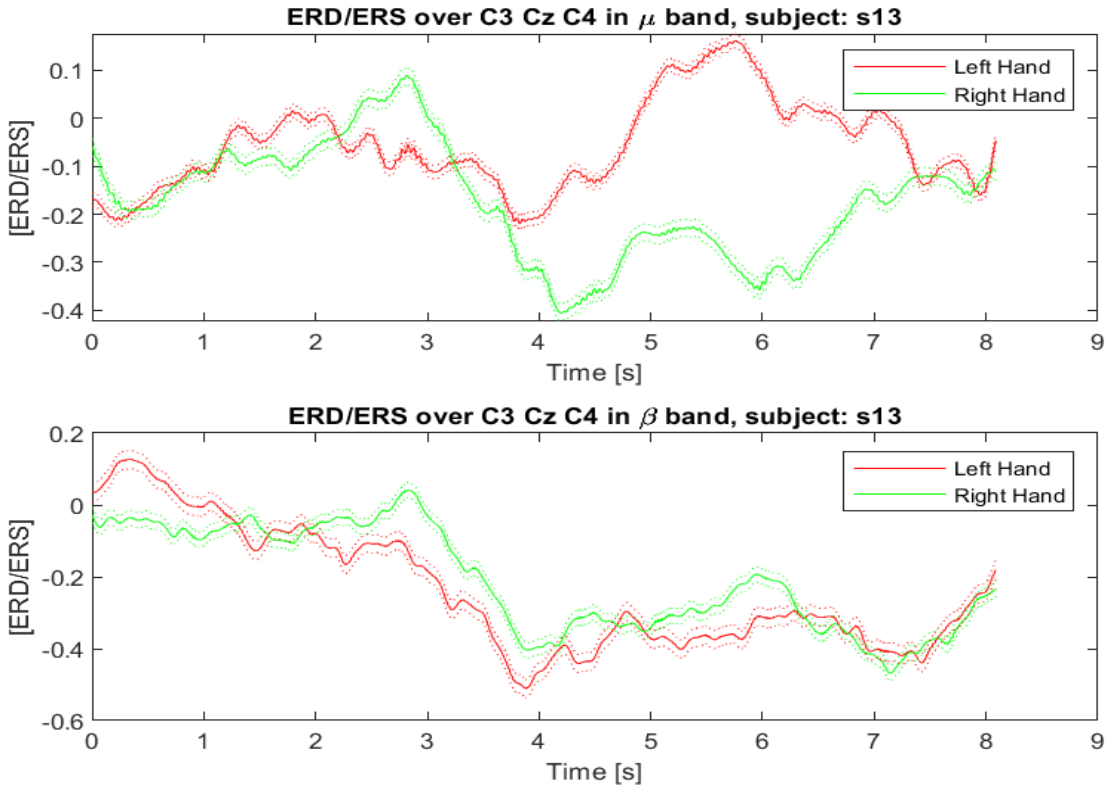

Figure 106: ERD/ERS over main target electrodes in μ and β bands for classes Right Hand and Left Hand, user s13.

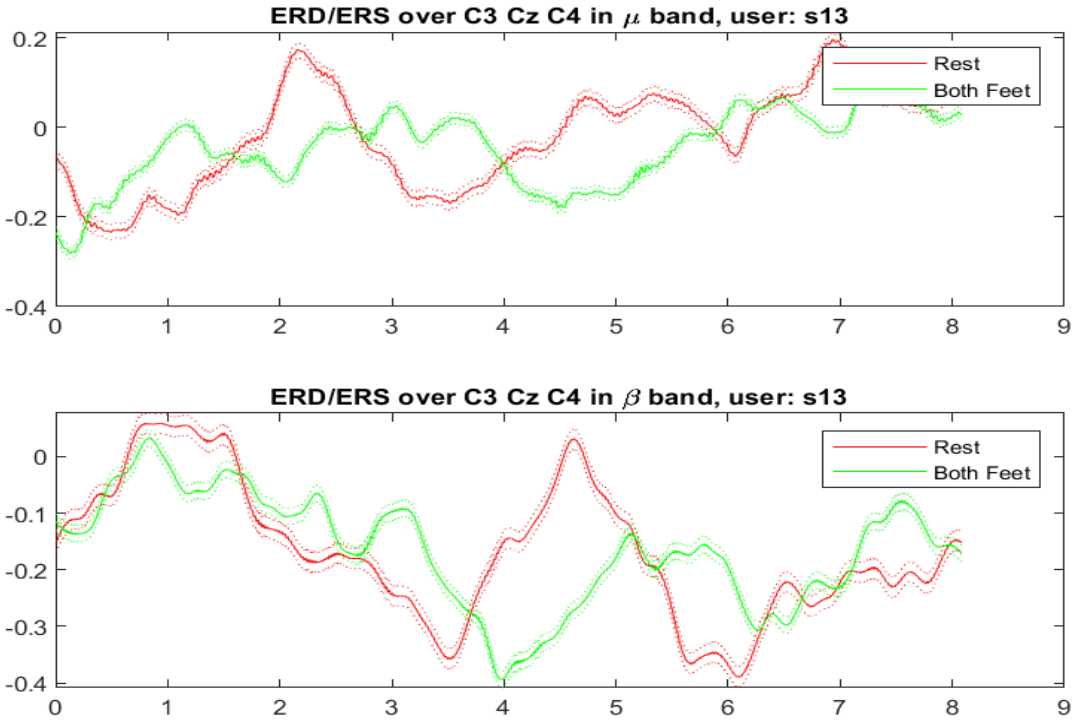

Figure 107: ERD/ERS over main target electrodes in μ and β bands for classes Both Feet and Rest, user s13.

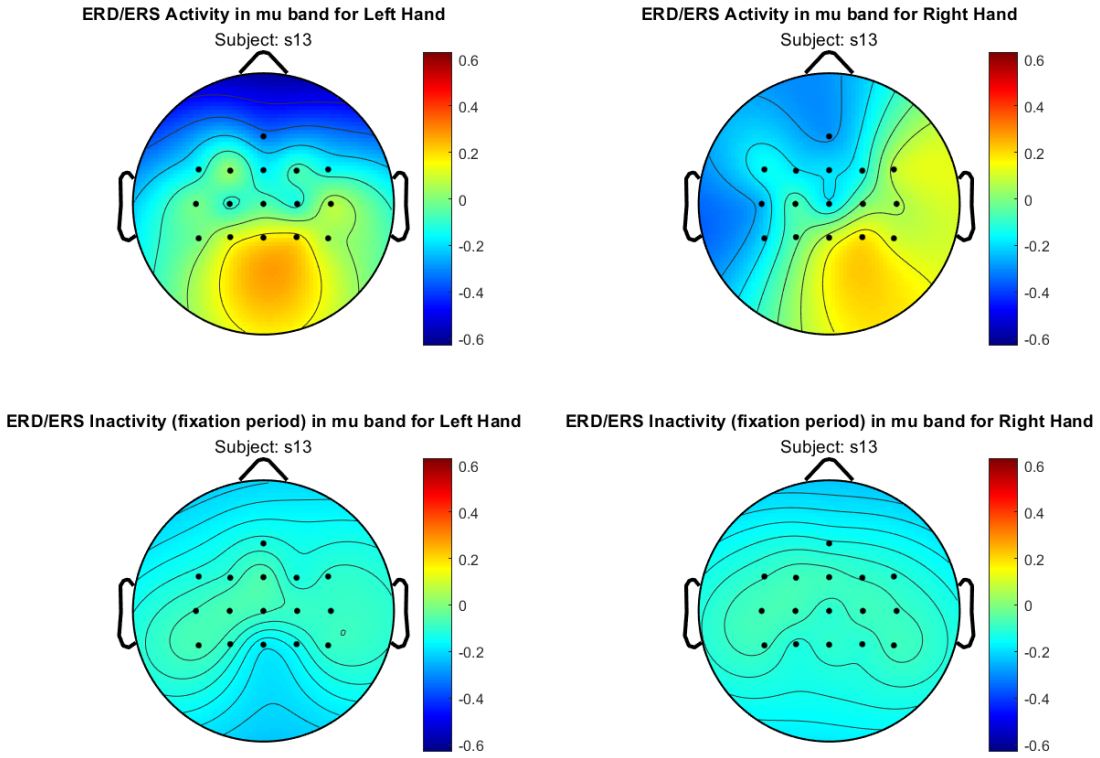

Figure 108: Topomaps related to the ERD/ERS of classes Right Hand and Left Hand, user s13.

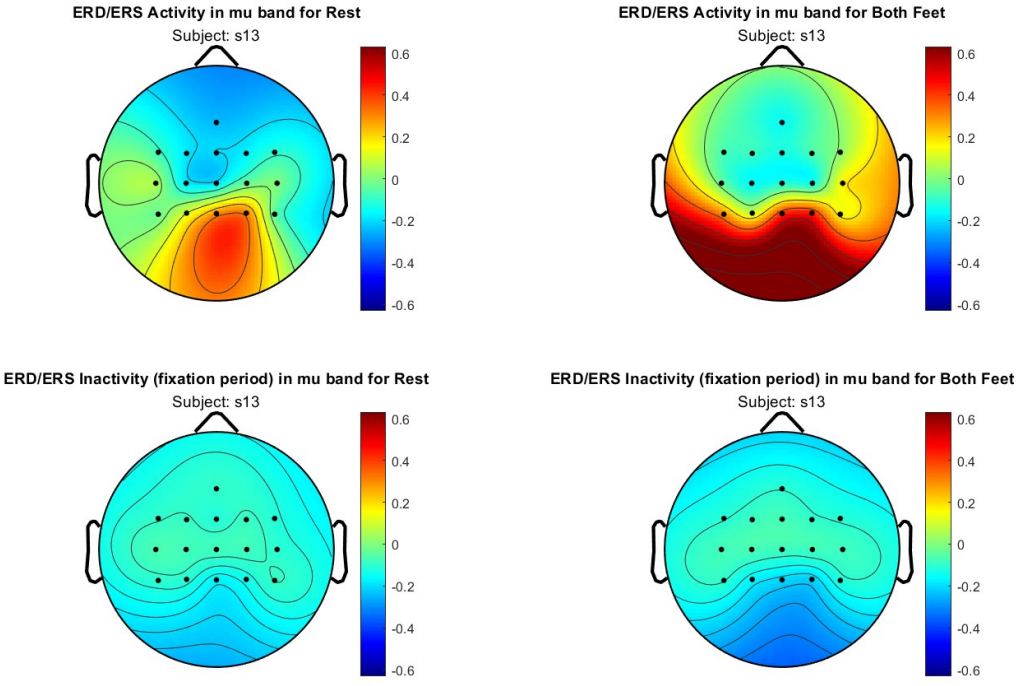

Figure 109: Topomaps related to the ERD/ERS of classes Both Feet and Rest, user s13.

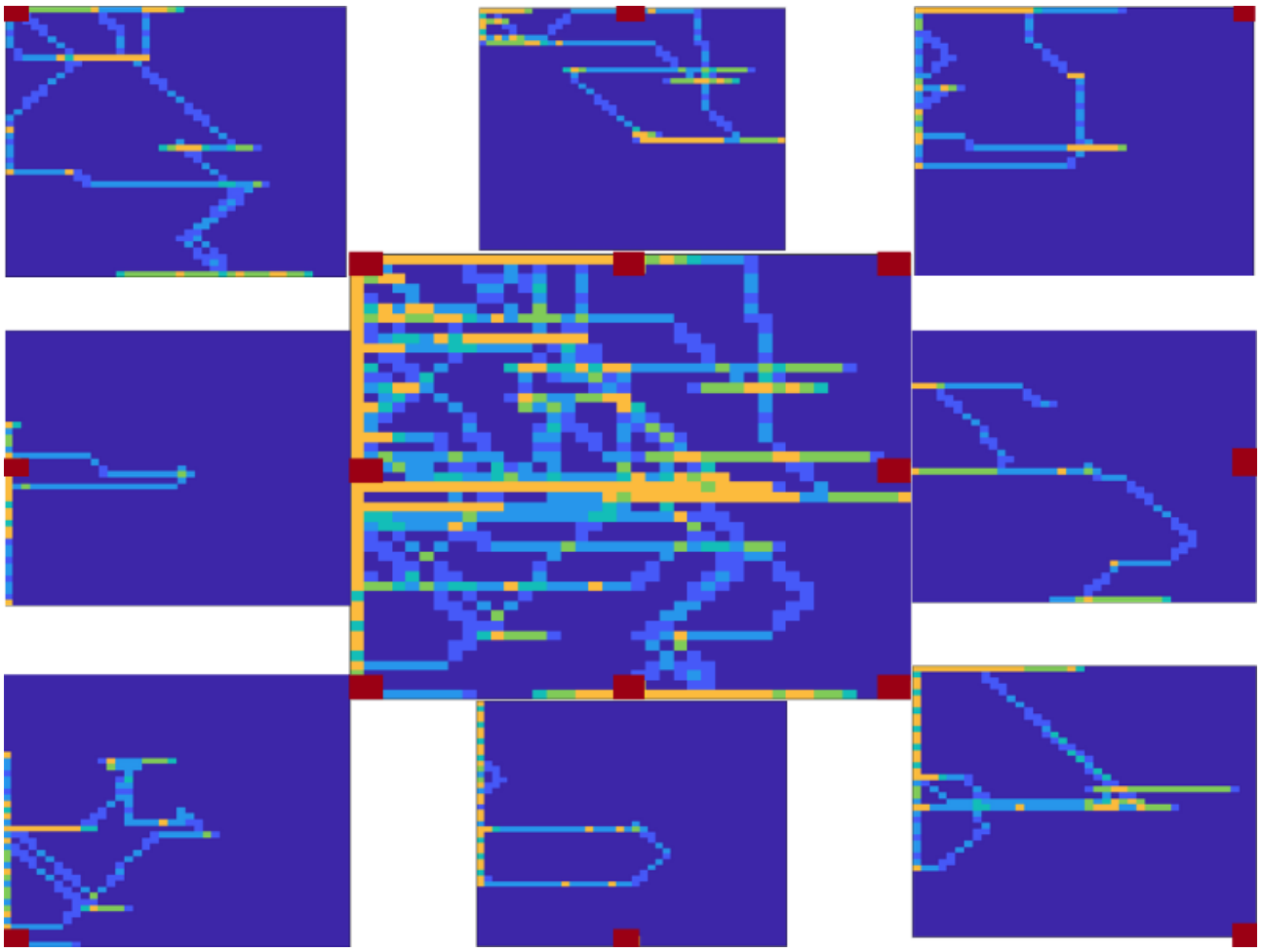

Figure 110: Heat maps of user s13, second setup.